A REGIONAL GEOCHEMICAL ATLAS FOR PART OF SOCORRO COUNTY, NEW MEXICO

by
James M. Watrus

A Thesis Submitted in Partial Fulfillment of the Requirements for
Master of Science in Geochemistry
May, 1998

New Mexico Institute of Mining and Technology
Socorro, New Mexico, USA

ABSTRACT

Accurate interpretations of geochemical data in environmental and mineral exploration studies require that the natural concentrations of elements in a study area be known. One way of providing these data is to create a regional geochemical atlas. As a trial for New Mexico, a regional geochemical atlas was created for part of Socorro County. The sampling protocol followed the recommendations set forth by the International Geological Correlation Programs Project 259 (Darnley et al., 1995). By following these recommendations the data from this project may eventually be incorporated into a global geochemical database. Samples were collected from within cells of a 3 X 3-km grid based on the UTM coordinate system. One sample site for each grid cell was selected based on an absence of obvious contamination, accessibility, and representation of the cell. Stream sediments were chosen as a sample media because they represent a composite of the < 150 μm sediment fraction taken over 50 m of the streambed. Samples were analyzed by wavelength dispersive x-ray fluorescence for SiO_2, Al_2O_3, CaO, Fe_2O_3, K_2O, MgO, MnO, Na_2O, P_2O_5, TiO_2, As, Ba, Cr, Cu, Ga, Mo, Nb, Ni, Pb, Rb, Sr, Th, U, V, Y, Zn, and Zr. The monitoring of analytical reproducibility as well as within stream variation involved the use of triplicate samples in an unbalanced two-level design. Analysis of international standard reference materials ensured the precision and accuracy of the data. Results show that nearly all elements have trends that are correlative with the varying geology of the region (e.g., Paleozoic sediments, and Tertiary andesitic and rhyolitic volcanics). There also exists the presence of three multi-element anomalous regions within the study area. These occur in the Magdalena Mountains, Socorro Peak, and Polvadera Mountain. The anomalous regions within the

Magdalena Mountains and Socorro Peak coincide with existing mining districts. The anomalous region at Polvadera Mountain is likely the result of the Precambrian granites as well as carbonatite dikes that occur in the region. A large arsenic anomaly is also present in the Chupadera Mountains and is coincident with the Luiz Lopez mining district.

ACKNOWLEDGEMENTS

There are many people I owe a large debt of gratitude for helping me to obtain this goal. First, I would like to thank Philip Kyle for his support and guidance throughout my stay in New Mexico. I would also like to thank him for introducing me to the interesting topic of regional geochemical mapping. Secondly, I would like to thank the members of my committee Virginia McLemore, Charles Chapin, and Dave Norman for their insights into this project. I would also like to thank Richard Chamberlain for helping me obtain access to EMRTC as well as his insights into geochemical mapping and the local geology.

I would also like to express my sincere gratitude to all of the geoscience volleyball team members who provided a great deal of entertainment these last two years. Now that you have finally removed the dead weight (Me), I know you will obtain the ultimate goal of intramural champions.

Finally, I would like to thank my parents and little brother for their support and words of encouragement throughout my long college career. Without their overwhelming support none of this would have been possible.

TABLE OF CONTENTS

LIST OF TABLES

LIST OF FIGURES

LIST OF ABBREVIATIONS AND TERMS

ppm = μg/g

Baseline: A line established with more than usual care which serves as a reference to which surveys are coordinated and correlated.

Clarke: The average abundance of an element in the crust of the earth.

Disclaimer: I would like to point out that the data in this project are the result of a preliminary investigation of surficial geochemistry based solely on stream sediments. There has been no attempt on my part to relate the surficial chemistry to the environmental guidelines the US Environmental Protection Agency has established for drinking water.

INTRODUCTION

"All life, and the quality of human life, is dependent upon the chemistry of the earth's surface layer."
Arthur Darnley, 1995

BACKGROUND

Geochemical information is becoming increasingly more important in the management of our environment because the quality of life depends on the chemistry of the earth's surface layer. One method of portraying information regarding surface layer chemistry is with the construction of regional geochemical atlases. A regional geochemical atlas serves two purposes. First, it provides a natural element baseline to monitor environmental change. Second, it delineates regions of large-scale anomalous elemental concentrations, and is thus widely used in mineral-resource exploration studies.

The development of a natural element baseline is probably the most important product of a geochemical atlas. Accurate interpretations of geochemical data in environmental and mineral exploration studies require that the natural concentrations of elements in a study area be known. A geochemical atlas can provide this information allowing the results from future studies easier to interpret. Natural element baselines can also be used as a means of monitoring changes at the earth's surface through time (Darnley et al., 1995).

The creation of a geochemical atlas provides valuable information regarding the occurrences of mineral resources. Delineation of regions of large-scale anomalous elemental concentrations is important for mineral resource management. With an ever-

increasing world population it is important that we begin to look for the mineral resources that will supply the industrial productivity needed in the future (Darnley et al., 1995).

Geochemical atlases can also provide important environmental information. Recently, environmental scientists have been working, in a "curative" manner, to solve existing problems such as the remediation of hazardous waste sites. However, the future of geochemistry will likely involve taking a "preventive" approach to environmental issues (Siegel, 1995). A geochemical atlas can be used in a preventive manner by providing information regarding the possible affects that future anthropogenic pollution may have on a region.

SIMILAR STUDIES

National Uranium Reconnaissance and Evaluation (NURE)

The NURE project was a large-scale geochemical mapping project conducted in the United States during the 1970's. The goal of this national project was to determine the uranium resources of the United States, and to make this information available to industry for future development. One of the methods involved in this program was the National Hydrogeochemical and Stream Sediment Reconnaissance Survey. This survey was conducted by the Department of Energy's Los Alamos Scientific Laboratory, Oak Ridge Gaseous Diffusion Plant, Savannah River Laboratory, and Lawrence Livermore Laboratory. The samples collected during this project were analyzed for uranium and other elements (DOE, 1979). Unfortunately each of the four labs had their own sampling and analytical procedures (SRL, 1977; LASL, 1978, and ORGDP, 1978). The result is a

database with information regarding uranium resources throughout the United States, but it is incomplete and incomparable with respect to other elements.

British Geological Survey

The British Geological Survey began its Geochemical Survey Program in 1975. The primary goal of this program is to identify new occurrences of metalliferous minerals and provide natural element baselines, which may be used to assess contaminated regions (BGS, 1992). The Geochemical Survey Program involves a systematic mapping of the geochemistry of Great Britain based on stream sediments. Each year this program samples approximately 5000 km^2 at a sampling density of approximately 1 sample per square km (Simpson et al., 1993). As of 1992, the British Geological Survey had published nine atlases in the series (BGS, 1992).

International Geological Correlation Program

In 1988 the Global Geochemical Mapping Project was launched with the formation of the International Geological Correlation Program (IGCP) Project 259. The goal of IGCP 259 was to determine how best to sample, map, and store the data for a worldwide geochemical mapping project. Project 259 was completed in 1995 with the release of a final report on their findings. The IGCP has broken the earth's land surface down into 5000, 160 x 160-km grids. The grids are then to be broken down further into cells for sampling of stream sediments, lake sediments, regolith, humus, and water. The project will involve many quality assurance measures, which will produce high-quality, comparable data worldwide. Project 259 has been continued as Project 360 with a goal of implementing the recommendations of the former project. In order to do this they first

need to obtain support, principally financial, for the development of a worldwide geochemical database (Darnley et al., 1995).

Other Organizations

Many other geological surveys have determined a need for such geochemical data. The Russians have recently started preliminary orientation surveys of their country based on the findings of the IGCP project. The goal of the Russian project is to compile a set of multi-purpose maps that relate to mineral exploration and environmental geology (Koval et al., 1995). Other geological surveys which have begun a geochemical sampling program include the Chinese, South Africans, and Western Europeans (Darnley et al., 1995; Labuschagne et al., 1993; Bolviken et al., 1996).

PURPOSE

The purpose of this project is to construct a high-quality, multi-element regional geochemical atlas for part of Socorro County, New Mexico. The sampling and analytical procedures for this project followed the recommendations set forth by the International Geological Correlation Programs Project 259 regarding stream sediment surveys (Darnley et al., 1995). By following these recommendations the data from this project may eventually be incorporated into a global geochemical database.

STUDY AREA

LOCATION

The study area for this project consists of approximately 3000 km^2 of Socorro County, New Mexico (Fig. 1). The eastern, western, and southern boundaries are defined

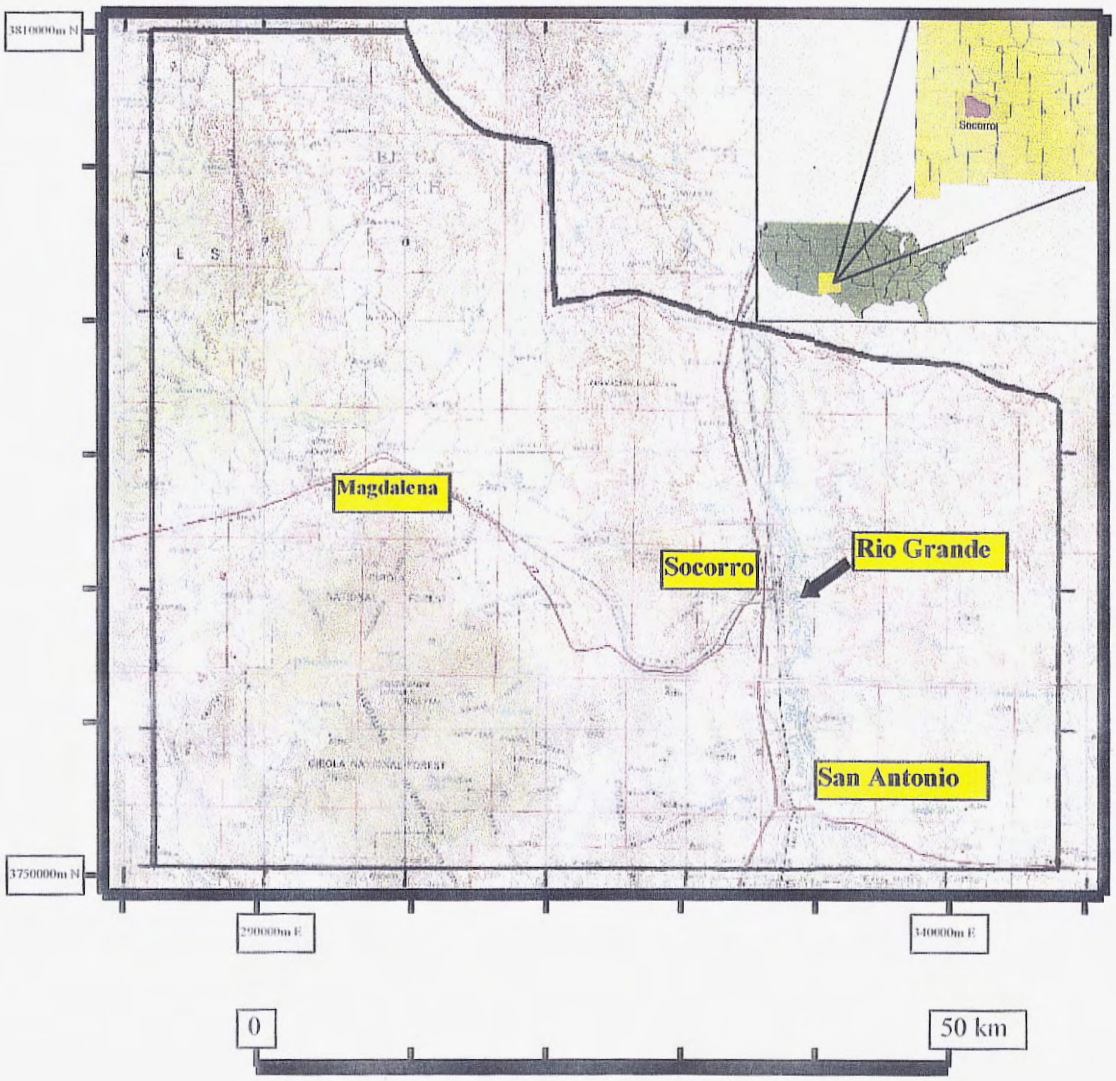

Figure 1. Location map of the study area.

by the following Universal Transverse Mercator coordinates; Zone 13S 357000m E, 282000m E, and 3750000m N. The northern boundary is defined by the Rio Salado in the west and the southern boundary of the Sevilleta National Wildlife Refuge in the central and eastern regions. Socorro County has a population of approximately 15,853. The major city within the county is Socorro with a population of approximately 9,000 (U.S. Bureau of Census, 1993). Other communities within the study area include Magdalena and San Antonio. Interstate 25 and the Rio Grande bisect the study area from north to south in the east-central region. Highway 380 and Highway 60 traverse the study area from east to west. Highway 60 extends from the western edge of the study area to Socorro while Highway 380 extends from San Antonio to the eastern margin of the study area. A large percentage of the study area is public land. The Bureau of Land Management, and US Forest Service administers this land. The primary use of the land in the study area is livestock grazing and some irrigated farming within the Rio Grande Valley (Johnson, 1988).

TOPOGRAPHY AND CLIMATE

Figure 2 shows pictures taken within the study area. Elevations in the study area range from a high of approximately 3286 m at South Baldy in the Magdalena Mountains to approximately 1380 m in the Rio Grande Valley. The central and western portions of the study area are characterized by high mountains including the Bear Mountains (northwest), Magdalena Mountains (southwest), Lemitar Mountains (north central), and Chupadera Mountains (south central) with the La Jencia Basin located between the

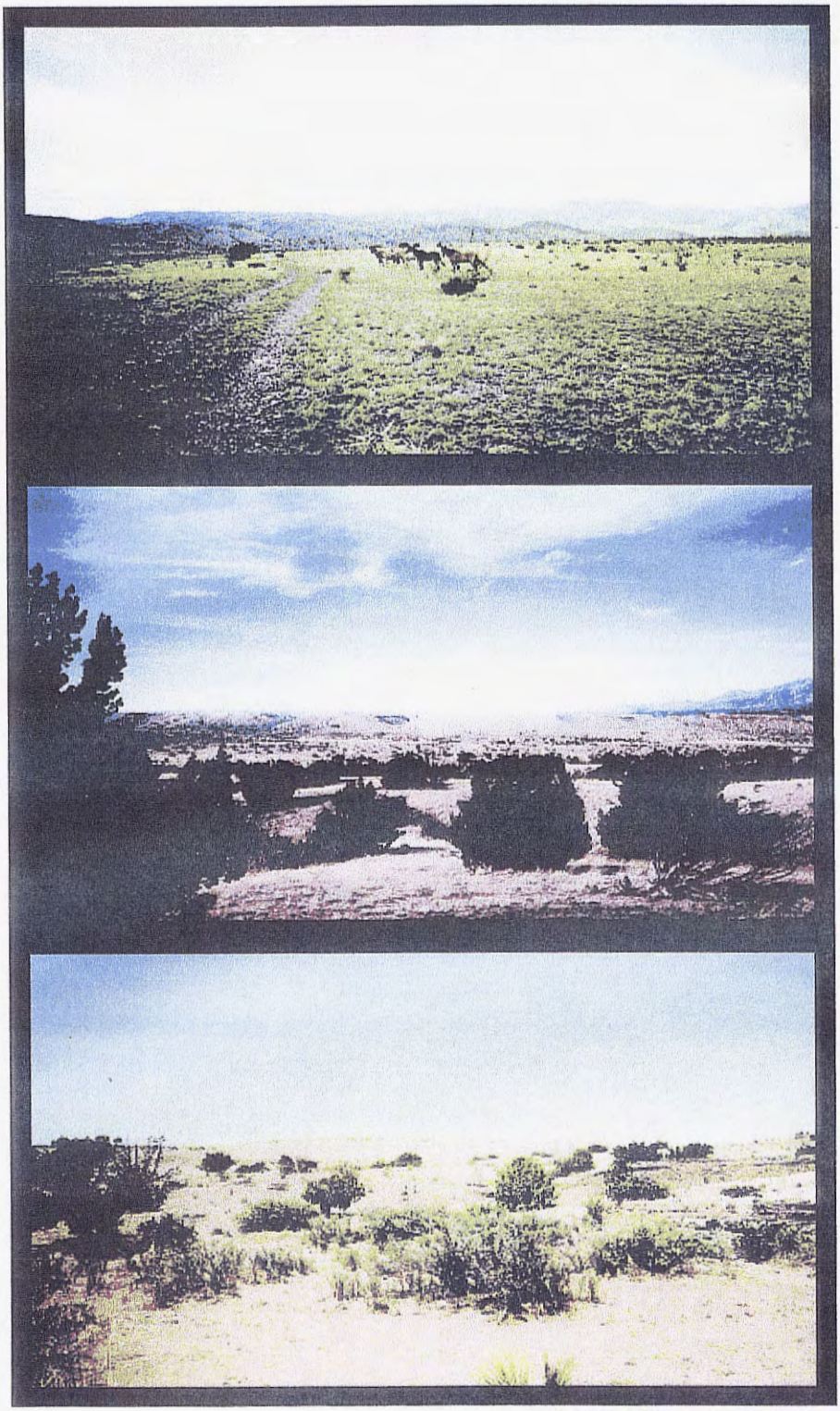

Figure 2. Three picture of the study area. The top picture shows the Magdalena Mountains in the distance, the middle is of the north-central region, and the bottom is typical of the area east of the Rio Grande.

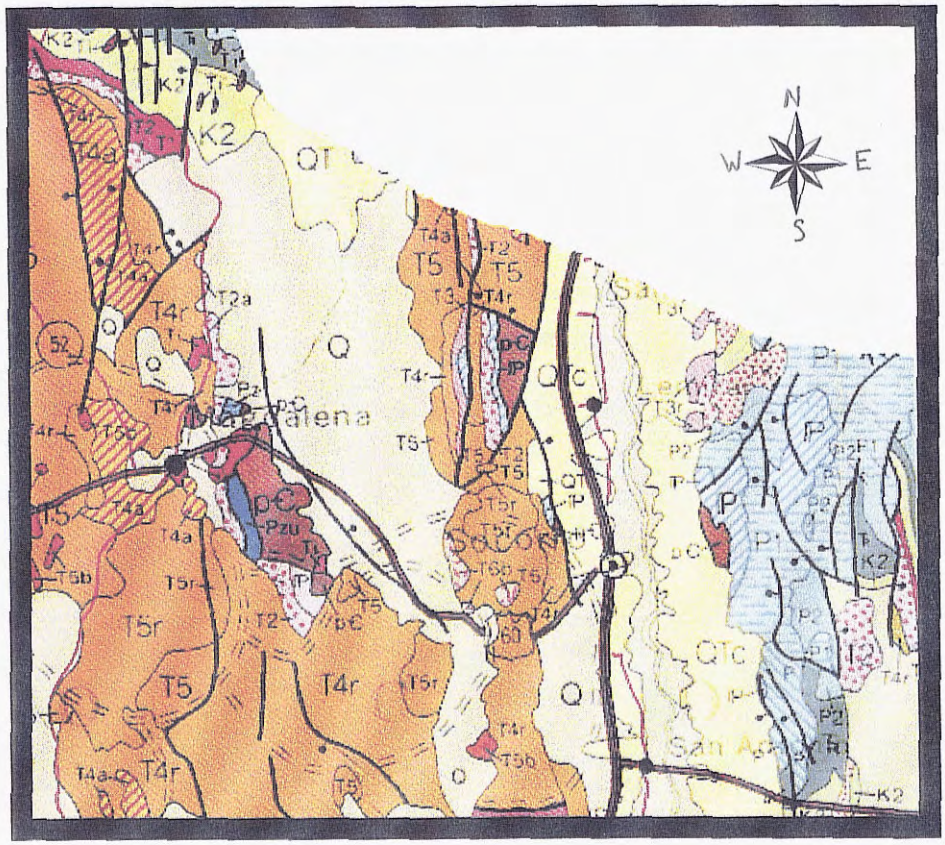

QUATERNARY SEDIMENTS

QUATERNARY / TERTIARY SEDIMENTS

TERTIARY RHYOLITES

TERTIARY ANDESITES

TERTIARY BASALTS

TERTIARY BASALTS

CRETACEOUS SEDIMENTARY ROCKS

TRIASSIC SEDIMENTARY ROCKS

PERMIAN SEDIMENTARY ROCKS

PENNSYLVANIAN SEDIMENTARY ROCKS

PRECAMBRIAN GRANITES AND QUARTZITES

FIGURE 2. Generalized geologic map of the study area (after, NMGS, 1982)

and metaigneous rocks. The Lemitar Mountains consist of Precambrian granites, gabbros, and metasedimentary-metavolcanic rocks (Osburn, 1984). Younger carbonatite dikes have intruded the Precambrian rocks in the Lemitar Mountains. These dikes are enriched in the rare-earth elements, niobium, uranium, thorium, and phosphate (McLemore, 1982).

Mississippian and Pennsylvanian

Mississippian and Pennsylvanian sedimentary rocks outcrop in the Magdalena Mountains, Lemitar Mountains, northwest region, and east of the Rio Grande within the study area. The Mississippian Caloso and Kelly Formations occur in the Magdalena Mountains. The Kelly Formation is also present in the Lemitar Mountains. The Caloso Formation is comprised of basal sands, arkoses, and shales overlain by a massive gray limestone, whereas the Kelly Formation is a gray to light-brown crinoidal limestone (Armstrong, 1958). The Pennsylvanian Sandia Formation occurs in the Magdalena and Lemitar mountains and east of the Rio Grande. The Sandia Formation consists of siltstones, sandstones, shales, conglomerates, and localized sandy limestones (Osburn, 1984). The Pennsylvanian Madera Formation crops out in the Magdalena and Lemitar mountains and east of the Rio Grande. The Madera Formation is a dark-gray to black fossiliferous micritic limestone with calcareous quartzites and black shales (Siemers, 1973). Osburn (1984) has mapped undivided Pennsylvanian rocks in the Lemitar Mountains and northwest section of the study area.

Permian

Permian sedimentary rocks make up a large portion of the rocks east of the Rio Grande. Smaller outcrops occur in the Magdalena and Lemitar mountains as well as the

northwestern section of the study area. East of the Rio Grande, Permian rocks consist of the Bursum, Abo, Yeso, Glorieta, and San Andres formations. In the northwest, the Glorieta and San Andres formations are present, whereas in the Magdalena Mountains the Abo, Yeso, Glorieta, and San Andres formations are present (Osburn, 1984).

The Bursum Formation consists of dark-red and green shales, limestones and red arkosic rocks in the upper beds. The Abo Formation consists of dark-red to brown, fine-grained sandstones with interbedded mudstones and siltstones (Osburn, 1984). The Yeso Formation consists of four members. The lower Meseta Blanca Sandstone is a pink to orange sandstone, the overlying Torres Member consists of interbedded sandstone, siltstones, limestones, and gypsum, the Canas Gypsum, overlies the Torres Member and is succeeded by the Joyita Sandstone which is a reddish brown calcareous sandstone (Siemers, 1973). The Glorieta Sandstone is a well-sorted, cross-bedded quartzose sandstone. The San Andres Limestone consists of limestones and dolostones with abundant gypsum and minor mudstones and siltstones.

Triassic and Cretaceous

Triassic sedimentary rocks crop out east of the Rio Grande and in the northwestern portion of the study area. Triassic rocks consist of the Chinle Formation, a red to purple sequence of mudstones and thin sandstones, and the Santa Rosa Sandstone. Cretaceous strata crop out east of the Rio Grande as well as in the northwestern section of the study area. The Cretaceous rocks within the study area have been broken down into two mapping units 1) the Dakota Sandstone which includes the Mancos Shale and Tres Hermanos Sandstone, and; 2) the Gallup Sandstone and overlying Crevasse Canyon Formation (Osburn, 1984). The Dakota Sandstone mapping unit is comprised of marine

and non-marine sandstones while the Gallup Sandstone mapping unit is composed of shoreface and nonmarine sandstones.

Tertiary

During the Tertiary extensive volcanism and local igneous intrusions were emplaced in the study area. Intrusive rocks in and near the Magdalena Mountains include the Anchor Canyon, Nitt, and Water Canyon stocks as well as the Hale Well Pluton and unnamed rhyolitic and monzonitic intrusives. The Baca Formation, consisting of red to buff sandstones, claystones, and conglomerates, was also deposited during the Tertiary. Tertiary volcanic rocks, including ash flows and lavas, range in composition from rhyolite to basaltic andesite (Osburn, 1984). The volcanics were erupted from various centers throughout the region during at least three eruptive cycles and dominate the west and central regions of the study area (Osburn and Chapin, 1983). The sedimentary Popotosa Formation consists of fanglomerates, mudstones, and sandstones. Within the study area the lowermost rocks are usually red, well-indurated mudflow deposits that are overlain by red and green claystones. These facies generally interfinger and grade into volcanic, piedmont-slope and alluvial fan deposits (Osburn, 1984).

Quaternary

Quaternary deposits occur throughout the study area. The deposits include basalt flows, the Sierra Ladrones Formation, as well as a wide variety of alluvial, colluvial, and eolian deposits. The Sierra Ladrones Formation consists of fanglomerates, plus channel and floodplain deposits of the ancestral Rio Grande. The deposits consist of poorly indurated buff to red fanglomerates intertonguing with light-gray sandstones, red to green mudstones and siltstones (Osburn, 1984).

TECTONIC HISTORY

Structurally the study area for this project is quite complex. The major tectonic feature within the study area is the Rio Grande rift. The rift is an area of north-trending crustal extension that is defined by a series of en echelon, north-northeast trending grabens, basins, and tilted fault blocks extending from central Colorado to Mexico (Chamberlain, 1983; and LASL, 1985). There have been two major episodes of extension in the Socorro area. The first extension was rapid and occurred between 28.8 and 27.4 Ma. The second episode was slower and occurred between 16 and 10 Ma. This second episode resulted in the uplift of the Lemitar Mountain block (Chapin and Cather, 1994). The regional strain is likely the result of thermal weakening realted to episodes of magmatism that occurred prior to and during tectonism within the area (Cather et al., 1994). The overall structural complexity of the study area can be seen in Osburn (1984).

MINERAL OCCURRENCES

Eleven mining districts are located within the study area (Fig. 4). Of the eleven very few have had any significant production (North, 1983). According to North and McLemore (1986), the precious metal occurrences within the region can be broken down into four groups: 1) volcanic-epithermal deposits; 2) carbonate hosted lead-zinc deposits; 3) sedimentary copper deposits; and 4) Precambrian vein and replacement deposits. A brief overview of each mining district is given below. The number following the district

MINERAL OCCURRENCES MAP

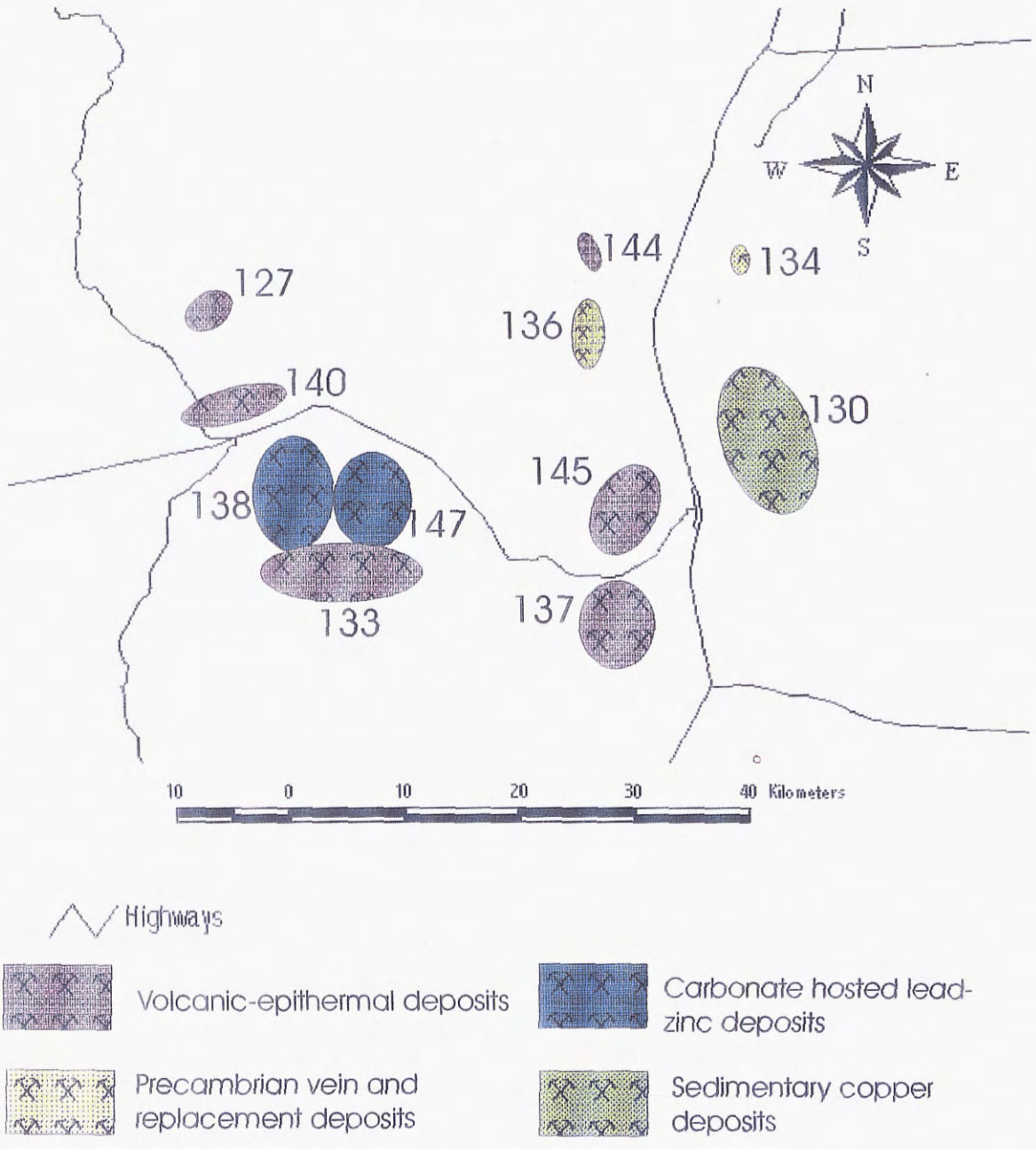

FIGURE 4. Approximate locations of mining districts within the study area (modified from, McLemore, in press).

name is the reference number that is keyed to figure 4 and is the same number used by McLemore (in press).

Bear Mountains District (127)

Copper, silver, antimony, and zinc occur within the Bear Mountains district; there has been no reported production (McLemore, in press). Prospects in this district are located at the head of Cedar Springs Canyon. Veins occur along a fault that cuts the La Jara Peak basaltic andesite and the Hells Mesa Tuff. Primary ore minerals include pyrite, quartz, and calcite. Oxidized minerals include chrysocolla, hematite, tripuhyite, and stibiconite (North, 1985).

Chupadero District (130)

The Chupadero district yielded copper and silver with trace amounts of uranium (McLemore, in press). Copper mineralization occurs irregularly within sandstones of the upper member of the Moya Formation. Copper minerals including malachite and azurite occur as cements and fracture fillings within the sandstone. Approximately 2000 tons of ore with an average of 2% copper and some silver were mined from these workings between 1958 and 1960 (Jaworski, 1973).

Hop Canyon District (133)

The Hop Canyon district yielded copper, lead, silver, and gold. The district also includes trace amounts of zinc, barite, and uranium (McLemore, in press). Mineralization within the district occurs in veins cutting the Hells Mesa Tuff and the Sawmill Canyon Formation. Prospects are also located within the Lemitar Tuff and an overlying andesite. Copper sulfides and copper carbonates are the major ore minerals within this district (North, 1983).

Joyita Hills District (134)

The Joyita Hills district yielded lead, silver, fluorite, and includes trace amounts of copper (McLemore, in press). Mineralization occurs in fissures in Precambrian rocks and along fault contacts with younger rocks. Flourite, barite, galena, chalcopyrite, bornite, and malachite are the ore minerals found within quartz gangue in this district (North, 1983).

Lemitar Mountains District (136)

The Lemitar Mountains district yielded copper, lead, silver and barite with trace amounts of zinc and uranium (McLemore, in press). Prospecting within this district began about 1880. Mineralization occurs in Precambrian rocks and along contacts between Precambrian and Paleozoic rocks. Veins within the district are generally thin and discontinuous (North, 1983).

Luis Lopez District (137)

The Luis Lopez district yielded manganese and includes trace amounts of gold, silver, zinc, lead, and tungsten (McLemore, in press). Mineralization within this district is associated with Tertiary volcanic rocks. Manganese production was from both open pit and underground operations in fissure veins and breccia zones along steeply dipping faults (Eggleston et al., 1983).

Magdalena District (138)

The Magdalena District has been an important source of zinc, lead, copper, silver, and gold. The district also includes trace amounts of fluorite and barite (McLemore, in press). The Magdalena District is the largest silver producer in Socorro County. The district was principally a lead and silver producer from about 1870 to 1900 and after 1900

became dominantly a zinc producer (North, 1983). The mineralization in this area occurs as limestone replacement deposits along faults within the Kelly Limestone. Large-scale mining in the district ceased during the 1950's (Gibbs, 1989).

North Magdalena District (140)

The North Magdalena district yielded lead, barite, silver, gold, and copper with trace amounts of vanadium and zinc (McLemore, in press). Ore was discovered in this district in 1863. The ore deposits within the district occur in veins in shear zones and faults within the La Jara Peak Basaltic Andesite (North, 1983).

San Lorenzo District (144)

The San Lorenzo district has produced copper and silver with trace amounts of uranium and gold (McLemore, in press). Mineralization occurs as fracture fillings along faults in andesite. Mineralization includes chrysocolla filling fractures with calcite (North, 1983).

Socorro Peak District (145)

The Socorro Peak district yielded lead and silver and contains barite, fluorite, gold, tungsten, vanadium, arsenic, and bromine (McLemore, in press). The district was an important silver producer during the 1880's. Mineralization occurs as veins along faults in the Socorro Peak Rhyolite and underlying Popotosa Formation (North, 1983).

Water Canyon District (147)

The Water Canyon District yielded copper, gold, silver, and lead. The district also contains zinc and manganese (McLemore, in press). Three geologic associations are found within the district. The first type is veins associated with volcanic rocks. The

second is vein replacement and skarn deposits within limestone and the third is veins along faults between Precambrian and Paleozoic rocks (North, 1983).

SAMPLING PROCEDURES

Before sampling began an orientation study was conducted. Details of the orientation study can be found in Appendix A. The orientation study helped to determine the final sampling procedures to be used in this project (Appendix B). First a grid, with 9 km^2 cells, was drawn on 1:100,000 topographic maps of the study area The Universal Transverse Mercator (UTM) system was chosen for use as the coordinate system for this project. Grid cells were named according to UTM convention with the southwest corner as a reference point (Merrill, 1986). The goal of the sampling program was to collect one sample from each of the grid cells. Stream sediments were chosen as the sampling media because they represent a composite of the lithological variations within a drainage basin (Darnley et al., 1995).

Samples were collected from first-order streams that have origins within the cell or a neighboring cell. Sample site selection was based on 1) the site being representative, 2) the lack of obvious contamination, and 3) accessibility. Samples were taken 50 m upstream from road crossings, culverts, or other sources of obvious contamination (Fig. 5). Non-contaminating field equipment was used in the sampling process and a GPS receiver was used to determine sampling locations (Fig. 6). Five grab samples were taken over 50 m of the streambed and combined to form one composite sample. Samples were sieved and the < 150 μm size fraction was collected and stored in polyethylene bags. Information regarding location, streambed characteristics, rock type, and

SAMPLE SITE SELECTION

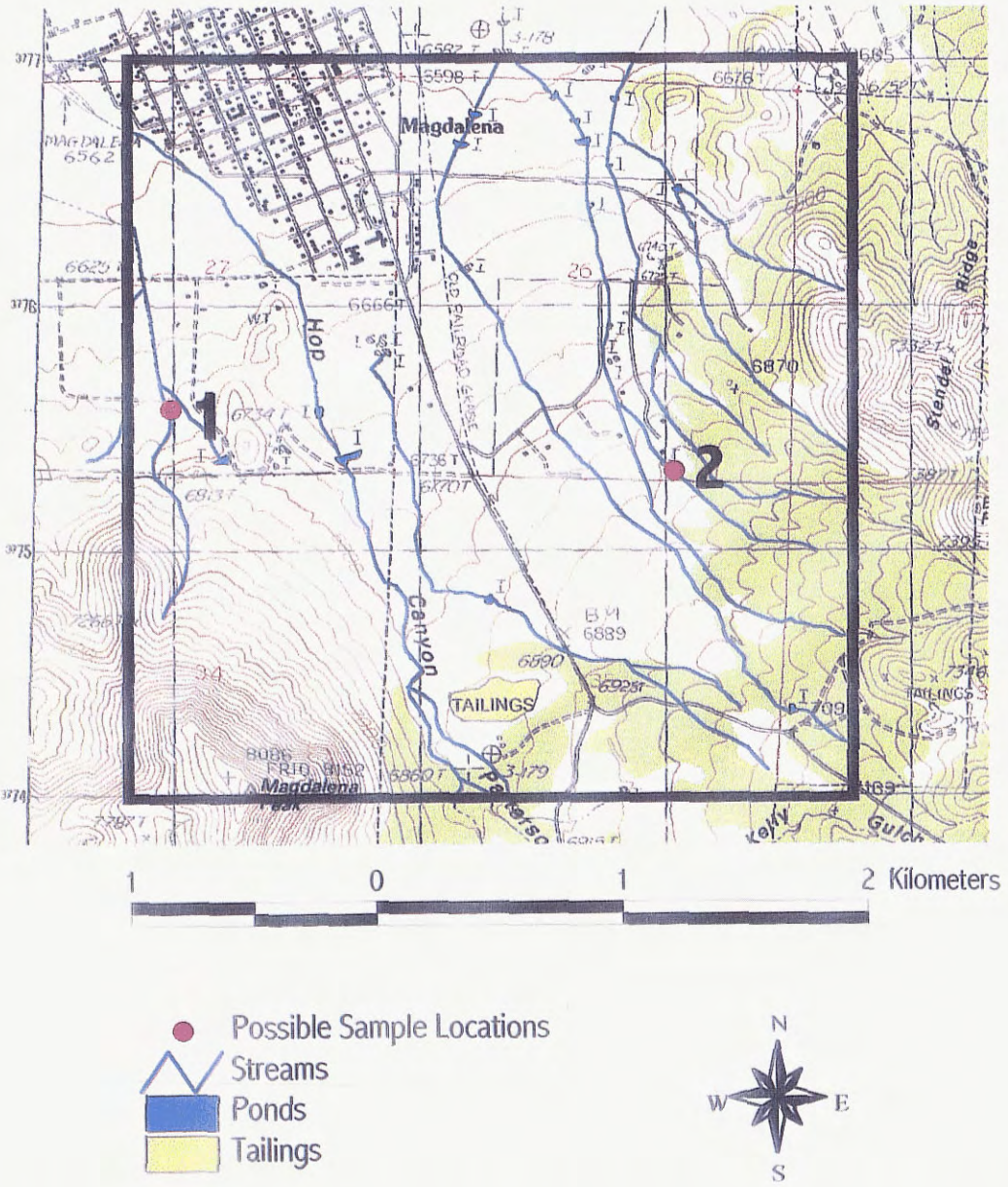

Figure 5. This figure shows two possible sample site locations. Note that the streams have their origins within the cell and are upstream of any sources of contamination (e.g. roads, tailings piles, and ponds).

Figure 6. Sampling equipment used as part of this study.

contamination were recorded on a standardized form (Fig. 7). Figure 8 shows the locations of the 254 samples collected for the study.

SAMPLE PREPARATION AND CHEMICAL ANALYSIS

Sieved samples were allowed to air dry at room temperature. Once dry, they were split using a stainless steel microsplitter with approximately 30 g being placed in plastic sampling vials. The remaining material was stored for possible future analysis. The samples were then ground to a fine powder, approximately –200 mesh, in a tungsten carbide swing mill. Tungsten carbide swing mills have been known to contaminate samples with tungsten and cobalt. Because neither of these elements were determined as part of this project the contamination can be ignored. Pressed powders and fusion disks were created following the methods described in Appendix B.

Wavelength dispersive x-ray fluorescence (WD-XRF) spectrometry was used to determine major and trace element concentrations of the samples. Major elements (SiO_2, TiO_2, Al_2O_3, Fe_2O_3, MnO, MgO, CaO, Na_2O, K_2O, and P_2O_5) were determined on fused glass disks. Trace elements (As, Ba, Cr, Cu, Ga, Mo, Nb, Ni, Pb, Rb, Sr, Th, U, V, Y, Zn, and Zr) plus Fe_2O_3, K_2O, MnO, and TiO_2 were determined on pressed powders (Fig. 9). The determination of K_2O on pressed powders required a conversion detailed in Appendix C. Analyses were made using a Philips model PW2400 WD-XRF spectrometer at the New Mexico Institute of Mining and Technology. An end window Rh-tube was used to excite the sample and fluorescent x-rays were detected using the spectrometer conditions shown in Table 1. Spectral analysis was done on an interfaced Gateway P5-66 computer using programs provided by Philips.

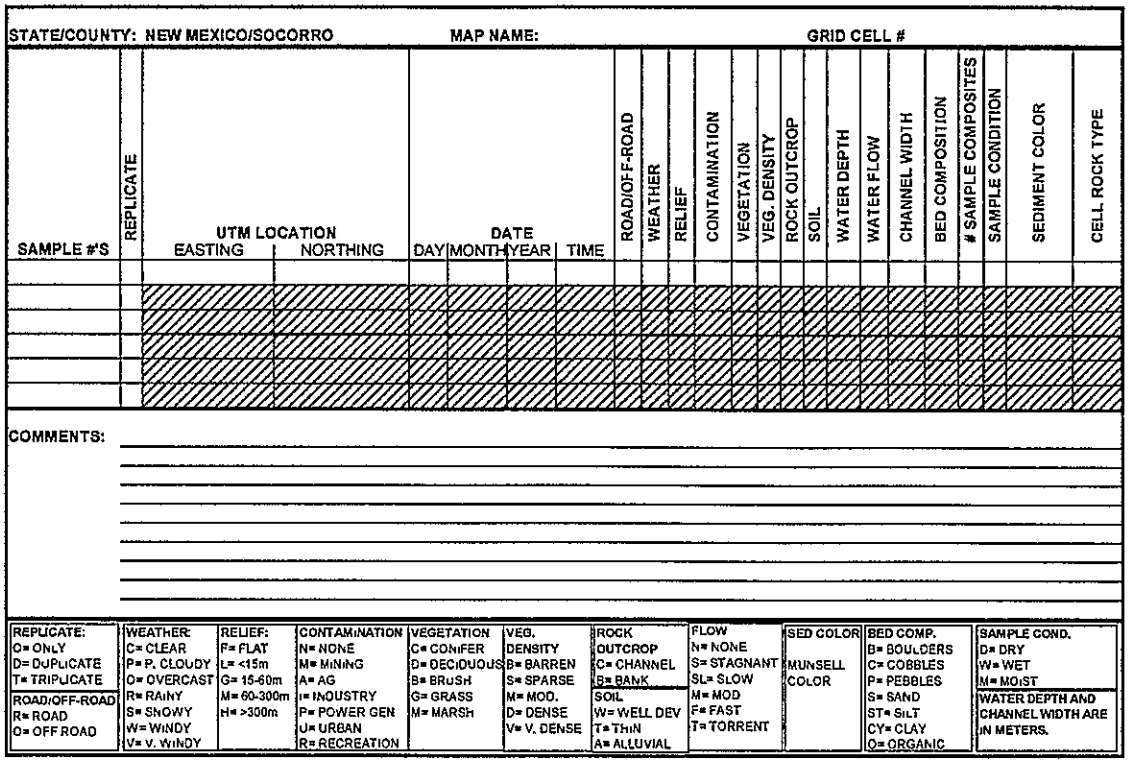

STATE/COUNTY: NEW MEXICO/SOCORRO MAP NAME: GRID CELL #

SAMPLE #'S	REPLICATE	UTM LOCATION EASTING	UTM LOCATION NORTHING	DATE DAY	DATE MONTH	DATE YEAR	TIME	ROAD/OFF-ROAD	WEATHER	RELIEF	CONTAMINATION	VEGETATION	VEG. DENSITY	ROCK OUTCROP	SOIL	WATER DEPTH	WATER FLOW	CHANNEL WIDTH	BED COMPOSITION	# SAMPLE COMPOSITES	SAMPLE CONDITION	SEDIMENT COLOR	CELL ROCK TYPE

COMMENTS:

REPLICATE:	WEATHER:	RELIEF:	CONTAMINATION	VEGETATION	VEG.	ROCK	FLOW	SED COLOR	BED COMP.	SAMPLE COND.
O= ONLY	C= CLEAR	F= FLAT	N= NONE	C= CONIFER	DENSITY	OUTCROP	N= NONE		B= BOULDERS	D= DRY
D= DUPLICATE	P= P. CLOUDY	L= <15m	M= MINING	D= DECIDUOUS	B= BARREN	C= CHANNEL	S= STAGNANT	MUNSELL	C= COBBLES	W= WET
T= TRIPLICATE	O= OVERCAST	G= 15-60m	A= AG	B= BRUSH	S= SPARSE	B= BANK	SL= SLOW	COLOR	P= PEBBLES	M= MOIST
ROAD/OFF-ROAD	R= RAINY	M= 60-300m	I= INDUSTRY	G= GRASS	M= MOD.	SOIL	M= MOD		S= SAND	WATER DEPTH AND
R= ROAD	S= SNOWY	H= >300m	P= POWER GEN	M= MARSH	D= DENSE	W= WELL DEV	F= FAST		ST= SILT	CHANNEL WIDTH ARE
O= OFF ROAD	W= WINDY		U= URBAN		V= V. DENSE	T= THIN	T= TORRENT		CY= CLAY	IN METERS.
	V= V. WINDY		R= RECREATION			A= ALLUVIAL			O= ORGANIC	

Figure 7. Stream sediment data form used in the study.

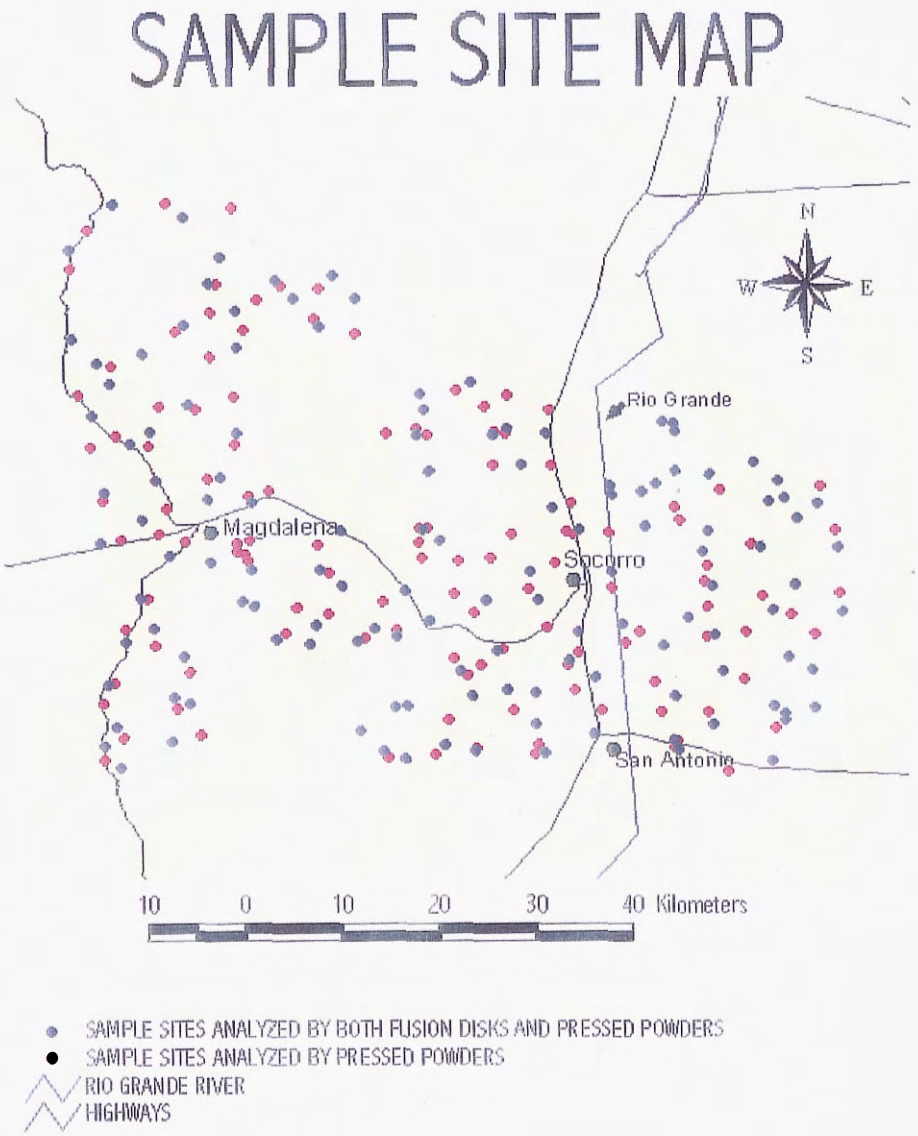

Figure 8. Location map of sample sites.

Analyzed by Fusion Disks

Analyzed by Pressed Powders

Analyzed by both Fusion Disks and Pressed Powders

Figure 9. Elements determined and method of determination.

TABLE 1. ANALYTICAL SETTINGS.

ELEMENT	LINE	kV	mA	CRYSTAL	ANGLE	COUNT TIME (s)	BKGRND. COUNT TIME (s)
SiO2	KA	30	100	PE_C	108.9953	20	
TiO2	KA	35	85	LIF200	86.1608	20	
TiO2*	KA	40	75	LIF200	86.1893	10	8
Al2O3	KA	30	100	PE_C	144.7941	20	
Fe2O3	KA	45	66	LIF200	57.4959	12	
Fe2O3*	KA	40	75	LIF200	57.4965	10	4
MnO	KA	45	66	LIF200	62.9634	12	
MnO*	KA	40	75	LIF200	62.9595	10	8
MgO	KA	30	100	PX1	23.1038	30	
CaO	KA	35	85	LIF200	113.1244	12	
Na2O	KA	30	100	PX1	27.9053	60	
K2O	KA	30	100	LIF200	136.7067	16	
K2O*	KA	40	75	LIF200	136.7076	10	8
P2O5	KA	30	100	Ge	141.0014	20	
As*	KA	60	50	LIF220	48.7583	60	50
Ba*	LA	60	50	LIF200	87.2005	100	40
Cr*	KA	60	50	LIF200	69.3454	50	20
Cu*	KA	60	50	LIF200	44.9783	40	20
Ga*	KA	60	50	LIF200	38.8926	40	20
Mo*	KA	60	50	LIF220	28.8399	60	10
Nb*	KA	60	50	LIF220	30.3704	60	20
Ni*	KA	60	50	LIF200	44.9430	40	20
Pb*	LB	60	50	LIF200	28.2296	60	40
Rb*	KA	60	50	LIF200	26.5872	30	40
Sr*	KA	60	50	LIF200	25.1101	30	30
Th*	LA	60	50	LIF200	27.4052	50	40
U*	LA	60	50	LIF220	37.2723	100	60
V*	KA	60	50	LIF220	123.1981	40	32
Y*	KA	60	50	LIF220	33.8330	50	20
Zn*	KA	60	50	LIF200	41.7562	40	20
Zr*	KA	60	50	LIF220	32.0208	50	20

* Settings for Pressed Powders

Table 1. Analytical settings of the WD-XRF spectrometer in the study.

QUALITY CONTROL

PROCEDURES

Quality control was an important aspect of this project throughout the sampling and analytical process. The two variables monitored in a quality control program are precision and accuracy. Precision is the ability to obtain the same result repeatedly, while accuracy is the proximity of a result to its true value. Regional geochemical mapping measures the natural variation of element abundances within the environment and therefore determination of relative abundances is more important than the absolute concentrations. This makes the precision of the data more important than its accuracy (Fletcher, 1981). Quality of the data was monitored with the use of an unbalanced two-level sampling design, as well as the use of both local and international standard reference materials.

An unbalanced two-level sampling design was employed on every 30^{th} site during the sampling process. Figure 10 shows a schematic of this sampling strategy. This strategy began with one sample site where two samples are collected in the normal manner. The second sample was collected from different locations within the stream. The first composite sample collected was later split into A and B for duplicate analysis. In this approach you obtain three samples for analysis from the same stream. Samples A and B allow monitoring of analytical variation while a comparison with sample C provides details about the natural within-stream variability (Darnley et al., 1995).

Both local in-house comparative standards and international standard reference materials (SRM's) were used in this project. Local in-house standards were collected from the Arroyo de la Parida and San Lorenzo Arroyo, both of which are located within

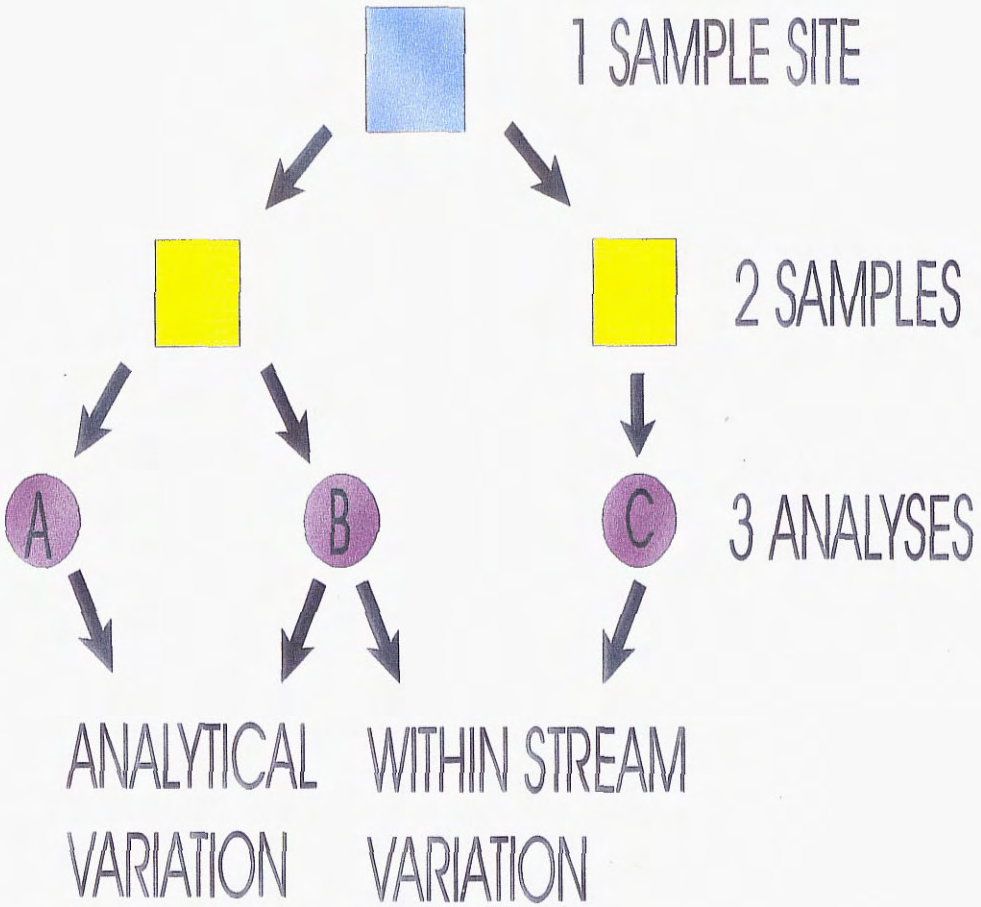

Figure 10. This schematic shows the sampling strategy used in the unbalanced two-level design. The analysis of samples A and B indicate the analytical variation while a comparison with sample C provides information regarding within-stream variation (after Darnley et al., 1995).

the study area. The in-house standards were collected and prepared in the same manner as the other samples for this study. Ten pressed powders were created from each of these samples. The two in-house standards were analyzed with every load of samples to monitor analytical precision. International reference materials were also analyzed for quality control. Descriptions of the standard reference materials are located in Appendix D. The primary standard reference material for this project was the National Institute of Standards and Technology SRM 2704 Buffalo River sediment, which was also analyzed with every load of samples. Other international SRM's that were analyzed as part of this project include stream sediments from the Geological Survey of Japan (Jsd-1, Jsd-2, and Jsd-3) and the Canadian Center for Mineral and Energy Technology (STSD-3, and STSD-4). The international SRM's were used to monitor analytical precision as well as the accuracy of the data.

RESULTS

Results from the quality control process indicate that the data from the project are both precise and accurate (Appendix D). Results from the two-level unbalanced sampling design indicate that there was little analytical or within-stream variation (Table 2). The largest variation shows up in the elements that are found in resistant minerals, such as zirconium. The low analytical variation means the spectrometer was working properly providing precise data. The low values found in within-stream variation indicate that the sampling process used was sufficient to provide an accurate chemical signature for the sample sites. Table 3 shows the results from the two in-house comparative standards. The low percent differences indicate the high precision of the data in this project. The highest differences occur in elements that are very near their lower limit of detection.

TABLE 2. UNBALANCED TWO-LEVEL DESIGN FOR SOC96030.

SAMPLE	SOC96030 A	SOC96030 B	SOC96030 C	MEAN OF A+B	ANALYTICAL VARIATION	WITHIN STREAM VARIATION
Fe2O3 (%)*	4.60	4.60	4.90	4.60	0.0	0.2
MnO (%)*	0.07	0.07	0.07	0.07	0.0	0.0
TiO2 (%)*	0.60	0.60	0.60	0.60	0.0	0.0
As (ppm)*	6	5	6	6	0.7	0.4
Ba (ppm)*	448	443	461	446	3.5	11.0
Cr (ppm)*	70	73	70	72	2.1	1.1
Cu (ppm)*	13	14	14	14	0.7	0.4
Ga (ppm)*	14	14	14	14	0.0	0.0
Mo (ppm)*	0	0	2	0	0.0	1.4
Nb (ppm)*	11	12	12	12	0.7	0.4
Ni (ppm)*	27	27	26	27	0.0	0.7
Pb (ppm)*	13	14	14	14	0.7	0.4
Rb (ppm)*	91	90	90	91	0.7	0.4
Sr (ppm)*	216	216	213	216	0.0	2.1
Th (ppm)*	8	7	10	8	0.7	1.8
U (ppm)*	3	3	3	3	0.0	0.0
V (ppm)*	81	76	81	79	3.5	1.8
Y (ppm)*	28	27	28	28	0.7	0.4
Zn (ppm)*	44	43	44	44	0.7	0.4
Zr (ppm)*	349	345	384	347	2.8	26.2
* Elements determined by Pressed Powders						

TABLE 2. This table shows the results of the unbalanced two-level sampling design for sample number SOC96030. The analytical variation is the mean deviation between samples A & B. The lack of analytical variation expresses the precision of the data obtained for this project. The within-stream variation is the mean deviation of sample C and the mean of A+B. The lack of within-stream variation expresses the quality of the sampling method used.

TABLE 3. IN-HOUSE COMPARATIVE STANDARDS						
	SOC96SRM1			SOC96SRM2		
		n= 23			n= 21	
	MEAN	STD DEV	C.V.	MEAN	STD DEV	C.V.
SiO2 (%)	70.62	0.1	0.1	61.49	0.1	0.1
Al2O3 (%)	7.40	0.0	0.2	12.93	0.0	0.2
CaO (%)	5.68	0.0	0.1	5.89	0.0	0.1
Fe2O3 (%)	2.89	0.0	0.0	5.28	0.0	0.1
Fe2O3* (%)	2.85	0.0	0.4	5.07	0.0	0.7
MgO (%)	1.67	0.0	0.3	1.66	0.0	0.4
K2O (%)	1.65	0.0	0.3	3.06	0.0	0.2
Na2O (%)	1.14	0.0	0.4	2.66	0.0	0.2
TiO2 (%)	0.51	0.0	0.2	0.86	0.0	0.1
TiO2* (%)	0.48	0.0	1.0	0.82	0.0	1.0
P2O5 (%)	0.09	0.0	0.8	0.20	0.0	1.0
MnO (%)	0.05	0.0	1.2	0.09	0.0	0.9
MnO* (%)	0.05	0.0	1.0	0.09	0.0	1.5
As (ppm)*	4	0.5	11.3	7	0.5	7.2
Ba (ppm)*	688	5.0	0.7	911	8.4	0.9
Cr (ppm)*	51	1.5	2.9	144	5.6	3.9
Cu (ppm)*	12	0.6	4.8	22	0.6	2.6
Ga (ppm)*	9	0.4	4.2	16	0.4	2.6
Mo (ppm)*						
Nb (ppm)*	8	0.5	6.9	12	0.7	5.5
Ni (ppm)*	15	0.4	2.9	34	0.6	1.8
Pb (ppm)*	13	0.5	4.1	18	0.8	4.4
Rb (ppm)*	60	0.6	0.9	137	0.6	0.5
Sr (ppm)*	207	0.7	0.3	615	1.8	0.3
Th (ppm)*	5	0.6	12.5	9	0.7	8.3
U (ppm)*	2	0.4	14.9	3	0.4	14.8
V (ppm)*	53	1.7	3.1	113	2.6	2.3
Y (ppm)*	21	0.6	2.7	29	0.6	1.9
Zn (ppm)*	35	0.4	1.1	62	0.4	0.6
Zr (ppm)*	428	4.1	1.0	297	5.3	1.8
C.V. = (Std Dev. / Mean) *100						
*Elements Determined by Pressed Powders,Others by Fusion Disk						

TABLE 3. This table shows the analytical variation for the two in-house comparative standards that were used in this project. The lack of variation is the result of the high precision of the XRF instrument. The largest variation occurs in elements very near their lower limit of detection.

Table 4 shows the results of the primary standard reference material for this project, SRM 2704. Once again the low standard deviations from this work indicate the spectrometer was providing precise data. Nearly all elements have means that overlap within standard deviations of the certified values for this reference material. This indicates the high accuracy of the data from this project. The element with the most difference is chromium. However, when looking at the chromium results from the other international standard reference materials, the means remain near the certified values until concentrations exceed 100 ppm.

DATA AND IMAGE PROCESSING

Data and image processing was performed on a personal computer. All of the field and analytical data for this project were stored in a Microsoft Access database. The database allowed for rapid querying, sorting, and analysis of the large amount of data that was collected. The database was then imported into a geographic information system (GIS), ArcView, for image processing. The GIS allowed for spatial analysis of the data with the result being a series of color contour plots of elemental concentrations within the study area. Contouring was performed using the inverse distance weighted method. In this method it is assumed that the variable being mapped has an influence that diminishes with distance from the sampling point (ESRI, 1996). Class intervals were broken down by percentiles. In general the percentiles used were 99, 98, 95, 90, 75, 50, 25, 15, and 5. Fewer class intervals were used when much of the data was below the lower limit of detection. Color choice for class intervals was based on a cold to hot trend with

TABLE 4. NIST SRM 2704.

	THIS WORK		REF. 1	
	n=18	n=21*		
	MEAN	Std. Dev.	MEAN	Std Dev.
SiO2 (%)	61.33	0.1	62.12	0.28
Al2O3 (%)	11.54	0.0	11.545	0.3
Fe2O3 (%)	5.71	0.0	5.876	0.14
Fe2O3* (%)	5.95	0.0		
CaO (%)	3.62	0.0	3.638	0.04
K2O (%)	2.37	0.0	2.409	0.05
MgO (%)	2.00	0.0	1.99	0.03
Na2O (%)	0.90	0.1	0.737	0.02
TiO2 (%)	0.74	0.0	0.762	0.03
TiO2* (%)	0.75	0.0		
P2O5 (%)	0.22	0.0	0.229	0.006
MnO (%)	0.07	0.0	0.072	0.007
MnO* (%)	0.08	0.0		
As (ppm)*	20	0.5	23.4	0.8
Ba (ppm)*	416	5.5	414	12
Cr (ppm)*	172	4.6	135	5
Cu (ppm)*	94	3.4	98.6	5
Ga (ppm)*	16	0.4	15	
Ni (ppm)*	44	0.7	44.1	3
Pb (ppm)*	160	1.4	161	17
Rb (ppm)*	101	0.6	100**	
Sr (ppm)*	131	0.6	130**	
Th (ppm)*	8	1.0	9.2**	
U (ppm)*	3	0.5	3.13	0.13
V (ppm)*	104	2.3	95	4
Zn (ppm)*	429	2.0	438	12
Zr (ppm)*	277	4.7	300**	
*Elements Determined by Pressed Powders				
** Noncertified values				

TABLE 4. This table shows the results of primary standard reference material NIST SRM 2704 compared to the reference values of Reed (1990). Nearly all elements overlap the certified values with the major exception being chromium. The lack of variation between this work and the referenced values expresses the accuracy of the data.

increasing elemental concentration. Both Microsoft Excel and WinStat were used for statistical analysis of the data. Excel was used to perform basic statistical analysis of the data including the determination of means and standard deviations. Excel was also used to create frequency distribution diagrams for the elements. WinStat was used to determine correlation coefficients for the elements.

DATA

INTRODUCTION

In this section the data is displayed for each element in alphabetical order. The discussion of each element begins with a brief overview of the geochemistry of that element along with any possible adverse health effects associated with the element. A table that shows the concentrations of the element in some typical rocks and soils follows. The table is then followed by a discussion and map of the distribution of the element within the study area. Included with the color contour maps is a statistical table describing the number of observations, maximum, minimum, mean, median, and standard deviation of the element as well as a frequency distribution diagram for the element. Included within the tables is the Clarke value for the element. The Clarke value was derived to act as a global datum in geochemical mapping. The Clarke value has been chosen as the average crustal abundance for the element (Fortescue, 1992). Unfortunately this number varies from author to author depending on their method of calculation.

ALUMINUM OXIDE

Geochemistry

The Al^{3+} valence state is the only stable state of aluminum in natural systems. Aluminum exhibits solid solutions with a large number of cations (Wedepohl, 1978). Aluminum may undergo isomorphous substitution for silicon (O'Neill, 1985). The solubility of aluminum during weathering is typically low. Sediments with high aluminum concentrations probably contain relatively unaltered detrital material containing alumino-silicate minerals. Aluminum in sediments is also present in clay minerals produced during the weathering of the original rock (Wedepohl, 1978). Table 5 shows the concentrations of aluminum oxide in some typical rocks.

Table 5 Aluminum Oxide (Al2O3%)

	Fortescue (1992)	Rose, Hawkes, and Webb (1991)	Wedepohl (1978)	Taylor and McLennan (1985)
Clarke	15.0			15.9
Ultramafic				
mafic				
granitic			13.86	
basalt			15.19	
andesite			17.26	
rhyolite			13.04	
sandstone			4.78	
limestone			0.81	
shale			15.47	
soils				
ores				

Data

Concentrations of aluminum oxide within the study area range from 5.33 to 16.62 % with a mean of 11.04 % (Fig. 11). This value is well below the Clarke value cited by Taylor and McLennan (1985) of 15.9 %. The lower mean, in the study area, is

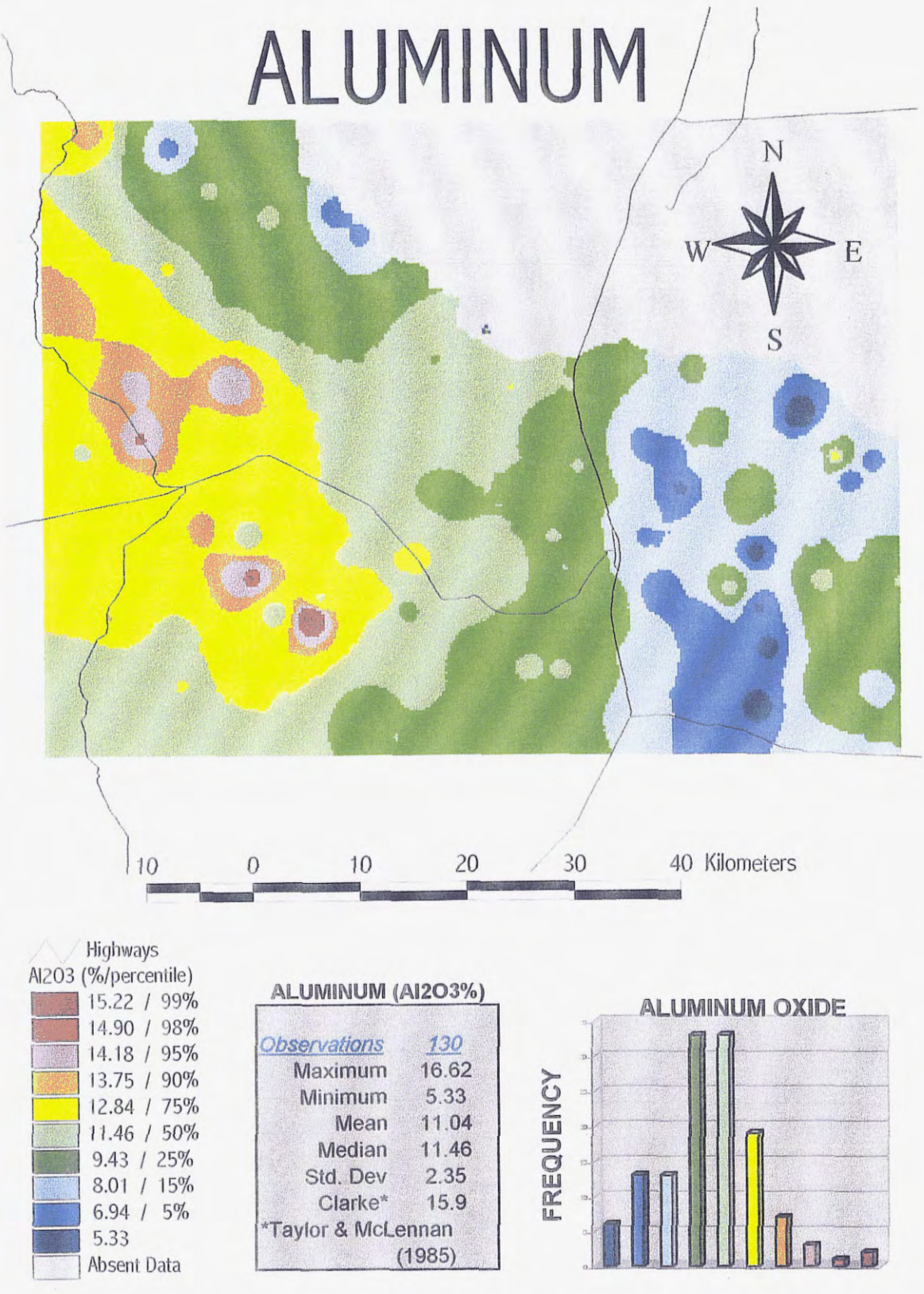

Figure 11. Aluminum oxide distribution within the study area.

likely a result of the large amount of rhyolites and sedimentary rocks within the study area and the arid to semi-arid climate.

Aluminum concentrations across the Paleozoic sedimentary rocks east of the Rio Grande and Cretaceous sedimentary rocks in the northwest region of the study area typically range from 5.33 to 11.46 %. These values are slightly higher than referenced values cited by Wedepohl (1978) for sedimentary rocks. The Tertiary rhyolites and basaltic andesites have aluminum concentrations that range from 9.43 to 16.62 %. Slightly higher overall concentrations occur on the western margin of the study area that is dominated by Tertiary basaltic andesites. This is consistent with the referenced values for igneous rocks cited by Wedepohl (1978).

ARSENIC

Geochemistry

Arsenic is a chalcophile element commonly associated with U, Sn, Bi, Mo, P, and F (Rose et al., 1979). There is a strong relationship between arsenic and gold and therefore As is commonly used as a pathfinder for Au, Ag, and the PGE's. As^{3+} substitutes for Si^{4+}, Al^{3+}, Fe^{3+}, and Ti^{4+} in silicates and As^{5+} substitutes for P^{5+} in phosphates (Wedepohl, 1978; and BGS, 1992). Arsenopyrite (FeAsS) is the most abundant arsenic mineral (Wedepohl, 1978). Hydrothermal alteration commonly results in an increase in arsenic concentrations. During weathering arsenic is concentrated in the clay size fraction. In stream sediments arsenic occurs mainly as As_2O_3, As_2O_5, and as sulfides FeAsS and As_2S_3 (BGS, 1992). Table 6 shows the concentrations of arsenic in some typical rocks and soils.

Arsenic was chosen as the number one hazardous substance for 1997 by the Agency for Toxic Substances and Disease Registry and the Environmental Protection Agency (ATSDR, 1997). Intake of high concentrations of arsenic can be fatal. At high concentrations, arsenic is known to damage tissues including nerves, stomach, intestines, and skin. At lower exposure levels arsenic may cause nausea, vomiting, diarrhea, decreased production of blood cells, abnormal heart rhythms, and blood vessel damage. Arsenic is also a known carcinogen. Because of the known health risks, the EPA has set a limit of 0.05 ppm for arsenic in drinking water (ATSDR, 1993a).

Table 6 Arsenic (ppm)

	Fortescue (1992)	Rose, Hawkes, and Webb (1979)	Wedepohl (1978)	Taylor and McLennan (1985)
Clarke	1.8			1.0
Ultramafic		1.0		
mafic		1.5		
granitic		2.1	1.5	
basalt			1.5	
andesite			2.8	
rhyolite			3.5	
sandstone		1.2	1.0	
limestone		1.1	1.0	
shale		12.0	13.0	
soils		7.5	5-10	
ores			280-700	

Data

Arsenic concentrations within the study area range from less than 4 ppm to a maximum of 253 ppm (Fig. 12). The mean of 8 ppm is greater than the 1-2 ppm range cited for the Clarke value (Table 6). However, it is very near the value cited for average soils (Rose et al., 1979; Wedepohl, 1978). This may be due to the enrichment of arsenic in the clay size fraction during the weathering process.

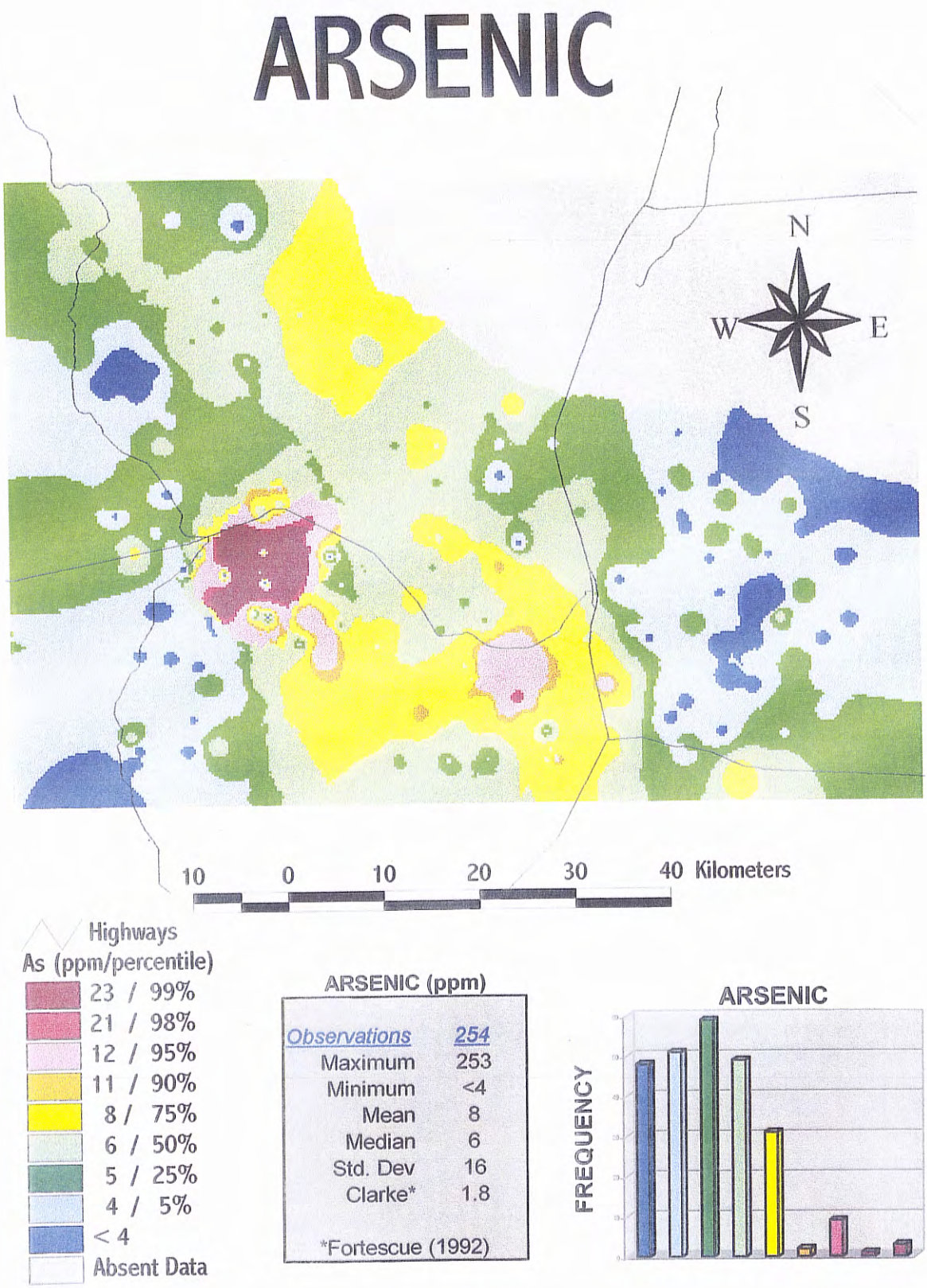

Figure 12. Arsenic distribution within the study area.

Arsenic concentrations across the Paleozoic sedimentary rocks east of the Rio Grande, Cretaceous sedimentary rocks in the northwest region of the study area, and Tertiary and Quaternary deposits in the southwest region, are typically less than 5 ppm. This is in good agreement with the reported values for both sandstones and limestones (Rose et al., 1979; Wedepohl, 1978).

Arsenic concentrations across the Tertiary rhyolites as well as the Quaternary piedmont-slope deposits in the La Jencia Basin are between 5 and 11 ppm. This is in agreement with the reported value for rhyolites, assuming an increase in concentration in the fine-grained sediment fraction related to weathering (Wedepohl, 1978). The Tertiary basaltic andesites located on the western margin of the study area have As concentrations of less than 5 ppm which is typical of basalts (Wedepohl, 1978).

Anomalously high arsenic concentrations occur in the northern Magdalena Mountains as well as the northern Chupadera Mountains. In the Magdalena Mountains, the arsenic anomaly coincides with the Magdalena mining district. Within this district, the maximum arsenic concentration is 253 ppm. In the Chupadera Mountains, the arsenic anomaly coincides with the Luiz Lopez mining district. The maximum concentration of As in this region is 24 ppm.

BARIUM

Geochemistry

Barium is a lithophile element (Rose et al., 1979). In igneous rocks barium occurs predominantly in potassium feldspars due to the substitution of Ba^{2+} for K^{+}. The Ba^{2+} ion may also substitute for Ca^{2+} in plagioclase, pyroxenes, and amphiboles (BGS,

1992). The barium content within igneous rocks typically increases with increasing SiO_2 concentration (Wedepohl, 1978). Barium concentrations within metamorphic rocks show wide variations even within individual rock types. Carbonatites commonly contain high concentrations of Ba. The average concentration of Ba in carbonatites is 3520 ppm (Wedepohl, 1978). Barite is the most common economic mineral of barium. High oxidation-potential fluids in the presence of sulfate result in the formation of barite. Barium is enriched in the silt and clay size fractions during weathering (Wedepohl, 1978). In stream sediments, barium occurs mainly in detrital feldspars, micas, and barite. Barium may also precipitate with manganese to form authigenic psilomelane (BGS, 1992). Table 7 shows the concentrations of barium in some typical rocks and soils.

Barium compounds that dissolve in water may be harmful to people. The intake of high levels of barium may result in difficulties breathing, increased blood pressure, changes in heart rhythms, stomach irritation, brain swelling, muscle weakness, and damage to vital organs. Because of the health risks of barium, the EPA has set a limit of 2 ppm of barium in drinking water (ATSDR, 1995a).

Table 7 Barium (ppm)

	Fortescue (1992)	Rose, Hawkes, and Webb (1979)	Wedepohl (1978)	Taylor and McLennan (1985)
Clarke	390.0			250.0
Ultramafic		0.4		
mafic		330.0		
granitic		840.0	732.0	
basalt			253.0	
andesite			703.0	
rhyolite			1127.0	
sandstone		170.0	316.0	
limestone		92.0	90.0	
shale		550.0	546.0	
soils		300.0	100-3000	

Data

Barium concentrations within the study area range from 319 to 2789 ppm (Fig. 13). The mean of 756 ppm is much larger than the referenced Clarke values of 390 and 250 ppm (Table 7). There are several potential reasons for this. The first is that barium is enriched in the silt and clay size fraction during weathering. Wedepohl (1978) reports values up to 3000 ppm of barium in soils. Another explanation is due to the large amount of barite that is found within the study area. This has the effect of raising the barium concentrations over rocks that usually contain low concentrations. The large amount of rhyolites within the study area may also result in a higher than normal mean for barium.

Barium concentrations across the Paleozoic sedimentary rocks east of the Rio Grande, Cretaceous rocks in the northwest region of the study area, and Tertiary and Quaternary sedimentary deposits in the southwest region range from 319 to 621 ppm. These numbers are in fair agreement with Wedepohl's (1978) value for sandstone of

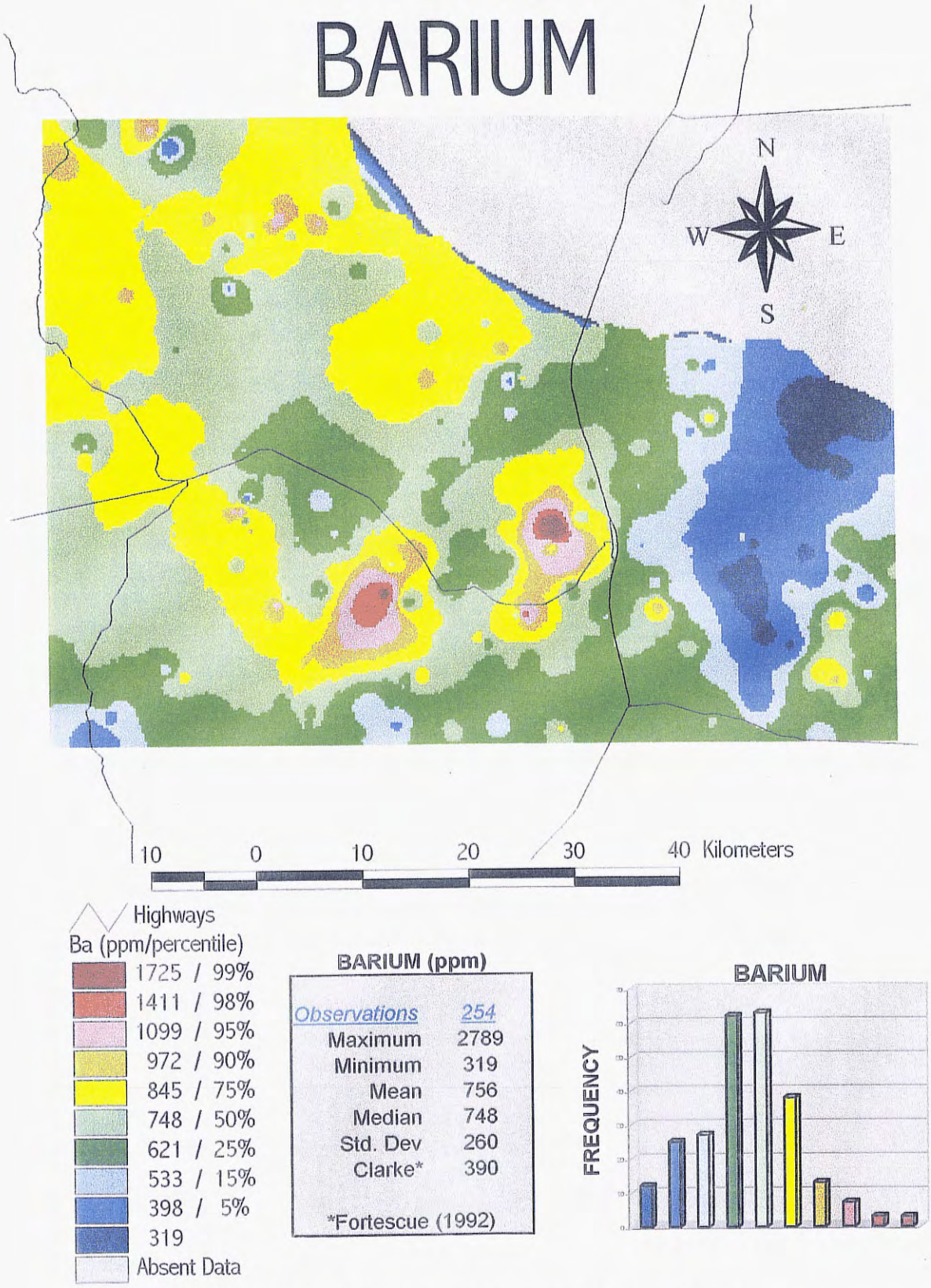

Figure 13. Barium distribution within the study area.

316 ppm. As mentioned previously these values may be slightly elevated due to the presence of barite deposits within the study area.

The Tertiary basaltic andesites as well as rhyolites, generally range from 621 to 1099 ppm barium. The Quaternary piedmont-slope deposits of the La Jencia Basin also fall within this range. The values for the basaltic andesites match the reported value for andesites of Wedepohl (1978) fairly well. However, the rhyolites in this area have lower barium concentrations than the reported mean, for rhyolites, of 1127 ppm (Wedepohl, 1978).

Anomalously high concentrations of barium occur in South Canyon (1719-1887 ppm), approximately 12.5 km east of South Canyon (1538 ppm), and on Socorro Peak (2789 ppm). The Socorro Peak anomaly coincides with the Socorro Peak mining district that is known to contain barite veins (North, 1983).

CALCIUM OXIDE

Geochemistry

Calcium is a major constituent of many minerals. Important magmatic calcium minerals include plagioclase feldspar, pyroxenes, and amphiboles. The most important calcium minerals at low temperatures include calcite, aragonite, anhydrite, gypsum, and dolomite. In sediments and sedimentary rocks calcium is generally present as either limestone or dolostone (Wedepohl, 1978). Table 8 shows calcium concentrations for some typical rocks.

Table 8 Calcium Oxide (CaO%)

	Fortescue (1992)	Rose, Hawkes, and Webb (1991)	Wedepohl (1978)	Taylor and McLennan (1985)
Clarke	7.20			7.40
Ultramafic				
mafic				
granitic			0.72	
basalt			12.42	
andesite			7.92	
rhyolite			0.61	
sandstone			5.47	
limestone			42.29	
shale			3.09	
soils				
ores				

Data

Calcium oxide concentrations within the study area range from 0.81 to 17.07 % with a mean of 4.08 % (Fig. 14). The mean of 4.08 % is lower than the cited Clarke value of Taylor and McLennan (1985). This is likely the result of the abundance of rhyolites within the study area.

The lowest concentrations of calcium oxide occur across the southern Magdalena Mountains where Tertiary rhyolites dominate. Calcium oxide concentrations in this region range from 0.81 to 3.82 %. These values are slightly higher than, but consistent with the reported average for rhyolites of 0.61 % (Wedepohl, 1978). In other areas dominated by Tertiary rhyolites and basaltic andesites, calcium oxide concentrations range from 2.79 to 5.22 %.

Calcium oxide concentrations across the Paleozoic sedimentary rocks east of the Rio Grande typically range from 5.22 to 8.27 %. These values are again consistent with

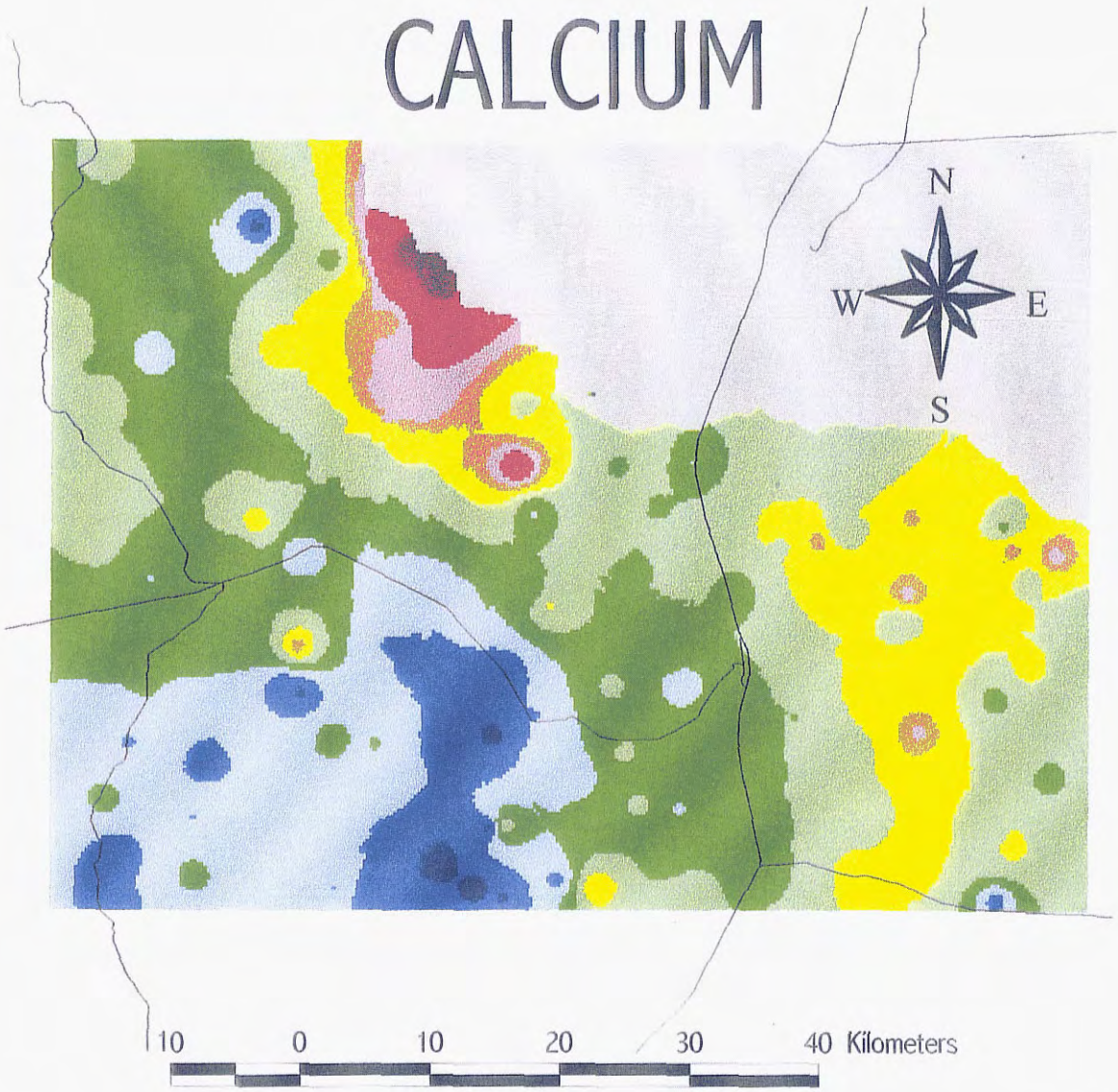

Figure 14. Calcium oxide distribution within the study area.

the value cited for sandstones of 5.47 % (Wedepohl, 1978). The highest concentrations of calcium oxide within the study area occur in the north-central region. Calcium oxide concentrations typically range from 5.22 to 17.07 % in this region. This is likely the result of both the presence of limestones and the large quantity of Ca-salts that occur in the Rio Salado and may be transported throughout the local area by wind.

CHROMIUM

Geochemistry

Chromium is a lithophile element that has a strong association with nickel and magnesium in ultramafic rocks (Rose et al., 1979). Chromium occurs in both hexavalent and trivalent states. Cr^{3+} replaces other elements, preferably aluminum, in a number of minerals (Wedepohl, 1978). Early in crystal fractionation Cr^{3+} is partitioned into spinels and pyroxenes (BGS, 1992). Sedimentary rocks contain chromium primarily in detrital phases such as chromite, magnetite, and ilmenite (BGS, 1992). Chromite is the only economic mineral of chromium. During weathering processes, chromium behaves similarly to iron and aluminum and is concentrated in the clay size fraction (Wedepohl, 1978). Table 9 shows the concentrations of chromium in some typical rocks and soils.

Table 9 Chromium (ppm)

	Fortescue (1992)	Rose, Hawkes, and Webb (1979)	Wedepohl (1978)	Taylor and McLennan (1985)
Clarke	122.0			185.0
Ultramafic		2980.0		
mafic		170.0		
granitic		4.1	10.0	
basalt			191.0	
andesite			55.0	
rhyolite			4.0	
sandstone		35.0	27.0	
limestone		11.0	1.2-16	
shale		90.0	83.0	
soils		43.0	37.0	
ores				

Data

Chromium concentrations within the study area range from 31 to 451 ppm (Fig. 15). The mean of 97 ppm is lower than the referenced Clarke values of 122 and 185 ppm (Table 9). The difference between the mean and Clarke values is likely due to the low abundance of ultramafic and mafic rocks within the study area.

Chromium ranges from 31 to 110 ppm across much of the study area. The low concentrations of chromium are a reflection of the low concentrations of chromium present in sedimentary and rhyolitic rocks (Wedepohl, 1978). Chromium concentrations in the northwest region of the study area range from 110 to 451 ppm. This is a reflection of the Tertiary basaltic andesites that occur in this region. These basalts outcrop elsewhere within the study area and are generally seen as individual contours within the 110 to 177 ppm range.

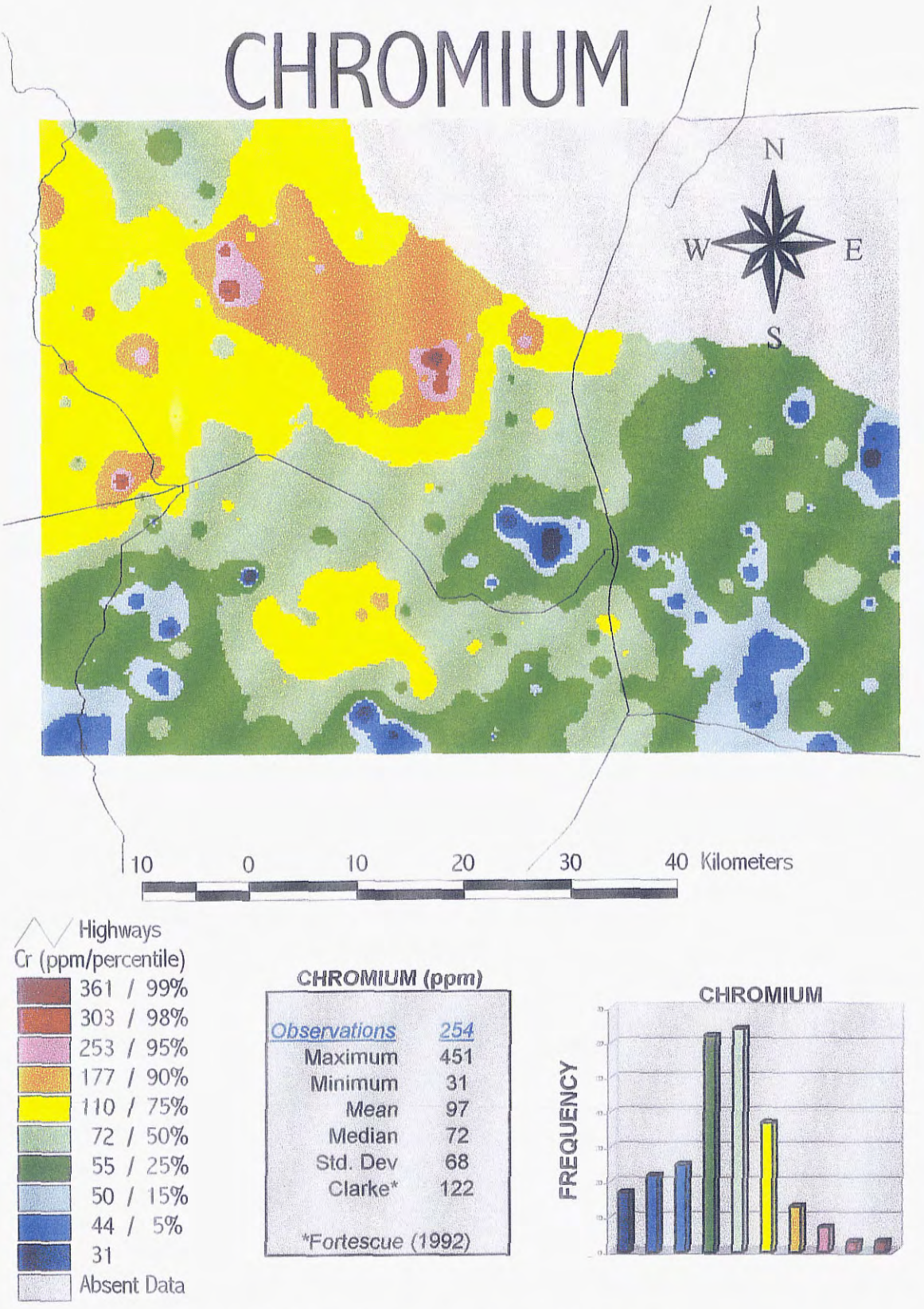

Figure 15. Chromium distribution within the study area.

COPPER

Geochemistry

Copper is a chalcophile element associated with Pb, Zn, Mo, Ag, Au, Sb, Se, Ni, Pt, and As in sulfide deposits (Rose et al., 1979). In nature copper occurs in three valence states Cu, Cu^{+}, and Cu^{2+} (Wedepohl, 1978). Cu^{+} is primarily concentrated in the early products of magmatic processes and tends not to be incorporated into silicates. Chalcopyrite ($CuFeS_s$) is a common accessory mineral in basic igneous rocks (BGS, 1992). During low-grade metamorphism copper can be redistributed but at higher grades copper becomes less mobile. During hydrothermal mineralization copper is concentrated within sulfide minerals (BGS, 1992). In stream sediments, copper is generally transported as detrital silicates except in mineralized areas where the sediments may contain copper sulfates, arsenates, oxides, carbonates and sulfides (Wedepohl, 1978; BGS, 1992). Copper is an important trace element in plants. Deficiencies in vegetation can occur where copper concentrations fall below 10 ppm in soils (Rose et al., 1979). Table 10 shows the concentrations for copper in some typical rocks and soils.

Table 10 Copper (ppm)

	Fortescue (1992)	Rose, Hawkes, and Webb (1979)	Wedepohl (1978)	Taylor and McLennan (1985)
Clarke	68.0			75.0
Ultramafic		42.0		
mafic		72.0		
granitic		12.0	13.0	
basalt			90.0	
andesite			55.0	
rhyolite			6.0	
sandstone		10.0	9.0	
limestone		5.0	4-6	
shale		42.0	39.0	
soils		15.0	18.0	
ores				

Data

Copper concentrations within the study area range from 8 to 1141 ppm with a mean of 31 and median of 20 ppm (Fig. 16). These values are well below the referenced Clarke values of 68 and 75 ppm (Table 10). This difference is again likely due to the low abundance of mafic and ultramafic rocks within the study area.

Copper concentrations across much of the Paleozoic sedimentary rocks east of the Rio Grande range from 8 to 14 ppm. A notable exception to this occurs on the eastern edge of these rocks where a single sample had a concentration of 68 ppm. This sample was taken east of the boundary defining the Chupadero mining district. However, it is likely the result of sedimentary red bed copper mineralization.

Copper concentrations across much of the rest of the study area range from 15 to 31 ppm. This is in fair agreement with the expected values for rhyolitic and andesitic rocks that crop out throughout much of the study area.

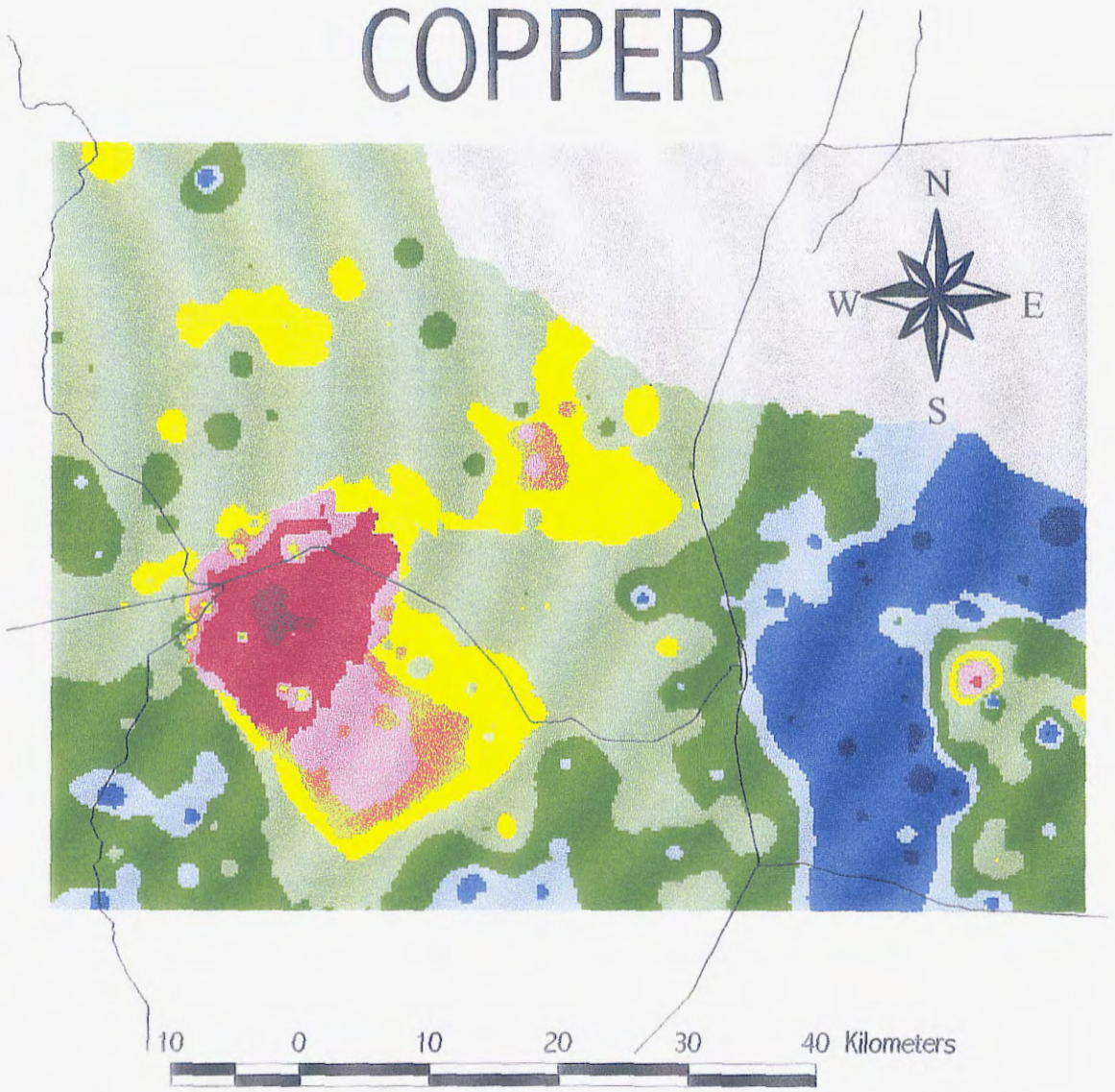

Figure 16. Copper distribution within the study area.

Anomalously high concentrations of copper occur in the northern Magdalena Mountains where copper obtains its maximum concentration of 1141 ppm. This area includes sample locations from north of the town of Magdalena extending southeast into the Copper Canyon region. This region coincides with the Northern Magdalena, Magdalena, Hop Canyon, and Water Canyon mining districts. Each of these districts has produced copper.

GALLIUM

Geochemistry

Gallium minerals are rare even though gallium is widespread in nature. Gallium is associated with aluminum in common minerals (Wedepohl, 1978). Feldspars and micas are the main host minerals for gallium in both igneous and metamorphic rocks (BGS, 1992). Gallium is uniformly distributed in most mafic, intermediate, and granitic rocks (Wedepohl, 1978). During metamorphism gallium is relatively immobile. Gallium behaves similarly to zinc under certain mineralizing conditions, which results in gallium enrichment in sphalerite (BGS, 1992). Gallium is enriched in the products of weathering in the same manner as aluminum (Wedepohl, 1978). Table 11 shows the concentrations of gallium in some typical rocks and soils.

Table 11 Gallium (ppm)

	Fortescue (1992)	Rose, Hawkes, and Webb (1979)	Wedepohl (1978)	Taylor and McLennan (1985)
Clarke	19.0			18.0
Ultramafic				
mafic				
granitic			18.5	
basalt			17.0	
andesite			21.0	
rhyolite				
sandstone			6.0	
limestone			2.5	
shale			23.0	
soils			10.0	
ores				

Data

Gallium concentrations within the study area range from 6 to 43 ppm with a mean of 15 ppm (Fig. 17). This is very near the referenced Clarke values of 18 and 19 ppm (Table 11).

Gallium concentrations across the Paleozoic sedimentary rocks east of the Rio Grande, and Cretaceous sedimentary rocks in the northwest region of the study area range from 6 to 15 ppm. This agrees well with the referenced value for gallium in sandstones of 6 ppm (Wedepohl, 1978). Gallium concentrations range from 13 to 17 ppm where Tertiary rhyolites outcrop. This is again consistent with values cited by Wedepohl (1978). The highest concentrations for gallium occur in the northwest section of the study area. This is consistent with the northwest section being dominantly composed of Tertiary andesites and silicic volcanic rocks.

Elevated concentrations of gallium occur southeast of the town of Magdalena. This region coincides with the Magdalena mining district where zinc has been produced.

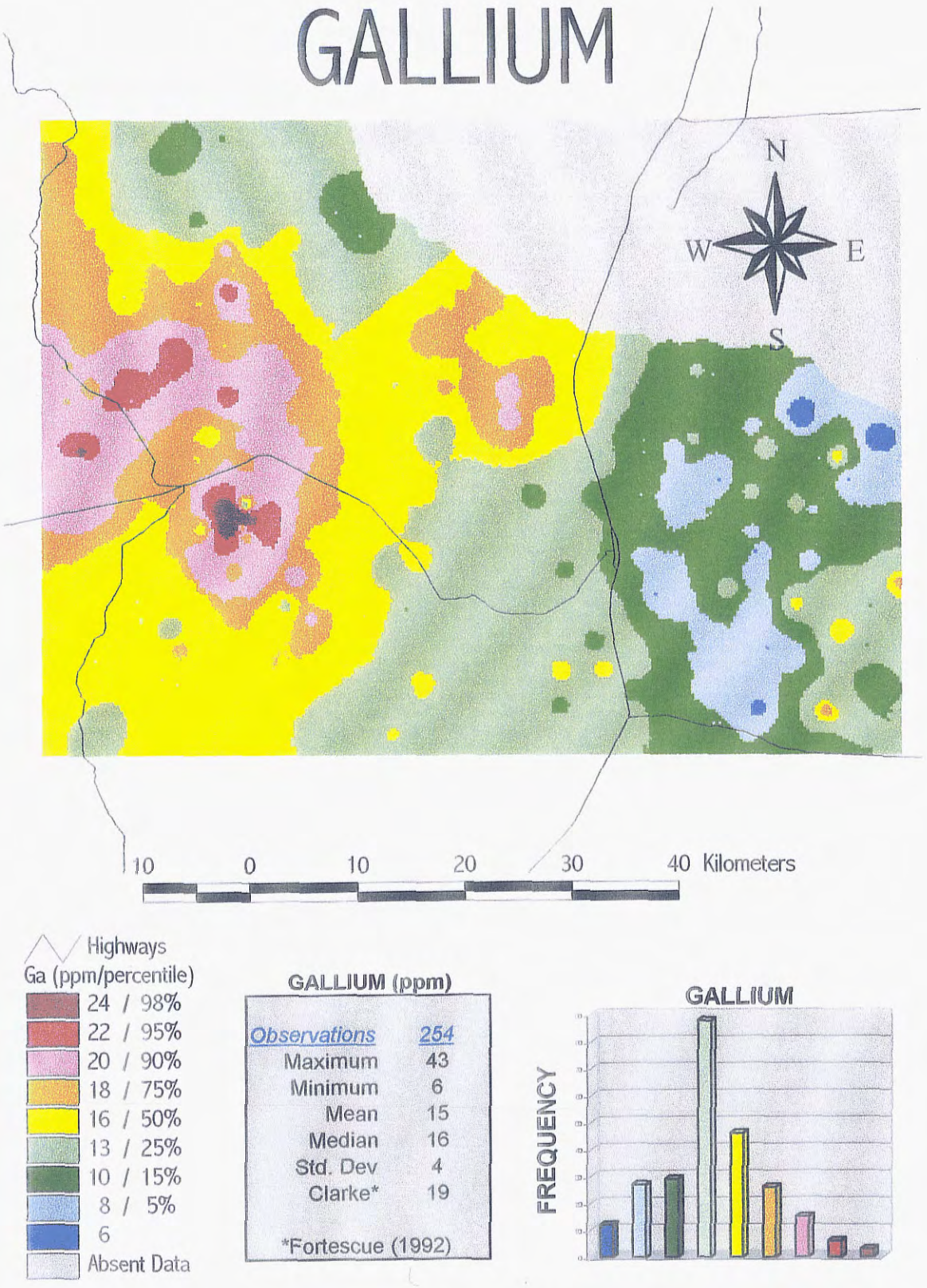

Figure 17. Gallium distribution within the study area.

The elevated concentrations in this area are likely due to the zinc related chalcophile behavior that causes gallium to be enriched in the mineral sphalerite.

IRON OXIDE

Geochemistry

Iron is a siderophile element that is enriched in mafic igneous rocks and ore deposits (Rose et al., 1979). Iron is a major constituent of biotites, olivines, pyroxenes, amphiboles, and is abundant in a variety of oxides and sulfides such as magnetite (Fe_3O_4) and pyrite (FeS_2) (BGS, 1992; Rose et al., 1979). A variety of factors including provenance, pH-Eh conditions, and diagenetic alteration influence the abundance of iron in sedimentary rocks (BGS, 1992). Secondary hydrous oxides are commonly the dominant iron phases in sediments. Enrichment in finer grained sediments is due to the interaction of hydrous oxides with the larger surface area of clay particles (BGS, 1992; Wedepohl, 1978). Iron is important for both plant and animal health. In plants iron is necessary for the synthesis of chlorophyll while in animals it is a constituent of hemoglobin in blood (Rose et al., 1979). Table 12 shows the concentrations of iron in some typical rocks and soils.

Table 12 Iron Oxide (Fe2O3%)

	Fortescue (1992)	Rose, Hawkes, and Webb (1979)	Wedepohl (1978)	Taylor and McLennan (1985)
Clarke	6.22			9.10
Ultramafic		9.43		
mafic		8.65		
granitic		1.42		
basalt				
andesite				
rhyolite				
sandstone		0.98	3.20	
limestone		0.38	0.50	
shale		4.70	6.50	
soils		2.10		
ores				

Data

Iron oxide concentrations within the study area range from 2 to 18.8 % with a mean of 6.1 % (Fig. 18). This value is very near the referenced Clarke value of 6.22 % (Fortescue, 1992).

Iron oxide concentrations across the Paleozoic sedimentary rocks east of the Rio Grande, Cretaceous sedimentary rocks in the northwest, and the Tertiary and Quaternary sediments in the southwest region of the study area range from 1 to 7.4 %. Sediments collected from areas of Tertiary rhyolites have iron oxide concentrations that range from 2.5 to 7.4 %. The highest concentrations of iron oxide occur in the northwest region of the study area. Concentrations within this region range from 7.5 to 18.8 %. This is the result of the northwest region being predominantly composed of Tertiary volcanic rocks.

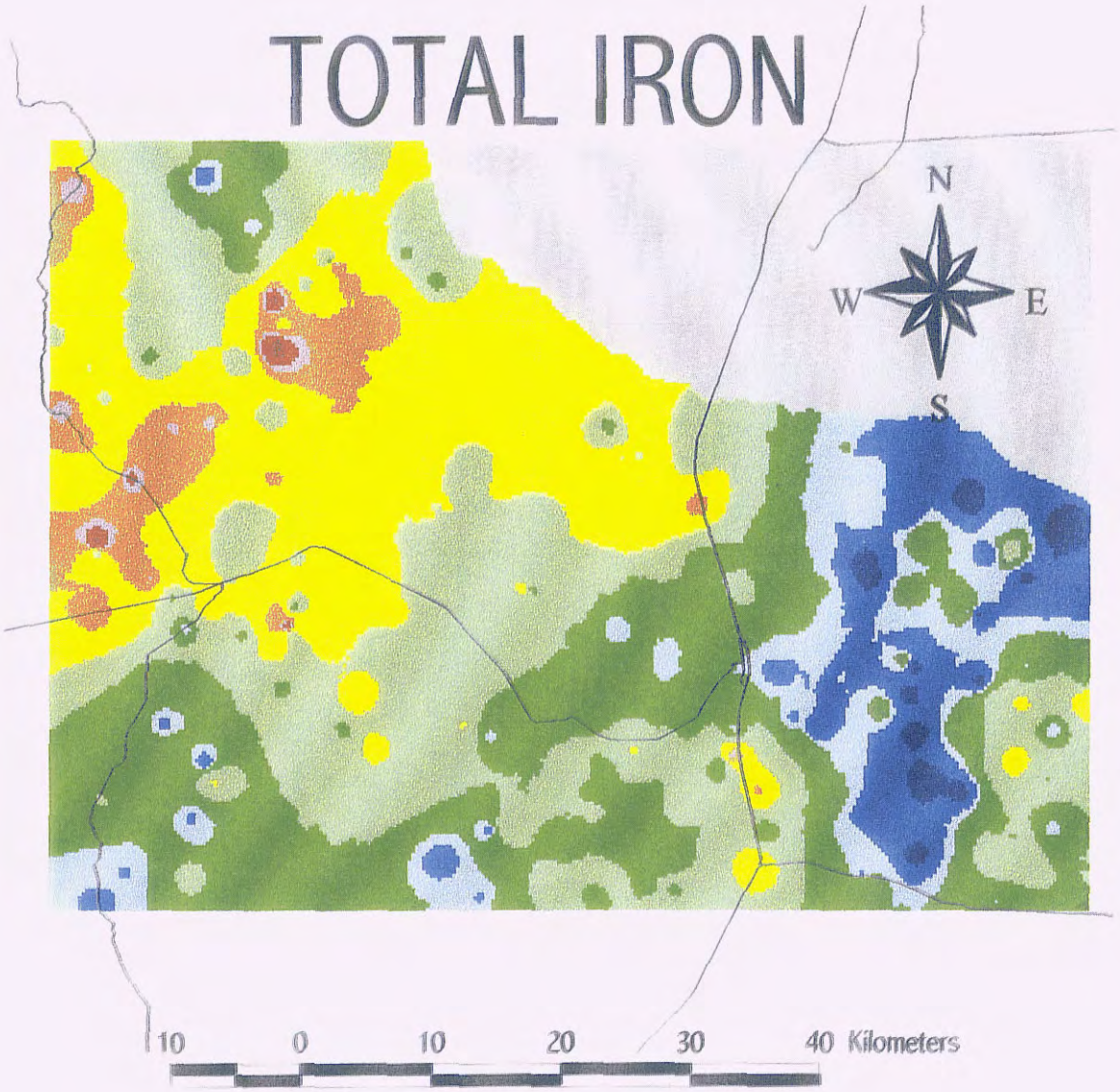

Figure 18. Iron oxide distribution within the study area.

Three locations south of Socorro along Interstate 25 have iron oxide concentrations above 7.5 %. These locations are likely the result of samples coming from drainages of the Luiz Lopez mining district. The locations also have high manganese concentrations and are likely the result of coprecipitation of iron and manganese oxides.

LEAD

Geochemistry

Lead is a chalcophile element associated with silver in many precious metal deposits and with iron, zinc, copper and antimony in sulfide deposits (Rose et al., 1979). The primary lead mineral is galena (PbS). Pb^{2+} may replace K^{+}, Sr^{2+}, Ba^{2+}, Ca^{2+}, and Na^{+} in rock forming minerals. Potassium feldspars are the major lead carriers in magmatic rocks (Wedepohl, 1978). Lead may be mobilized during low-grade metamorphism but has a low rate of mobility during chemical weathering (BGS, 1992; Wedepohl, 1978). This low mobility is due in part to lead's tendency for adsorption to Mn-Fe oxides and organic matter (Rose et al., 1979) as well as the formation of lead carbonate and sulfate crusts in arid climates. In sediments lead is found principally in detrital micas and feldspars as well as clay minerals (Wedepohl, 1978). The contamination of stream sediments by atmospheric dust near roads, metallic detritus, and paints is widespread (BGS, 1992). Table 13 shows the concentrations of lead in some typical rocks and soils.

Lead was chosen as the number 2 hazardous substance for 1997 by the Agency for Toxic Substances and Disease Registry and the Environmental Protection Agency (ATSDR, 1997). Lead can adversely affect almost every organ and system within the human body. The most sensitive to lead is the central nervous system. Exposure to lead

is even more dangerous for young children and unborn children. The Centers for Disease Control and Prevention (CDC) recommends that all children be screened for lead poisoning at least once a year. Because of the health effects associated with lead. the EPA has set a limit of 15 ppb of lead in drinking water (ATSDR, 1993b).

Table 13 Lead (ppm)

	Fortescue (1992)	Rose, Hawkes, and Webb (1991)	Wedepohl (1978)	Taylor and McLennan (1985)
Clarke	13.0			8.0
Ultramafic		1.0		
mafic		4.0		
granitic		18.0	23.0	
basalt			6.2	
andesite			10.6	
rhyolite			26.9	
sandstone		10.0	10.0	
limestone		5.0	3.0	
shale		25.0	21.6	
soils		17.0	16.0	
ores				

Data

Lead concentrations within the study area range from 6 to 11258 ppm with a median value of 20 ppm (Fig. 19). This value is slightly higher than the Clarke value cited by Fortescue (1992) of 13 ppm. This is likely the result of the abundance of granites and silicic volcanic rocks as well as mining districts within the study area.

Lead concentrations across the Paleozoic sedimentary rocks east of the Rio Grande, and Cretaceous sedimentary rocks in the northwest range from 6 to 17 ppm. These values are consistent with the values for sedimentary rocks cited by Rose et al. (1979) and Wedepohl (1978). In most areas dominated by Tertiary rhyolites and basaltic andesites, lead concentrations range from 17 to 42 ppm.

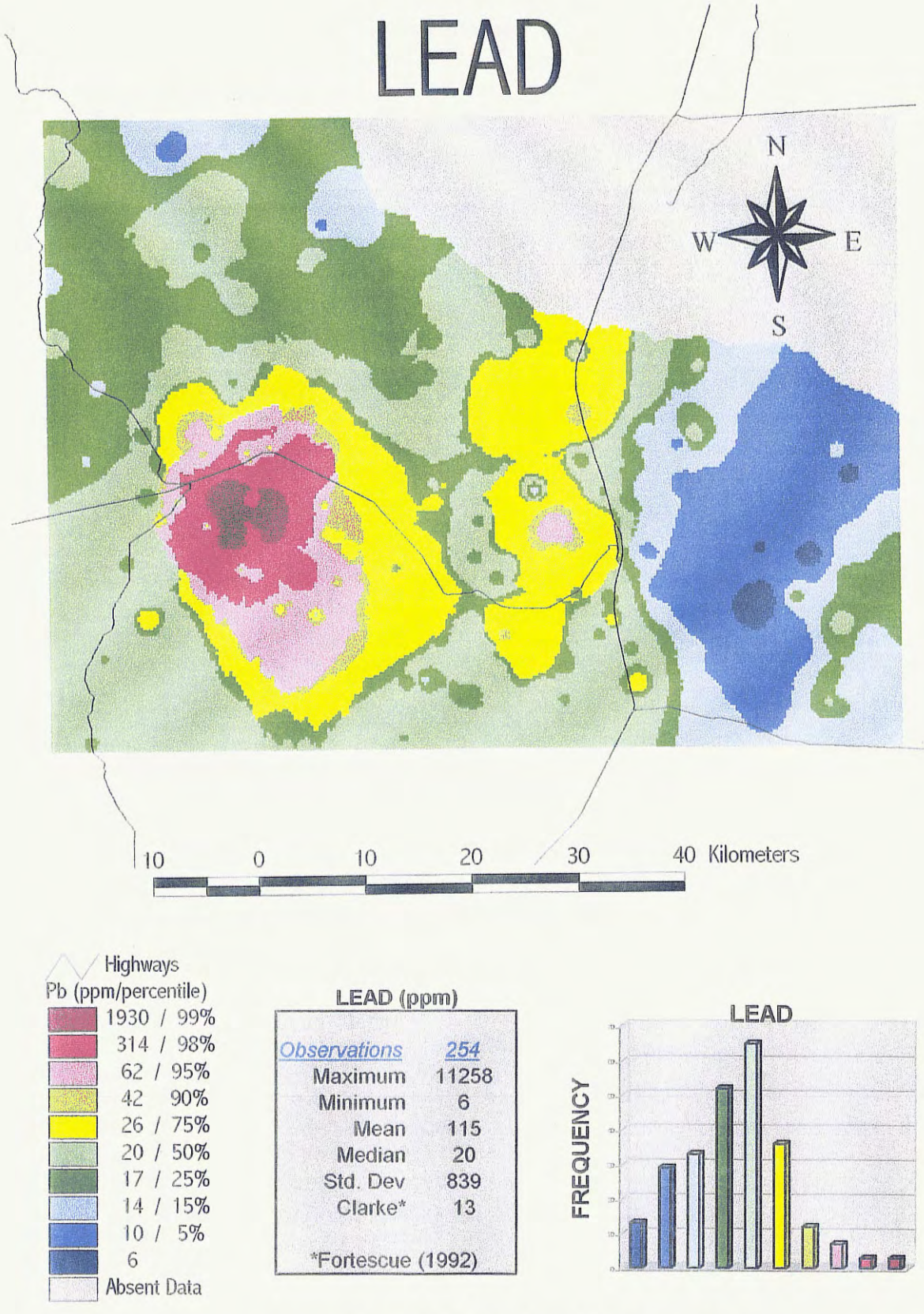

Figure 19. Lead distribution within the study area.

Anomalously high lead concentrations occur at Socorro Peak, Copper Canyon, and near the town of Magdalena. All of these locations are associated with the known mining districts of Socorro Peak, Water Canyon, Hop Canyon, Magdalena, and North Magdalena. The maximum lead concentration of 11,258 ppm was found within the Magdalena mining district.

MAGNESIUM OXIDE

Geochemistry

During magmatic processes magnesium is concentrated in the early differentiates and is a major constituent in rock forming minerals such as olivine and pyroxene (BGS, 1992). Magnesium is present in many silicate minerals many of which involve solid solutions between Mg^{2+} and Fe^{2+} (Wedepohl, 1978). Magnesium distribution seems to be relatively unaffected by medium to high-grade metamorphism. However, magnesium may be mobilized during greenschist facies alteration and contact metamorphism of carbonates (BGS, 1992). Weathering leads to the fractionation of magnesium from iron and other cations. This results in the formation of magnesium sheet silicate and carbonate minerals (Wedepohl, 1978). Minerals such as olivines, pyroxenes, amphiboles, chlorite, and micas break down rapidly and contribute to a large percentage of the detrital magnesium in stream sediments. Carbonates such as dolomite are also important under certain conditions. In sedimentary rocks magnesium occurs in dolomite, chlorite, ankerite, and glauconite (BGS, 1992). Table 14 shows the concentration of magnesium in some typical rocks.

Table 14 Magnesium Oxide (MgO%)

	Fortescue (1992)	BGS (1992)	Wedepohl (1978)	Taylor and McLennan (1985)
Clarke	4.9			5.3
Ultramafic		6.0		
mafic		4.5		
granitic		< 1	0.52	
basalt			6.34	
andesite			4.36	
rhyolite			0.32	
sandstone			0.70	
limestone				
shale			1.50	
soils				
ores				

Data

Magnesium oxide concentrations within the study area range from 0.54 to 2.95 % with a mean of 1.55 % (Fig. 20). The mean of 1.55 % is significantly lower than the Clarke value of 4.9 to 5.3 (Table 14). This is likely a reflection of the low percentage of ultramafic and mafic rocks within the study area.

The lowest concentrations of magnesium oxide within the study area occur in the southern region. This area is dominated by Tertiary rhyolites. In regions dominated by Tertiary volcanic rocks magnesium oxide concentrations typically range from 0.54 to 2.54 %. These values are consistent with those cited for rhyolites but are lower than cited values for either basalts or andesites (Wedepohl, 1978). Magnesium oxide concentrations across the Paleozoic sedimentary rocks east of the Rio Grande typically range from 1.50 to 2.95 %. These values are higher than the referenced value for

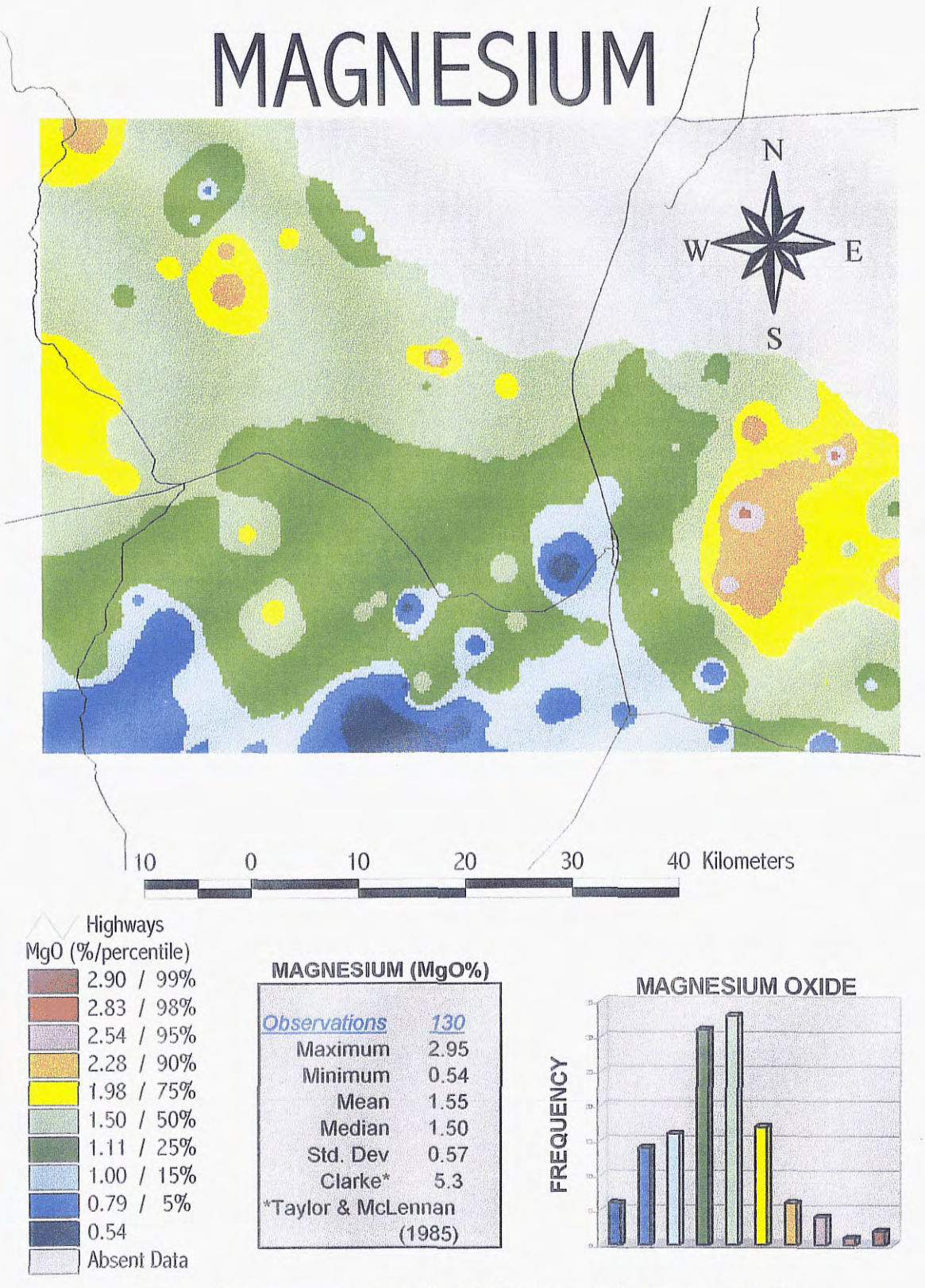

Figure 20. Magnesium oxide distribution within the study area.

SAMPLE LOCATIONS OVERLAY

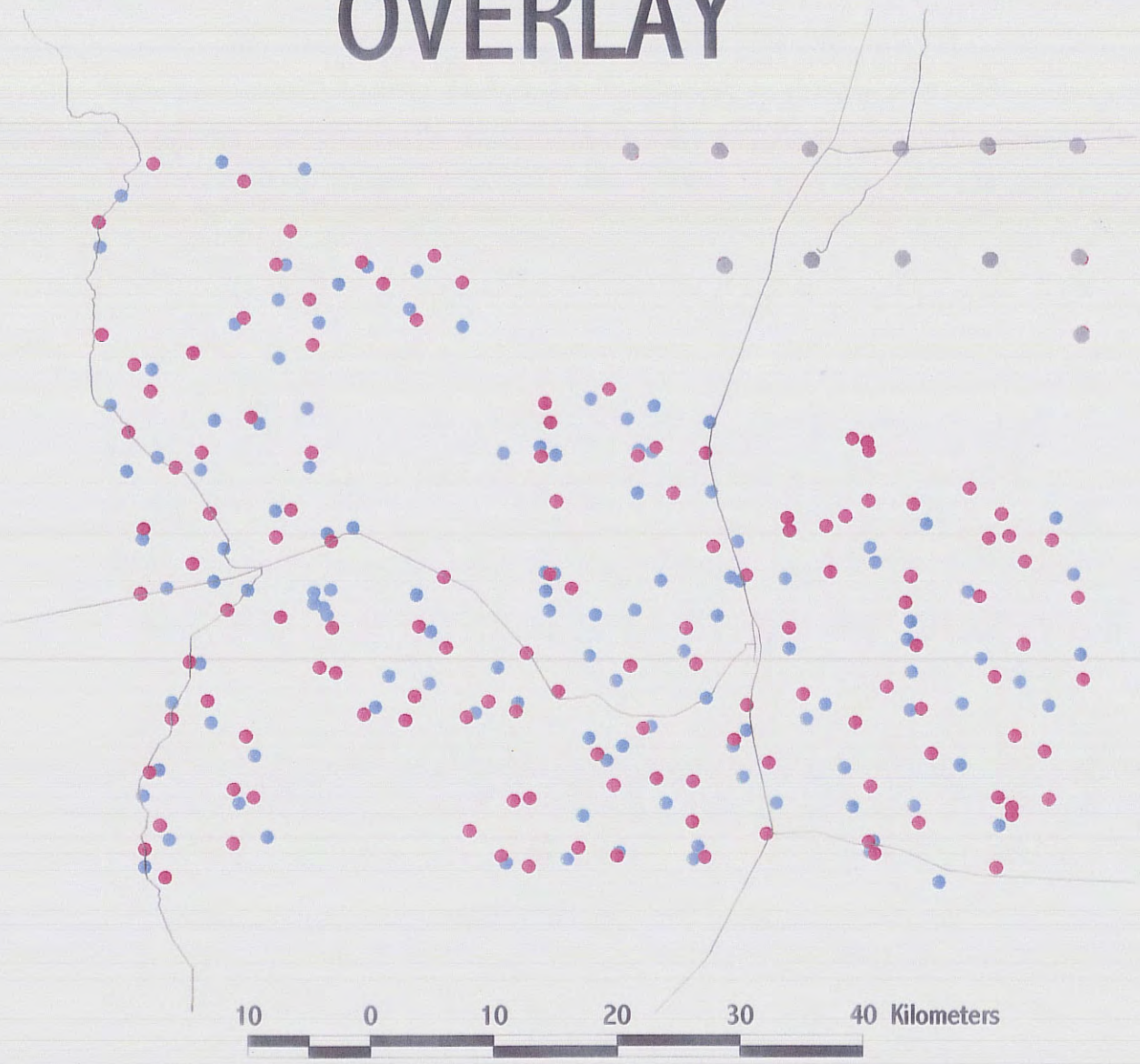

NOT AN EXACT OVERLAY

MINERAL OCCURRENCES OVERLAY

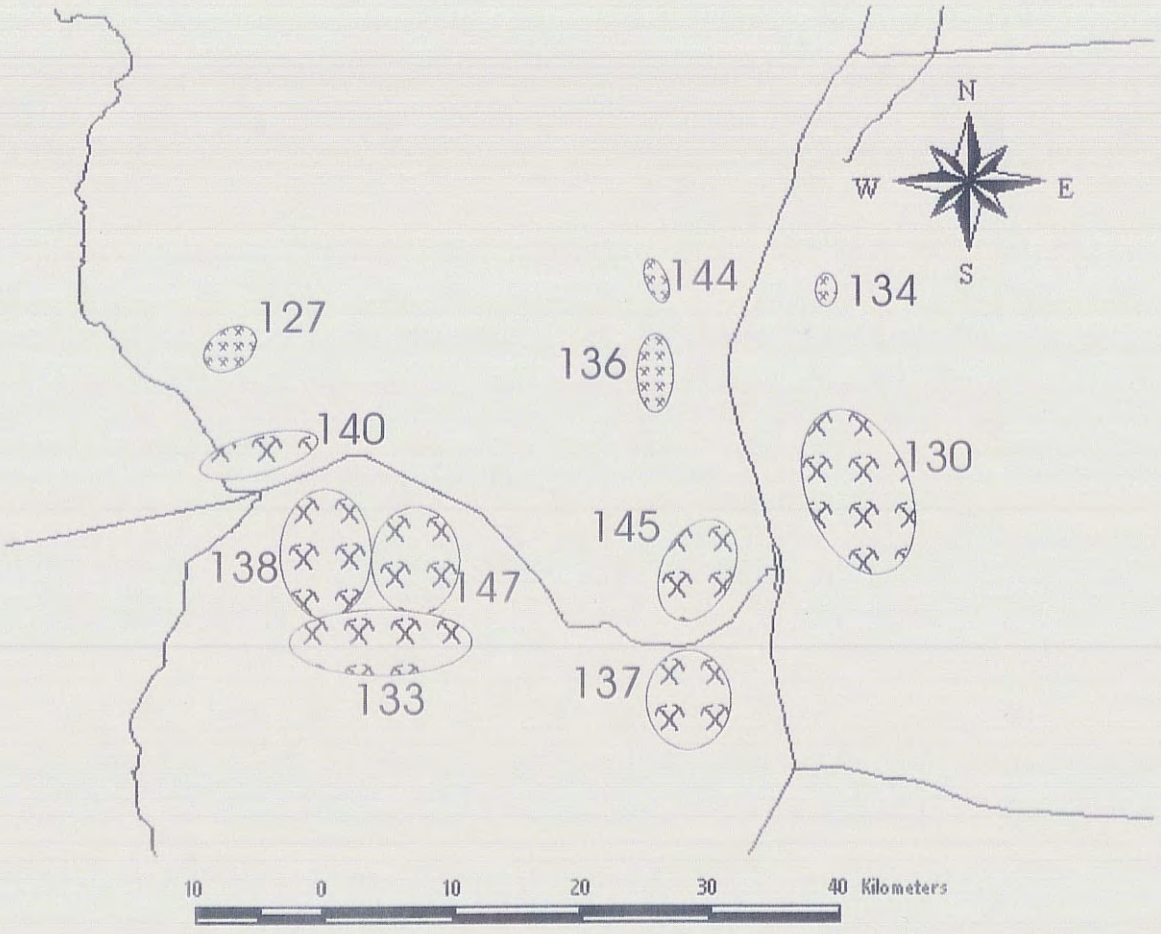

FIGURE 4. Approximate locations of mining districts within the study area (modified from, McLemore, in press).

NOT AN EXACT OVERLAY

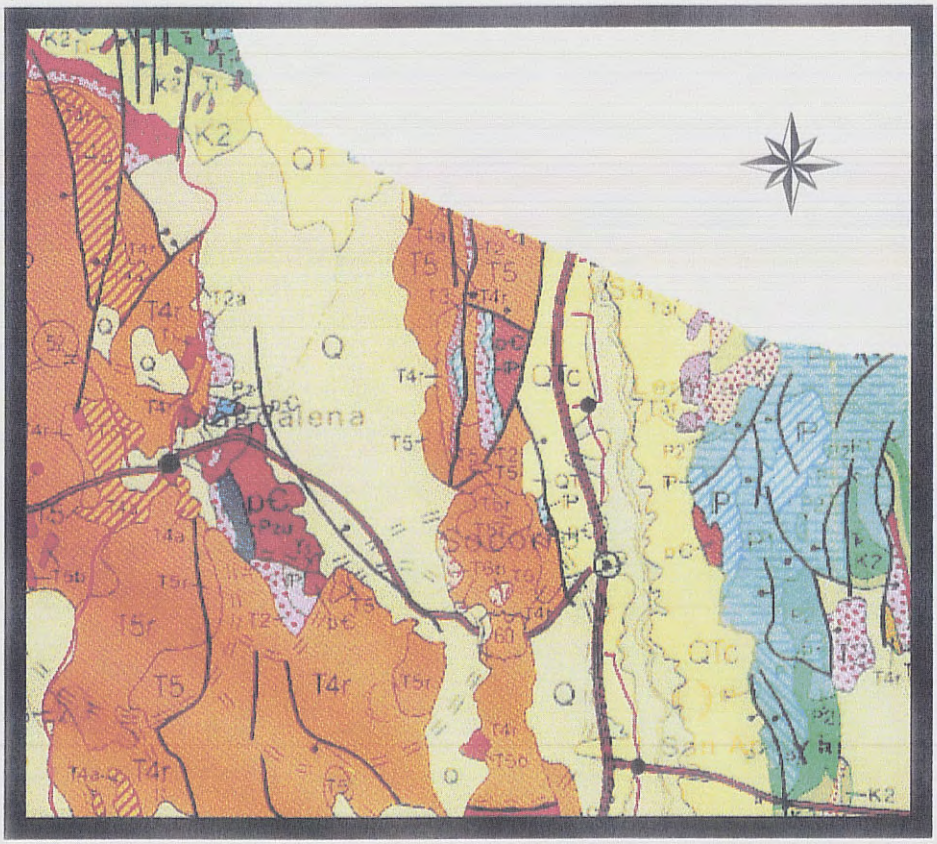

FIGURE 2. Generalized geologic map of the study area (after, NMGS, 1982)

NOT AN OVERLAY

sandstones of 0.70 %. This is likely a reflection of an igneous or metamorphic source for the sandstones.

MANGANESE OXIDE

Geochemistry

Manganese is a lithophile element associated with magnesium and iron silicates and is enriched in mafic and ultramafic rocks (BGS, 1992; Rose et al., 1979). Manganese occurs naturally in minerals as Mn^{2+}, Mn^{3+}, and Mn^{4+}. Mn^{2+} is the most stable species under most geological conditions and may substitute for Fe^{2+}, Mg^{2+}, and Ca^{2+} in igneous and metamorphic rocks (Wedepohl, 1978). Manganese is immobile during metamorphism but may be mobilized as a result of hydrothermal activity during regional metasomatism (BGS, 1992). During weathering and sediment formation Mn^{4+} forms its own minerals (Wedepohl, 1978). The precipitation of manganese oxides can scavenge trace elements such as Ba, Cu, and Zn (BGS, 1992). Table 15 shows the concentrations of manganese in some typical rocks and soils.

Table 15 Manganese Oxide (MnO%)

	Fortescue (1992)	Rose, Hawkes, and Webb (1979)	Wedepohl (1978)	Taylor and McLennan (1985)
Clarke	0.106			
Ultramafic		0.104		
mafic		0.150		
granitic		0.039		
basalt			0.170	
andesite			0.150	
rhyolite			0.080	
sandstone				
limestone		0.110		
shale		0.085		
soils		0.032		

Data

Manganese oxide concentrations within the study area range from less than 0.04 to 0.20 % with a mean of 0.1 % (Fig. 21). This mean value is very near the cited reference of 0.106 % given by Fortescue (1992).

Manganese oxide concentrations across the Paleozoic sedimentary rocks east of the Rio Grande, and Cretaceous sedimentary rocks in the northwest section of the study area range from less than 0.04 to 0.07 %. The Tertiary rhyolites and basaltic andesites have manganese oxide concentrations that that range from 0.05 to 0.16 %.

Enrichment of manganese oxide occurs in discrete samples in the northwest region, Magdalena Mountains, and south of Socorro along Interstate 25. In the northwest region, the enrichment is likely due primarily to the presence of Tertiary andesites. In the Magdalena Mountains the anomalous values of manganese oxide are coincident with the Magdalena, and Water Canyon mining districts. The highest concentration of manganese oxide (0.26 %) was found in the Water Canyon district. Manganese oxide enrichment south of Socorro is strongly related to iron oxide enrichment in the same samples. One explanation for this is the coprecipitation of manganese and iron oxides

An interesting note on the manganese oxide concentrations is the general lack of a significant anomaly located southeast of Socorro in the Luis Lopez mining district. The major element produced in this district is manganese and bed material within streams sampled in this region generally contained coatings of the manganese oxide psilomelane.

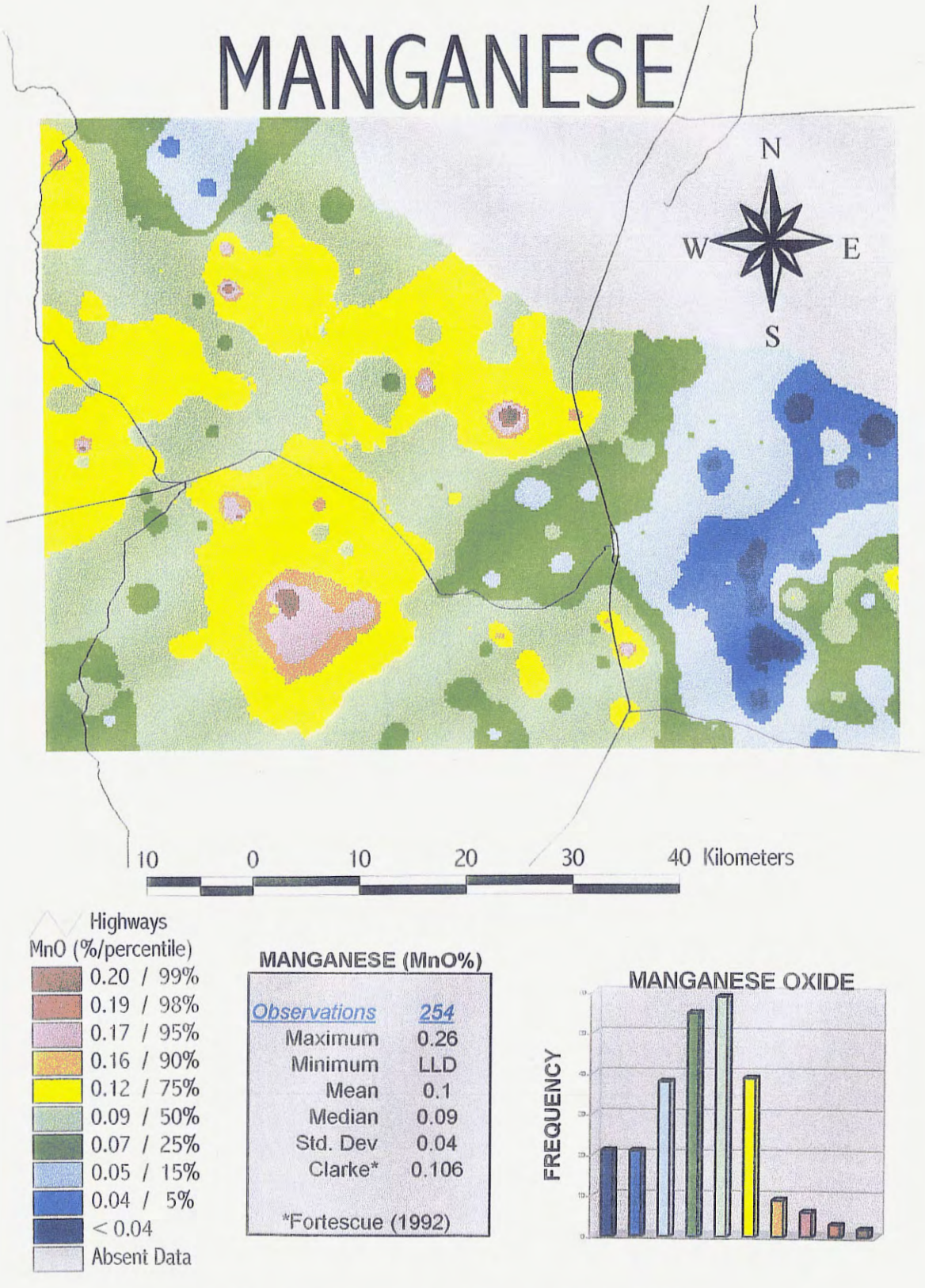

Figure 21. Manganese oxide distribution within the study area.

MOLYBDENUM

Geochemistry

Molybdenum is a siderophile element with a complex chemistry that involves a range of natural ions from Mo^{3+} to Mo^{6+} (Rose et al., 1979; Wedepohl, 1978). Molybdenum is preferentially accumulated in titanium, iron, and tungsten minerals such as sphene, ilmenite, titanomagnetite, and biotite. Metamorphic sequences show no consistent enrichment or depletion of molybdenum (Wedepohl, 1978). Molybdenum weathers quickly and is more mobile under alkaline, oxidizing conditions (BGS, 1992). Table 16 shows the concentrations of molybdenum in some typical rocks and soils.

Table 16 Molybdenum (ppm)

	Fortescue (1992)	Rose, Hawkes, and Webb (1979)	Wedepohl (1978)	Taylor and McLennan (1985)
Clarke	1.2			1.0
Ultramafic		0.3		
mafic		1.5		
granitic		1.3	1.1	
basalt			1.2	
andesite				
rhyolite				
sandstone		0.2	0.3	
limestone		0.4	0.4	
shale		2.6	0.7-2	
soils		2.5	2.0	
carbonatite			50.0	

Data

Molybdenum concentrations within the study area range from less than 2 to 13 ppm with a mean of 2 ppm (Fig. 22). This value is very near the Clarke value of 1.2 ppm and the referenced values for soils of 2 to 2.5 ppm (Table 16).

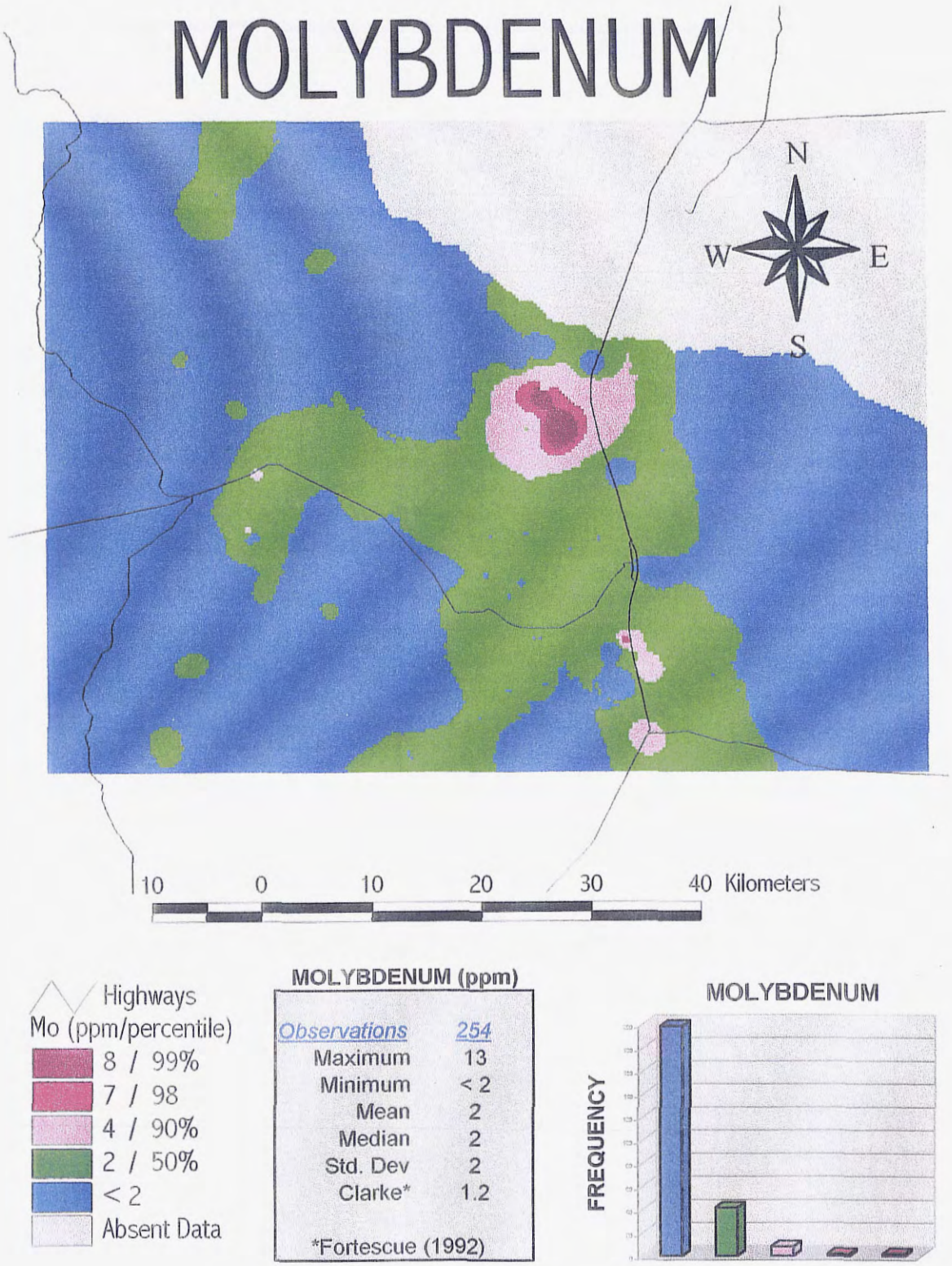

Figure 22. Molybdenum distribution within the study area.

Most of the samples within the study area have molybdenum concentrations lower than the detection limit of 2 ppm. This is consistent with the Clarke values cited by Fortescue (1992), and Taylor and McLennan (1985). The highest concentrations of molybdenum occur in the Polvadera Peak region where carbonatite dikes outcrop. The maximum value of 13 ppm is below the mean for carbonatites. However, Wedepohl (1978) gave a range of molybdenum concentrations in carbonatites of 4 to 100 ppm. Therefore, the carbonatites are a likely cause for the anomaly located near Polvadera Peak. Three locations south of Socorro along Interstate 25 have molybdenum concentrations above 4 ppm. These locations correspond to samples enriched in both manganese and iron oxides as well.

NICKEL

Geochemistry

Nickel is both a siderophile and to a lesser extent chalcophile element that is associated with magnesium and cobalt in ultramafic and mafic rocks, and with cobalt, copper, and platinum in sulfide deposits (Rose et al., 1979). A strong correlation exists between nickel, magnesium, and chromium, especially in basaltic rocks (Wedepohl, 1978). Nickel does not form any common rock-forming minerals. Ni^{2+} is intermediate in size between Mg^{2+} and Fe^{2+} and as such substitutes for them during fractionation. During fractionation nickel is partitioned into minerals such as olivine, orthopyroxene, and spinels (BGS, 1992; Wedepohl, 1978). During weathering nickel is readily mobilized but becomes coprecipitated with iron and manganese oxides (Wedepohl, 1978). In sedimentary rocks nickel is present in detrital ferromagnesian silicates, primary iron

oxides, hydrous iron and manganese oxides, and clay minerals (BGS, 1992). Table 17 shows the concentrations of nickel in some typical rocks and soils.

Table 17 Nickel (ppm)

	Fortescue (1992)	Rose, Hawkes, and Webb (1979)	Wedepohl (1978)	Taylor and McLennan (1985)
Clarke	99.0			105.0
Ultramafic		2000.0	1450.0	
mafic		130.0		
granitic		4.5	10.9	
basalt			134.0	
andesite			18.0	
rhyolite			< 6	
sandstone		20.0	21.0	
limestone		2.0	1.5	
shale		68.0	71.0	
soils		17.0	14.0	
ores				

Data

Nickel concentrations within the study area range from 10 to 79 ppm with a mean of 26 ppm (Fig. 23). This value is well below the referenced Clarke values of 99 and 105 ppm but is reasonably close to the 14 to 17 ppm cited for soils (Table 17). This difference is again likely due to the scarcity of mafic and ultramafic rocks within the study area.

Nickel concentrations across the Paleozoic sedimentary rocks east of the Rio Grande, Cretaceous sedimentary rocks in the northwest, Tertiary and Quaternary sediments in the southwest region, and areas dominated by Tertiary rhyolites range from 10 to 21 ppm. The values for sedimentary rocks are consistent with the values cited for sandstone by Wedepohl (1978) and Rose et al..(1979). The concentrations in areas

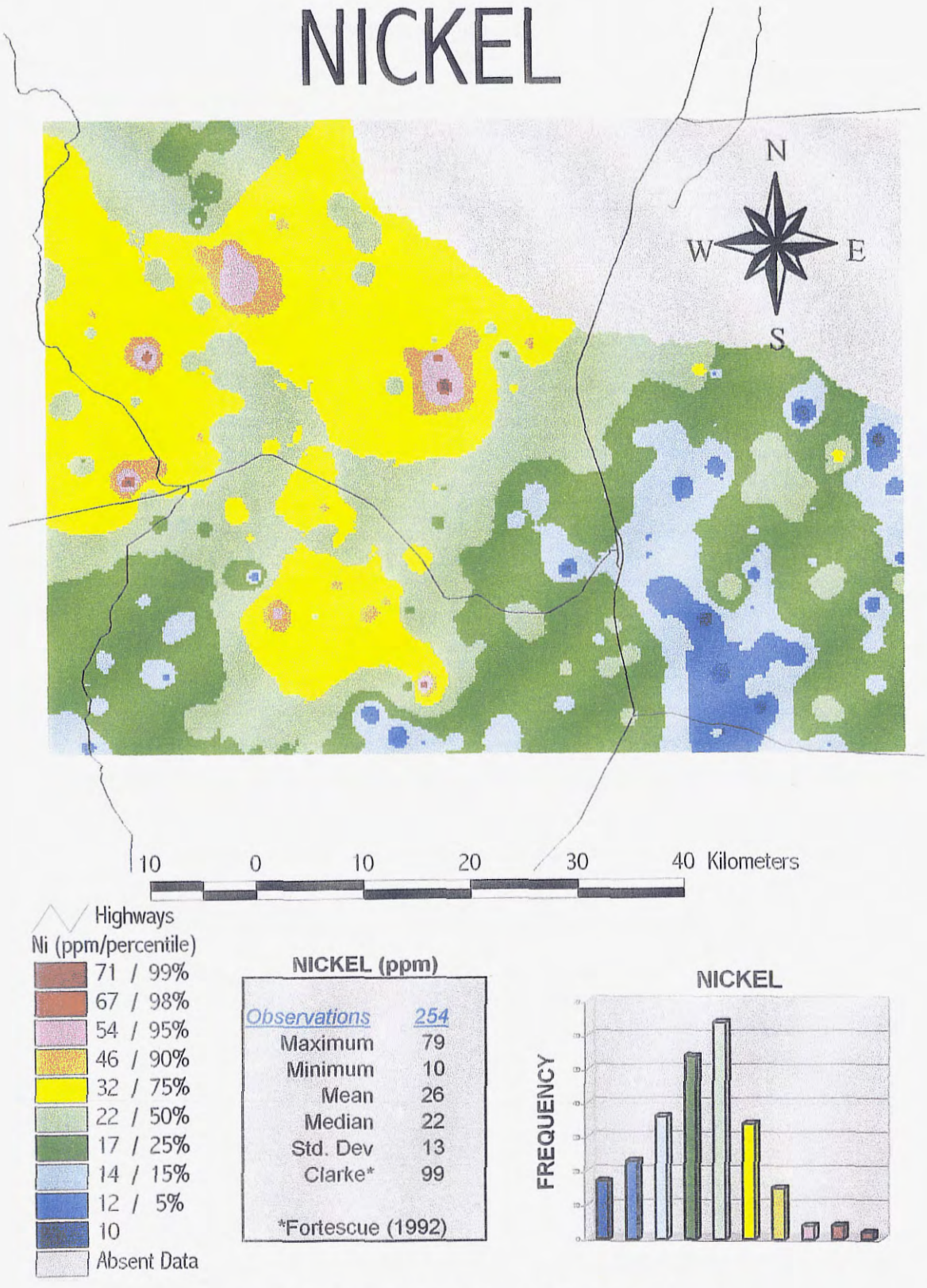

Figure 23. Nickel distribution within the study area.

dominated by Tertiary rhyolites are greater than the value cited by Wedepohl (1978) of less than 6 ppm.

Elevated concentrations of nickel occur in the northwest region, Magdalena Mountains, and a site located between the Magdalena and Chupadera Mountains. Elevated concentrations within the northwest region are related to the presence of Tertiary basaltic andesites. In the Magdalena Mountains nickel is enriched in Copper Canyon. This is likely the result of nickels association with copper in sulfide deposits as described by Rose et al. (1979).

NIOBIUM

Geochemistry

Niobium is a lithophile element having a strong association with tantalum. Niobium is also associated with titanium, rare earth elements, uranium, thorium, and phosphorus in alkaline igneous rocks (Rose et al., 1979). Niobium accumulates during magmatic fractionation and thus later differentiates have increased abundances. Titanium minerals are the major host phases of Nb in magmatic rocks (Wedepohl, 1978). Table 18 shows the concentrations of niobium in some typical rocks and soils.

Table 18 Niobium (ppm)

	Fortescue (1992)	Rose, Hawkes, and Webb (1979)	Wedepohl (1978)	Taylor and McLennan (1985)
Clarke	20.0			11.0
Ultramafic		1.0		
mafic		20.0		
granitic		20.0	23.5	
basalt			10.0	
andesite			4.3	
rhyolite			28.0	
sandstone			20.0	
limestone				
shale		20.0	10.0	
soils		15.0	12.0	
ores				

Data

Niobium concentrations within the study area range from 4 to 45 ppm with a mean of 15 ppm (Fig. 24). The mean value lies between those cited for the Clarke of 11 to 20 ppm (Table 18) and is equal to the value cited by Rose et al. (1979) for soils of 15 ppm.

Niobium concentrations across the Paleozoic sedimentary rocks east of the Rio Grande and Cretaceous rocks in the northwest section of the study area range from 4 to 11 ppm. These values are lower than the cited values for sandstones and shales given by Wedepohl, (1979) and Rose et al. (1979). Concentrations across regions dominated by Tertiary basaltic andesites range from 11 to 18 ppm which is consistent with the 10 to 20 ppm range cited for mafic rocks (Wedepohl, 1978; Rose et al., 1979). In areas where Tertiary rhyolites are dominant, niobium concentrations range from 18 to 45 ppm. This is consistent with the value cited by Wedepohl (1978) for rhyolites of 28 ppm.

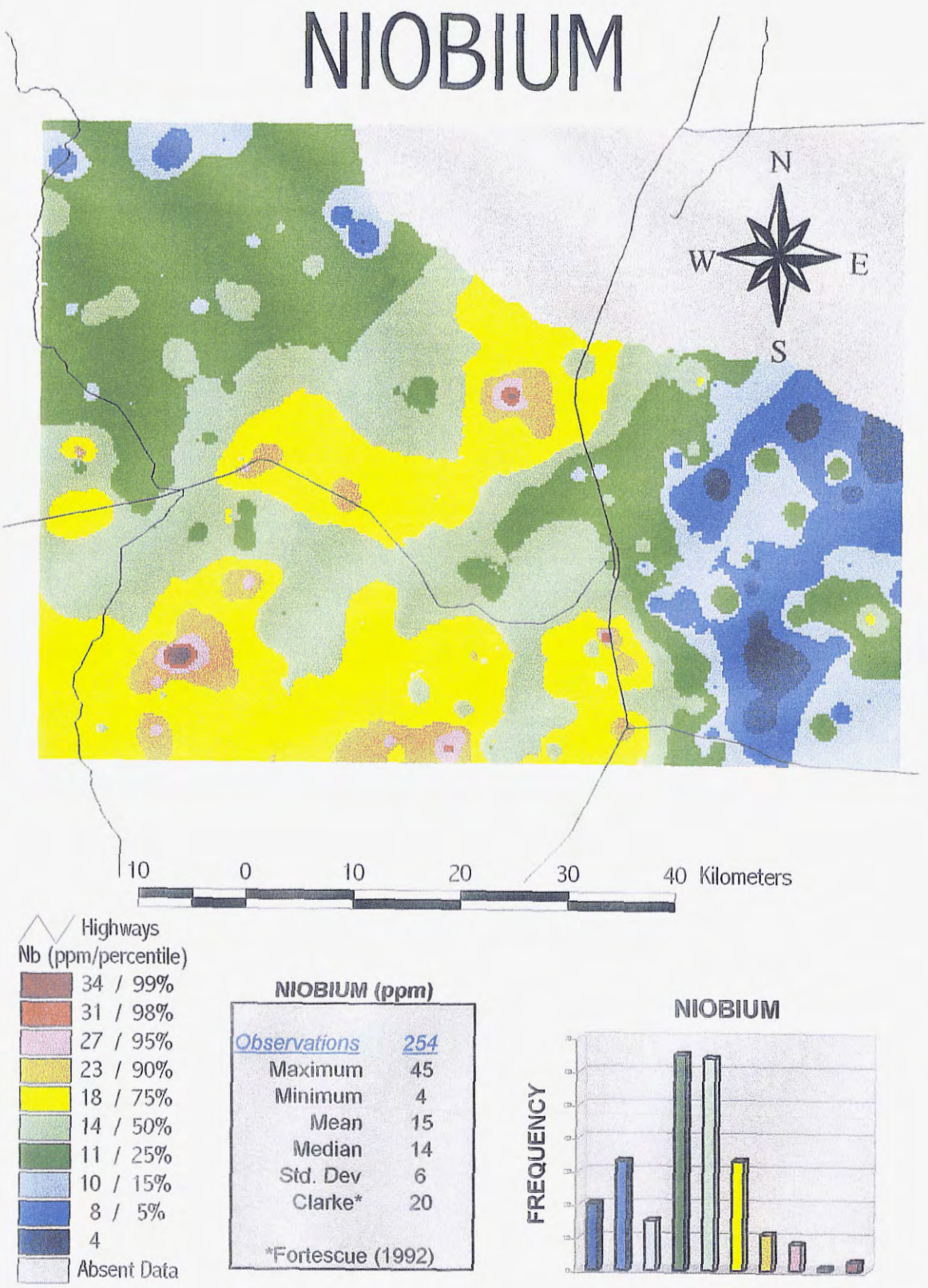

Figure 24. Niobium distribution within the study area.

PHOSPHORUS OXIDE

Geochemistry

Phosphorus in the lithosphere takes the form of P^{5+} in the phosphate ion $(PO_4)^{3-}$. The most abundant phosphate mineral is apatite (Wedepohl, 1978). Apatite is commonly associated with niobium and the rare earth elements in alkaline igneous rocks (Rose et al., 1979). There is a gradual decrease of phosphorus with increasing acidity of magmatic rocks (Wedepohl, 1978). Phosphorus has a low to intermediate mobility with apatite being the primary phosphorus mineral in sediments (Rose et al., 1979). Phosphorite deposits within the United States are commonly enriched in uranium and vanadium (Wedepohl, 1978). Table 19 shows the concentrations of phosphorus in some typical rocks.

Table 19 Phosphorus Oxide (P2O5%)

	Fortescue (1992)	Rose, Hawkes, and Webb (1991)	Wedepohl (1978)	Taylor and McLennan (1985)
Clarke	0.2			
Ultramafic			0.05	
mafic				
granitic			0.20	
basalt			0.56	
andesite			0.28	
rhyolite			0.13	
sandstone			0.04	
limestone			0.07	
shale			0.15	
soils				
ores				

Data

Phosphorus oxide concentrations within the study area range from 0.050 to 0.465 % with a mean of 0.128 % (Fig. 25). The mean of 0.128 % is lower than the cited

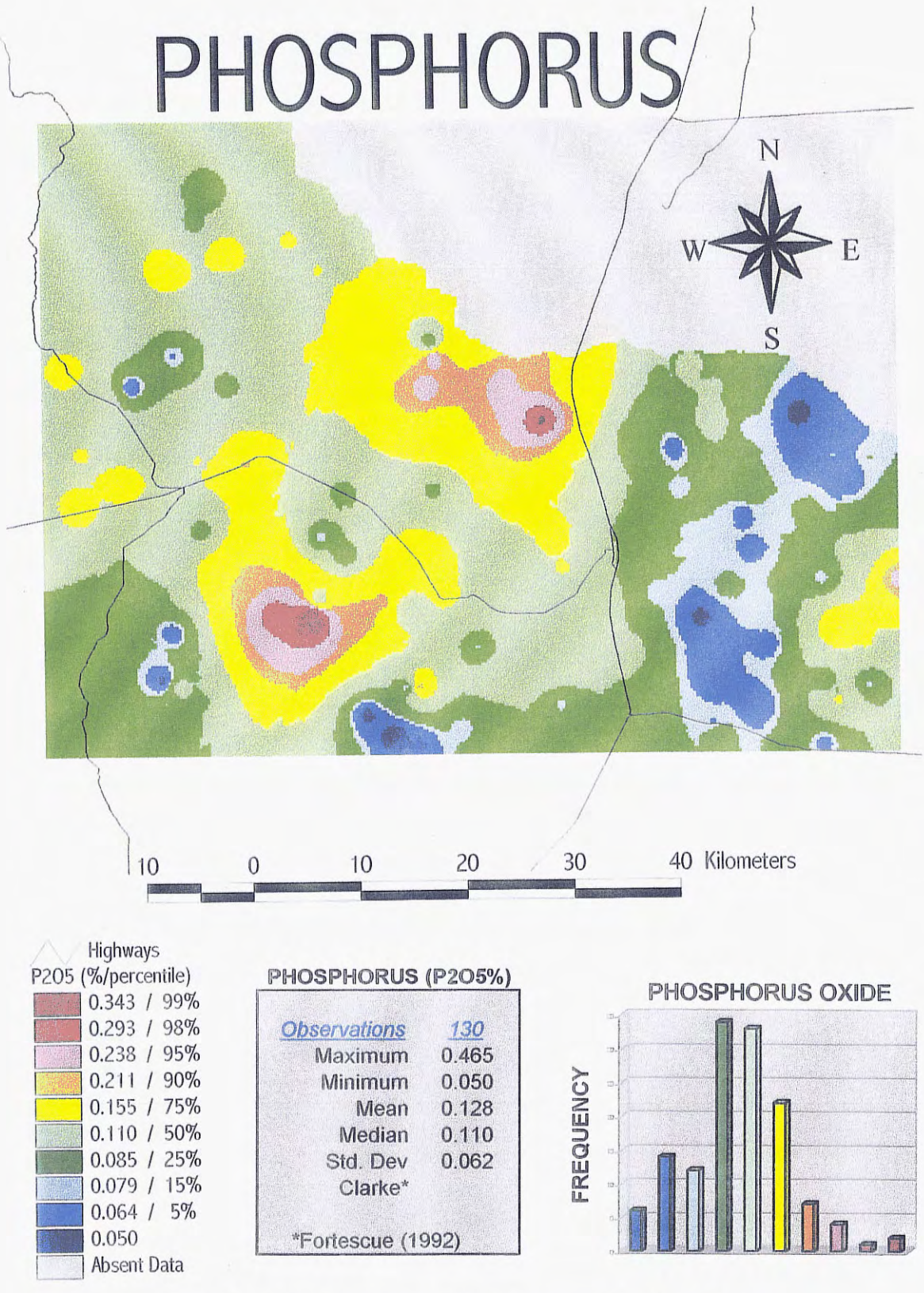

Figure 25. Phosphorus oxide distribution within the study area.

Clarke value of 0.2 % (Fortescue, 1992). This is likely the result of the low percentage of mafic rocks within the study area.

Phosphorus oxide concentrations across the Paleozoic sedimentary rocks east of the Rio Grande range from 0.050 to 0.110 %. These values are consistent with the cited values for sedimentary rocks of 0.04 to 0.15 % (Wedepohl, 1978). Phosphorus oxide concentrations in areas dominated by Tertiary rhyolites and basaltic andesites typically range from 0.085 to 0.211 %.

The highest concentrations of phosphorus oxide within the study area occur in Water Canyon, Copper Canyon, and Polvadera Mountain. In the Polvadera Mountain region the abundance of phosphorus oxide can be attributed to the carbonatite dikes in that region.

POTASSIUM OXIDE

Geochemistry

The majority of potassium within the earth's crust is contained in alkali feldspars (Wedepohl, 1978). Potassium is a lithophile element that is common to many mineral deposits (Rose et al., 1979). There is a strong similarity between K^+ and Rb^+ that allows a mutual substitution of the two elements. Potassium has a moderately high mobility restricted by adsorption to clay minerals and uptake by plants and animals (Rose et al., 1979). The potassium content of sandstones is principally a function of potassium feldspars, potassium micas, and glauconite. The concentrations of potassium in sedimentary rocks increases with decreasing grain size (Wedepohl, 1978). Table 20 shows the concentrations of potassium in some typical rocks and soils.

Table 20 Potassium Oxide (K2O%)

	Fortescue (1992)	Rose, Hawkes, and Webb (1991)	Wedepohl (1978)	Taylor and McLennan (1985)
Clarke	2.1			1.1
Ultramafic			0.70	
mafic				
granitic			4.11	
basalt			0.70	
andesite			2.04	
rhyolite			4.58	
sandstone			1.48	
limestone			0.31	
shale			2.45	
soils			1.68	
ores				

Data

Potassium oxide concentrations within the study area range from 0.82 to 4.52 % with a mean of 2.37 % (Fig. 26). The mean of 2.37 % is consistent with the Clarke value cited by Fortescue (1992) of 2.1 %.

Potassium oxide concentrations across the Paleozoic sedimentary rocks east of the Rio Grande and Cretaceous sedimentary rocks in the northwest range from 0.82 to 2.34 %. These values are consistent with those cited by Wedepohl (1978) for sedimentary rocks of 0.31 to 2.45 %. In areas dominated by Tertiary basaltic andesites, potassium oxide concentrations range from 0.82 to 2.75 %. Once again this is consistent with values cited by Wedepohl (1978) for basalts and andesites. Potassium oxide concentrations within areas dominated by Tertiary rhyolites typically range from 2.34 to 4.52 %.

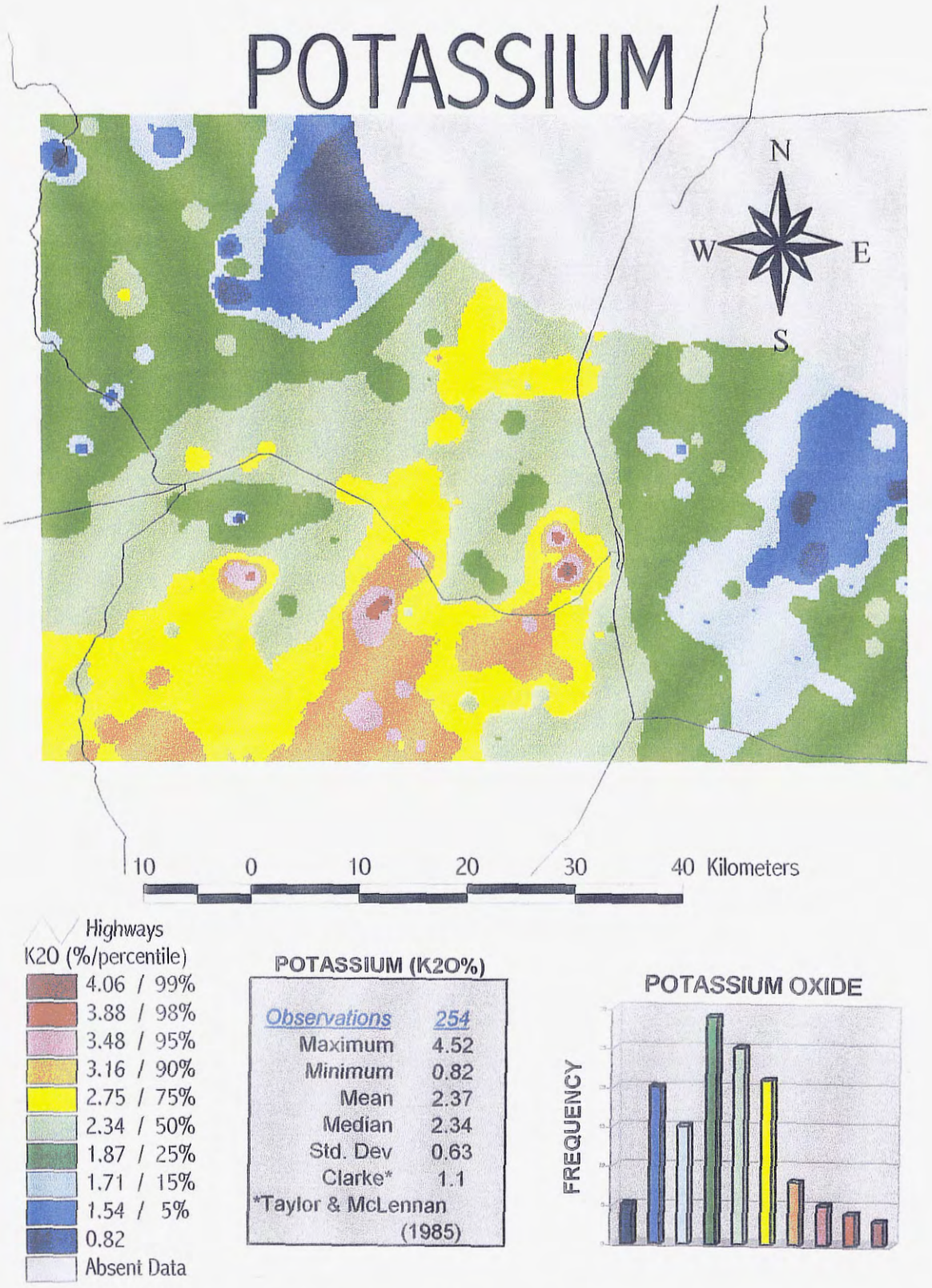

Figure 26. Potassium oxide distribution within the study area.

Potassium oxide enrichment occurs in two principal regions within the study area. The first region extends from Socorro Peak into the Chupadera Mountains while the other region occurs in South Canyon. This zone of enrichment does not match the expected zone of potassium metasomatism shown by Ennis (1996). This may in part be related to the breakdown of potassium into the clay size fraction that is easily removed. It may also be the result of the potassium alteration being restricted to lithology.

RUBIDIUM

Geochemistry

Rubidium is a lithophile element that is associated with potassium in igneous and sedimentary rocks (Rose et al., 1979). Rubidium does not form minerals of its own but is dispersed principally in potassium minerals such as micas and potassium feldspars (Wedepohl, 1978). In sedimentary rocks Rb is found in K-feldspars, micas, and clay minerals (BGS, 1992). Rubidium concentrations in regional metamorphism do not vary until the granulite facies (Wedepohl, 1978). Table 21 shows the concentrations of rubidium in some typical rocks and soils.

Table 21 Rubidium (ppm)

	Fortescue (1992)	Rose, Hawkes, and Webb (1979)	Wedepohl (1978)	Taylor and McLennan (1985)
Clarke	78.0			32.0
Ultramafic		0.14	0.2	
mafic		32.0		
granitic		276.0	190.0	
basalt			47.0	
andesite			73.0	
rhyolite			217.0	
sandstone		40.0	46.0	
limestone		56.0	45.0	
shale		143.0	164.0	
soils		35.0	140.0	
ores				

Data

Rubidium concentrations within the study area range from 38 to 294 ppm with a mean of 100 ppm (Fig. 27). This mean is higher than the Clarke value of 78 ppm cited by Fortescue (1992). The higher mean is likely the result of the abundance of rhyolites within the study area.

Rubidium concentrations across the Paleozoic sedimentary rocks east of the Rio Grande, Cretaceous sedimentary rocks in the northwest, and Tertiary basaltic andesites in the west range from 38 to 119 ppm. These values are consistent with those cited by Rose et al. (1979) and Wedepohl, (1979) for sedimentary and basaltic rocks. Regions dominated by Tertiary rhyolites have rubidium concentrations that range from 93 to 294 ppm. Once again these values are consistent with the value cited by Wedepohl (1978) of 217 ppm for rhyolites.

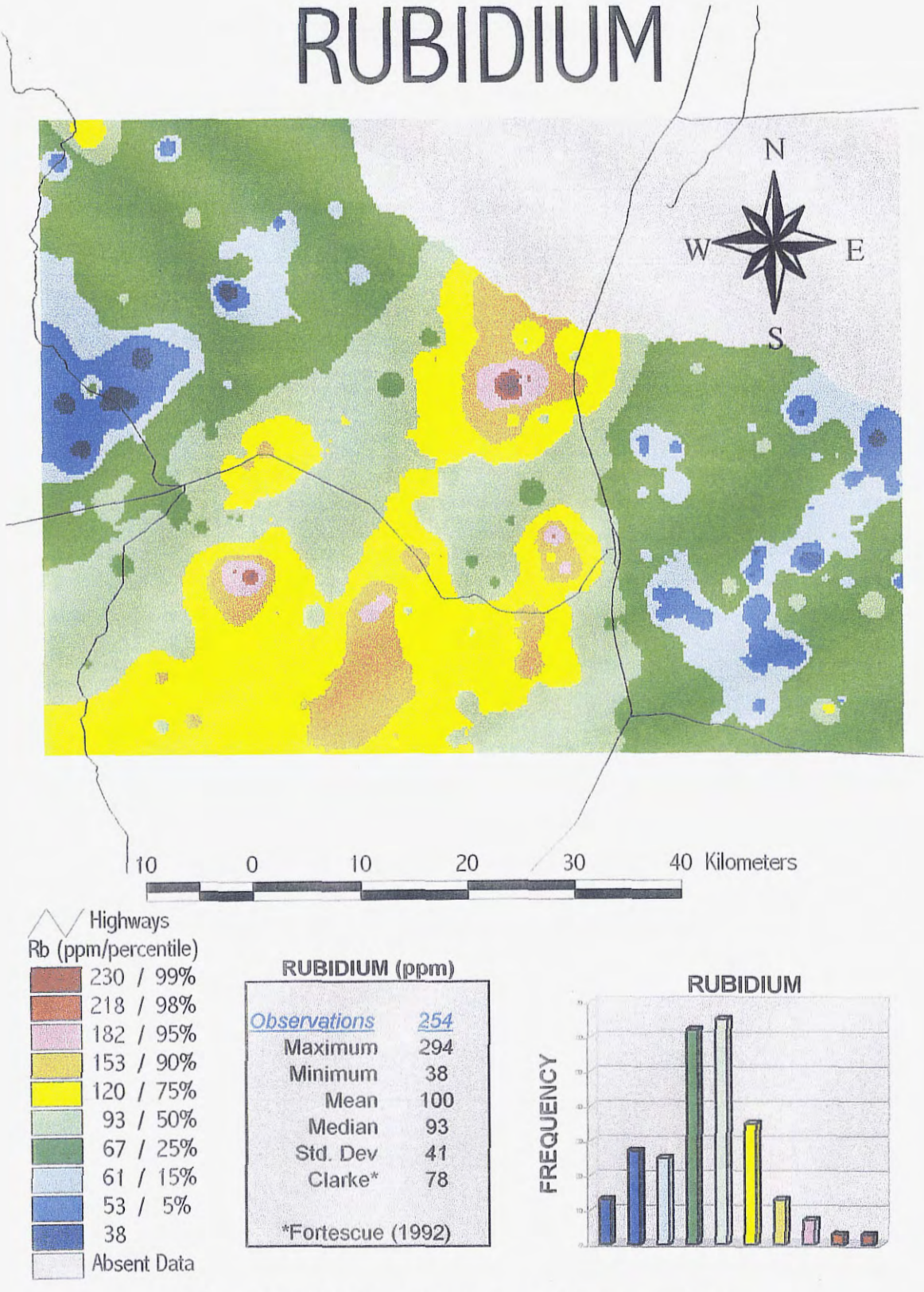

Figure 27. Rubidium distribution within the study area.

SILICON OXIDE

Geochemistry

Silicon is a major constituent in most rock-forming minerals and is commonly used as a measure of the degree of magmatic differentiation. Minerals such as olivines, pyroxenes, and amphiboles will weather quickly while quartz is highly resistant to weathering processes. The abundance of silica is sedimentary environments is highly variable and dependent on source areas and the amount of chemical precipitation which occurs. Table 22 shows the concentrations of silica in some typical rocks.

Table 22 Silicon Oxide (SiO2%)

	Fortescue (1992)	Rose, Hawkes, and Webb (1991)	Wedepohl (1978)	Taylor and McLennan (1985)
Clarke	59.3			57.3
Ultramafic			43.8	
mafic				
granitic			72.1	
basalt			50.1	
andesite			54.2	
rhyolite			73.7	
sandstone				
limestone				
shale				
soils				
ores				

Data

Silicon oxide concentrations within the study area range from 45.71 to 75.62 % with a mean of 64.50 % (Fig. 28). The mean of 64.50 % is slightly higher than the cited Clarke values of 57.3 and 59.3 % (Table 22). This is likely the result of the large percentage of quartz sandstones within the study area.

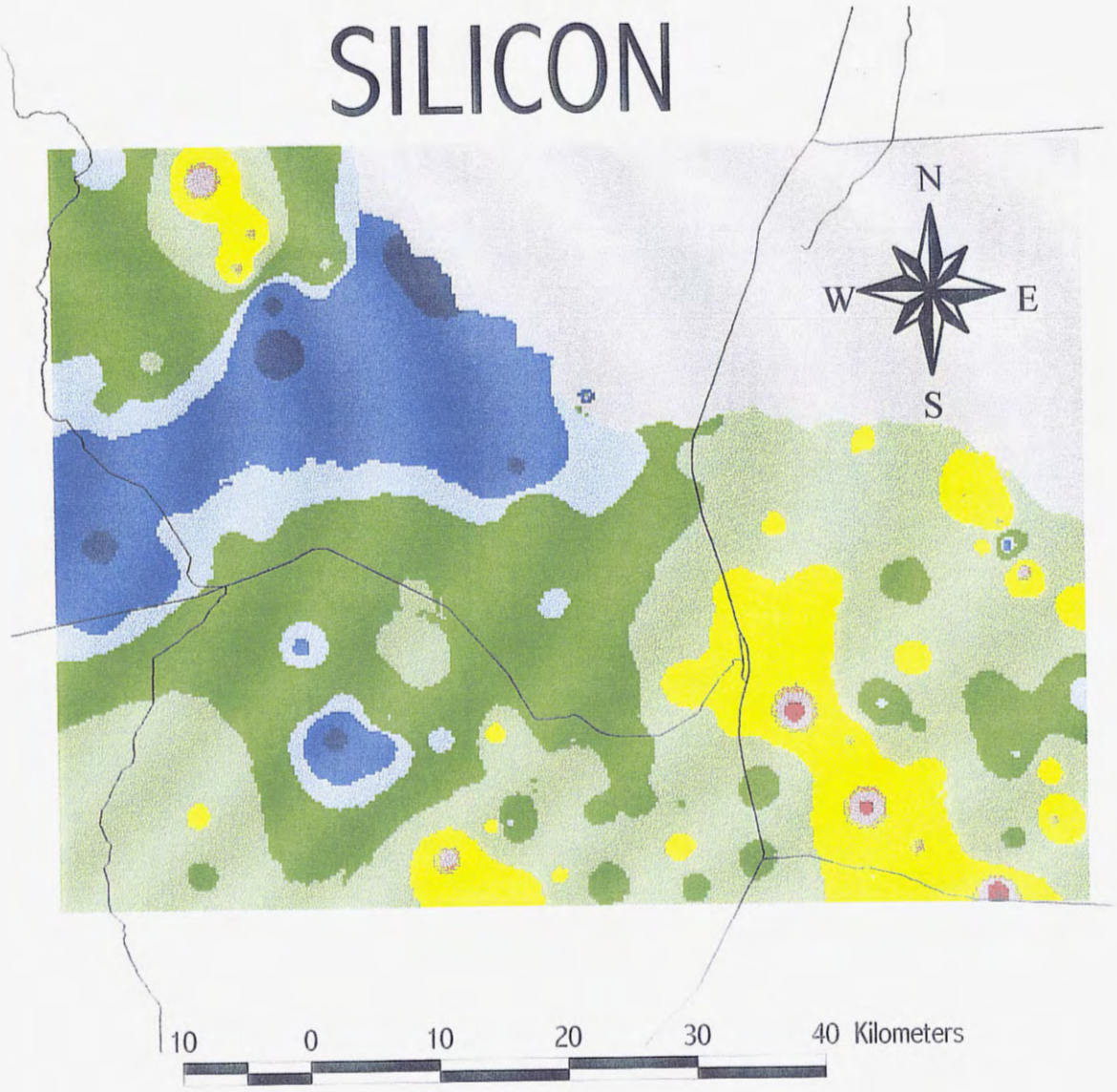

Highways
SiO2 (%/percentile)
75.31 / 99%
74.57 / 98%
73.12 / 95%
72.44 / 90%
69.41 / 75%
65.38 / 50%
60.26 / 25%
57.58 / 15%
51.30 / 5%
45.71
Absent Data

SILICON (SiO2%)

Observations	130
Maximum	75.62
Minimum	45.71
Mean	64.50
Median	65.38
Std. Dev	6.62
Clarke*	57.3

*Taylor & McLennan (1985)

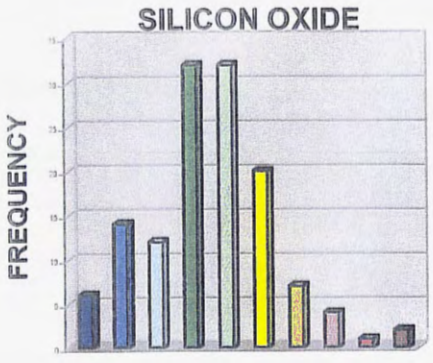

Figure 28. Silicon oxide distribution within the study area.

Silicon oxide concentrations are the lowest across the western portion of the study area. In this area, Tertiary basaltic andesites dominate and silicon concentrations range from 45.71 to 60.26 %. This range is consistent with the reported values of Wedepohl (1978) for basalts and andesites. Silicon oxide concentrations across areas dominated by Tertiary rhyolites range from 60.26 to 72.44 %.

The highest concentrations of silicon oxide within the study area are associated with the Paleozoic sedimentary rocks east of the Rio Grande, Cretaceous sedimentary rocks in the northwest region, and Quaternary sediments associated with the Rio Grande. Concentrations in these areas range from 60.26 to 75.62 %.

SODIUM OXIDE

Geochemistry

There is a close relationship between sodium, potassium, and calcium. In rock-forming minerals sodium is commonly replaced by ions such as Ca^{2+} and K^{+}. The majority of sodium within the earth's crust is contained in feldspars. Sodium is also important in micas, amphiboles, and pyroxenes. Sodium is soluble but with a low mobility during regional metamorphism. Sodium's low mobility leads to the formation of albite porphyroblasts during metamorphism. Sodic plagioclase is an important contributor to sodium in soils (Wedepohl, 1978). Sodium may be rapidly leached out of soils unless adsorbed to clays and organic matter (O'Neill, 1985). Table 23 shows the concentrations of sodium in some typical rocks and soils.

Table 23 Sodium Oxide (Na2O3%)

	Fortescue (1992)	Rose, Hawkes, and Webb (1991)	Wedepohl (1978)	Taylor and McLennan (1985)
Clarke	2.5			3.1
Ultramafic			0.10	
mafic				
granitic			3.48	
basalt			3.11	
andesite			3.58	
rhyolite			3.38	
sandstone			1.40	
limestone			0.17	
shale			0.80	
soils			0.84	
ores				

Data

Sodium oxide concentrations within the study area range from 0.46 to 3.63 % with a mean of 1.72 % (Fig. 29). The mean of 1.72 % is less than the cited Clarke value of 3.1 % (Taylor and McLennan, 1985).

Sodium oxide concentrations are the lowest across the Paleozoic sedimentary rocks east of the Rio Grande and the Cretaceous sedimentary rocks in the northwest region of the study area. Sodium oxide concentrations within these units range from 0.46 to 1.24 %. These values are lower than those cited for sedimentary rocks, but are very near the cited value for soils (Wedepohl, 1978). Concentrations of sodium oxide in areas dominated by Tertiary rhyolites typically range from 1.24 to 2.71 %. These values are significantly lower than the values cited by Wedepohl (1978) for rhyolites.

The highest concentrations of sodium oxide within the study area are associated with the Tertiary basaltic andesites located on the western boundary. Concentrations of

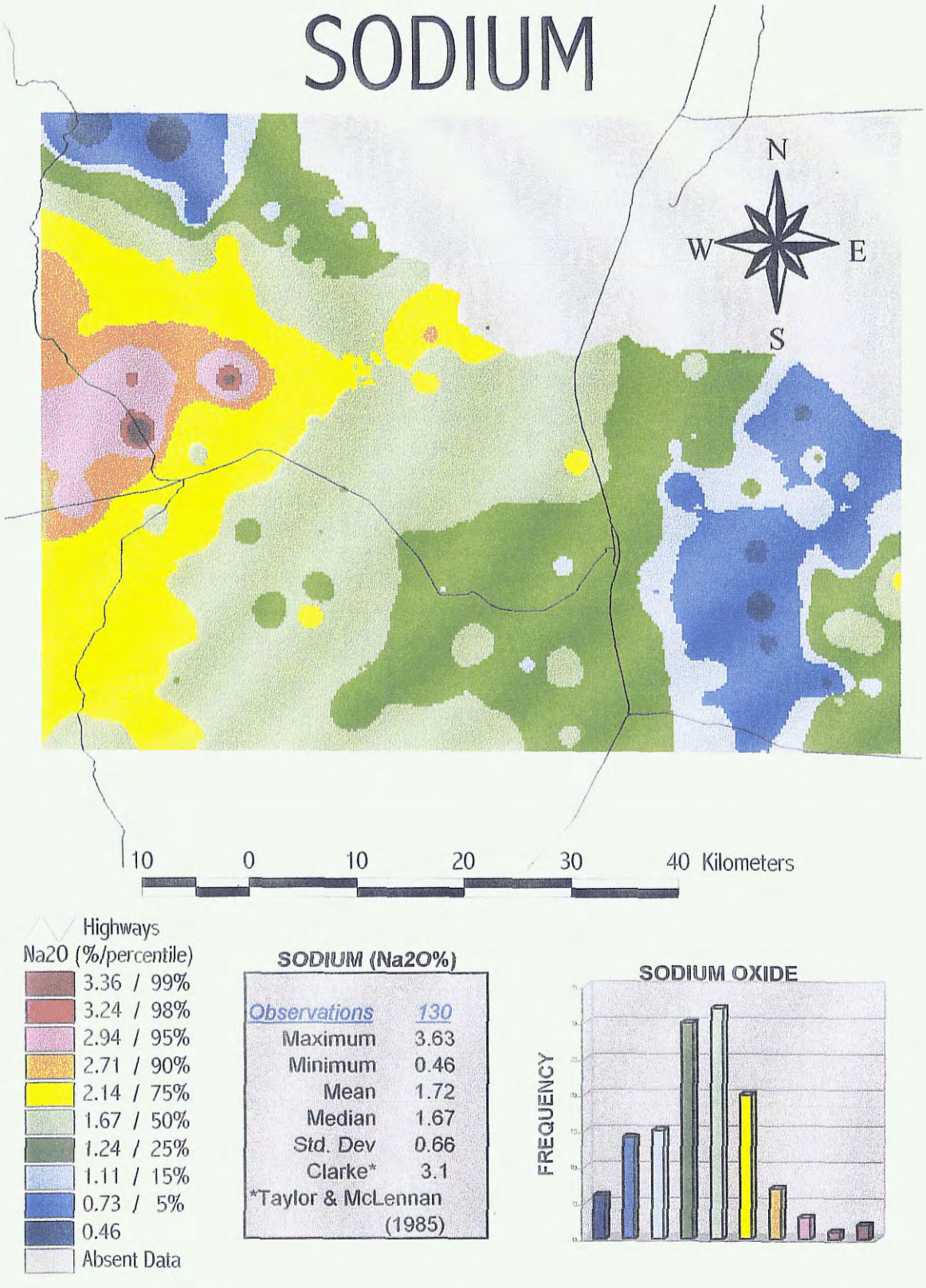

Figure 29. Sodium oxide distribution within the study area.

sodium oxide in this area range from 2.14 to 3.63 %. This is consistent with values cited by Wedepohl (1978) for basalts and andesites.

STRONTIUM

Geochemistry

Strontium is a lithophile element associated with calcium and barium (Rose et al., 1979). Most of the Sr within the earth's crust is dispersed in rock forming and accessory minerals (Wedepohl, 1978). Sr^{2+} is intermediate in size between Ca^{2+} and K^{+} and therefore may substitute in both plagioclase and potassium feldspars. Due to mid-stage fractionation, Sr is enriched in intermediate igneous rocks (BGS, 1992). Strontium is relatively immobile during high-grade metamorphism, but may be redistributed during contact metamorphism and hydrothermal alteration (BGS, 1992). Strontium is generally less mobile than calcium during weathering (Wedepohl, 1978). Strontium in stream sediments occurs principally in lithic fragments and detrital feldspars. In sedimentary rocks it is found in the Ca^{2+} and Ba^{2+} lattice sites of carbonates and sulfates (BGS, 1992). Table 24 shows the concentrations of strontium in some typical rocks and soils.

Table 24 Strontium (ppm)

	Fortescue (1992)	Rose, Hawkes, and Webb (1979)	Wedepohl (1978)	Taylor and McLennan (1985)
Clarke	384.0			260.0
Ultramafic		5.8	< 65.0	
mafic		465.0		
granitic		100.0	147.0	
basalt			554.0	
andesite			577.0	
rhyolite			40.0	
sandstone		20.0	40-150	
limestone		610.0		
shale		300.0	130-280	
soils		67.0	240.0	
ores				

Data

Strontium concentrations within the study area range from 115 to 1157 ppm with a mean of 384 ppm (Fig. 30). This mean is exactly equal to Fortescue's (1992) cited Clarke value of 384 ppm.

Strontium concentrations are the lowest across the Paleozoic sedimentary rocks east of the Rio Grande and the Cretaceous sedimentary rocks in the northwest section of the study area. Concentrations in these regions range from 115 to 215 ppm. These values are consistent with those for sandstones but may be elevated due to the presence of both limestones and shales in these areas. Strontium concentrations across the Tertiary rhyolites range from 115 to 466 ppm. These values are well above the value cited by Wedepohl (1978) for rhyolites of 40 ppm.

The highest concentrations of strontium within the study area occur in the western region. Strontium concentration in this area range from 466 to 1157 ppm and are the

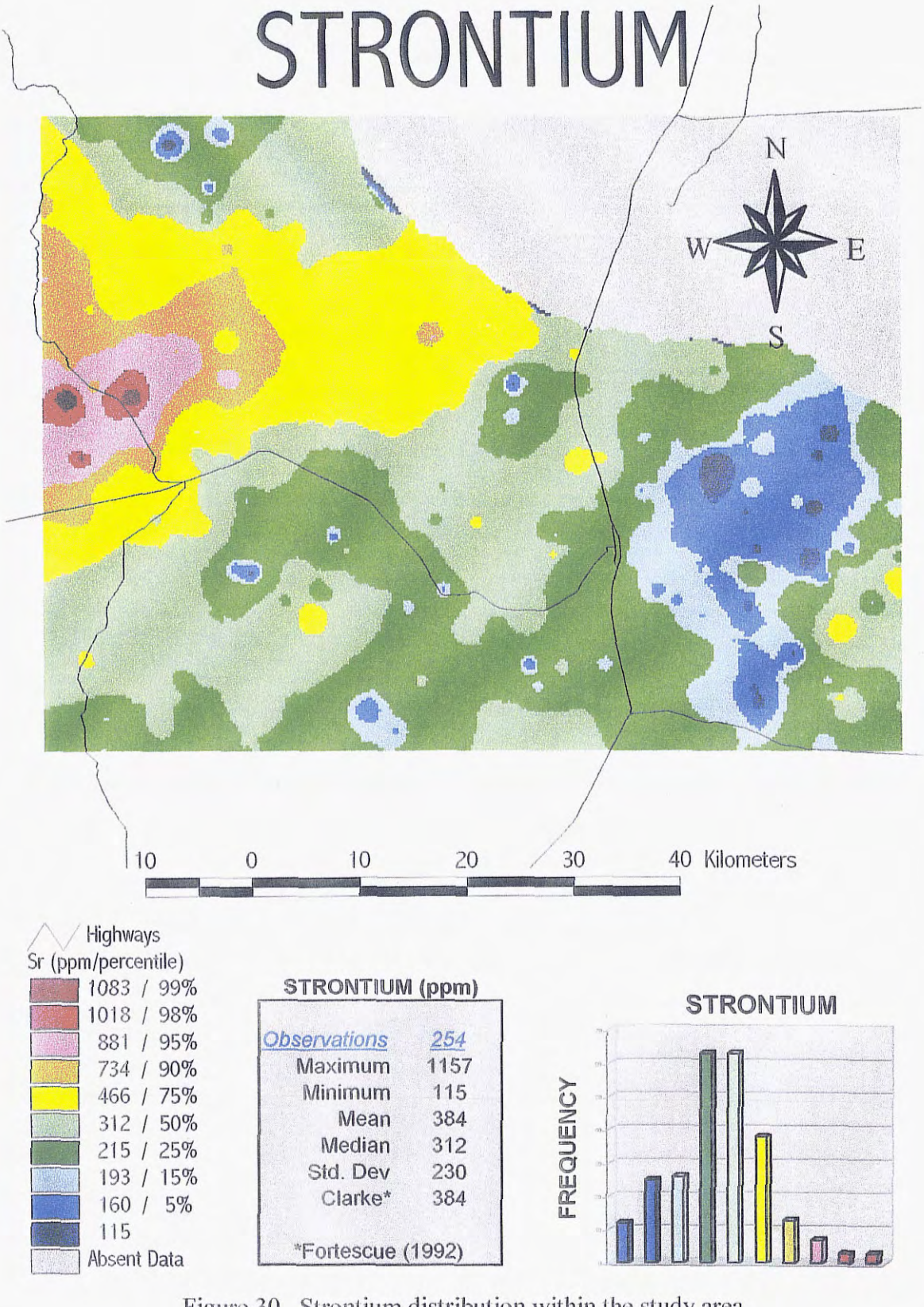

Figure 30. Strontium distribution within the study area.

result of the Tertiary basaltic andesites which occur in this area. These values are consistent with the values cited by Wedepohl (1978) and Rose et al. (1979) for basalts.

THORIUM

Geochemistry

Thorium is a lithophile element occurring in accessory minerals of igneous rocks (Rose et al., 1979). Similarities in ionic size, electron configuration, and bond character are the main reasons for the close relationship between thorium, cesium, uranium, and zirconium (Wedepohl, 1978). Thorium tends to be incorporated in primary minerals in igneous rocks, thus reducing its ability to concentrate in late-stage fluids (Wedepohl, 1978). Thorium occurs in monazite and as a minor constituent in allanite, sphene, and zircon. These minerals occur with gold, magnetite, and other heavy minerals (Rose et al., 1979). Concentrations of thorium in metamorphic rocks are highly variable (Wedepohl, 1978). The relatively immobile thorium is concentrated in residual materials such as weathered rocks and soils. This concentration leads to a fractionation between uranium and thorium as oxidation of uranium forms a soluble uranyl ion (Wedepohl, 1978). Table 25 shows the concentration of thorium in some typical rocks and soils.

Table 25 Thorium (ppm)

	Fortescue (1992)	Rose, Hawkes, and Webb (1979)	Wedepohl (1978)	Taylor and McLennan (1985)
Clarke	8.1			3.5
Ultramafic		0.004		
mafic		2.7		
granitic		20.0	10-20	
basalt			0.5-2	
andesite				
rhyolite				
sandstone		5.5	1.7	
limestone		1.7	1.1	
shale		12.0	13.1	
soils		13.0		
ores				

Data

Thorium concentrations within the study area range from less than 3 to 55 ppm with a mean of 11 ppm (Fig. 31). This value is slightly higher than Fortescue's (1992) Clarke of 8.1 ppm. This is likely the result of the abundance of rhyolites within the study area as well as the increased concentration of thorium in residual materials.

Thorium concentrations across the Paleozoic sedimentary rocks east of the Rio Grande, Cretaceous sedimentary rocks in the northwest, and Tertiary basaltic andesites in the west range from less than 3 to 12 ppm. These values are consistent with values cited for sedimentary rocks and basalts (Rose et al., 1979; Wedepohl, 1978). Thorium concentrations across the Tertiary rhyolites range from 8 to 43 ppm. These values are again consistent with the values cited by Rose et al. (1979) for granites of 20 ppm.

Elevated concentrations of thorium occur in the Hop Canyon and North Magdalena mining districts as well as in the Polvadera Mountain region. The highest

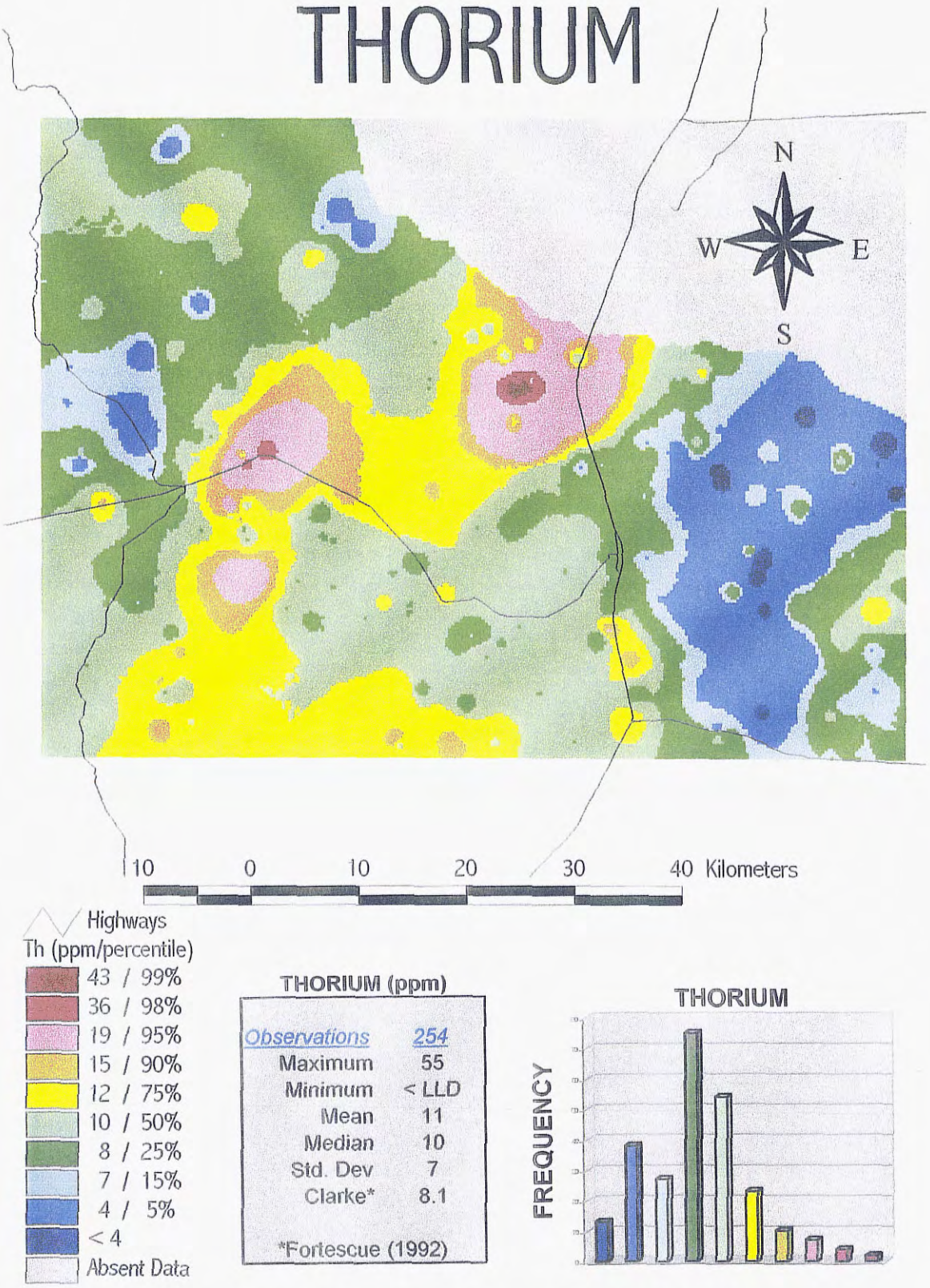

Figure 31. Thorium distribution within the study area.

concentrations within the study area occur at Polvadera Mountain and are likely the result of Precambrian granites as well as the carbonatite dikes.

TITANIUM OXIDE

Geochemistry

Titanium in minerals occurs principally in the tetravalent oxidation state (Wedepohl, 1978). During magmatic processes Ti^{4+} is partitioned into iron-titanium oxides such as ilmenite and magnetite and TiO_2 phases such as rutile and anatase (BGS, 1992). Titanium may partially replace Al^{3+}, Fe^{3+}, Nb^{5+}, Ta^{5+}, and Mn^{3+} in a large number of minerals (Wedepohl, 1978). Concentrations of titanium in sedimentary rocks are determined by the abundance of detrital oxides and silicates. The largest proportion of titanium in stream sediments occurs in minerals such as rutile, ilmenite, and sphene (BGS, 1992). Table 26 shows the concentrations of titanium in some typical rocks.

Table 26 Titanium Oxide (TiO2%)

	Fortescue (1992)	Rose, Hawkes, and Webb (1979)	Wedepohl (1978)	Taylor and McLennan (1985)
Clarke	0.7			0.9
Ultramafic			1.7	
mafic				
granitic			0.20-0.37	
basalt				
andesite			1.31	
rhyolite			0.17-0.22	
sandstone				
limestone			0.03	
shale			0.87	
soils				
ores				

Data

Titanium oxide concentrations within the study area range from < 0.5 to 3.4 % with a mean of 0.9 % (Fig. 32). The mean of 0.9 % is identical to the Clarke value cited by Taylor and McLennan (1985).

Titanium oxide concentrations are the lowest across the Paleozoic sedimentary rocks east of the Rio Grande. In this region concentrations typically range from < 0.5 to 0.6 %. This value is consistent with Wedepohl's (1978) cited values for sedimentary rocks. The Cretaceous sedimentary rocks in the northwest region of the study area have slightly higher concentrations of titanium oxide. In areas dominated by Tertiary rhyolites, titanium oxide concentrations range from 0.6 to 1.6 %. This range is considerably higher than that cited by Wedepohl (1978) for rhyolites.

The highest concentrations of titanium oxide in the study area are located in the west and are associated with Tertiary basaltic andesites. Titanium oxide concentrations within this area range from 1.1 to 3.4 %. This is consistent with Wedepohl's (1978) reference for andesites.

URANIUM

Geochemistry

Uranium is a lithophile element commonly associated with vanadium, arsenic, phosphorus, molybdenum, selenium, lead, and copper in the Colorado Plateau as well as cobalt and silver in some sulfide deposits (Rose et al., 1979). Uranium in minerals has valence states of 4^+, 5^+, and 6^+. Uranium occurs in a variety of minerals but is concentrated in a few species of minor abundance. The most abundant uranium mineral

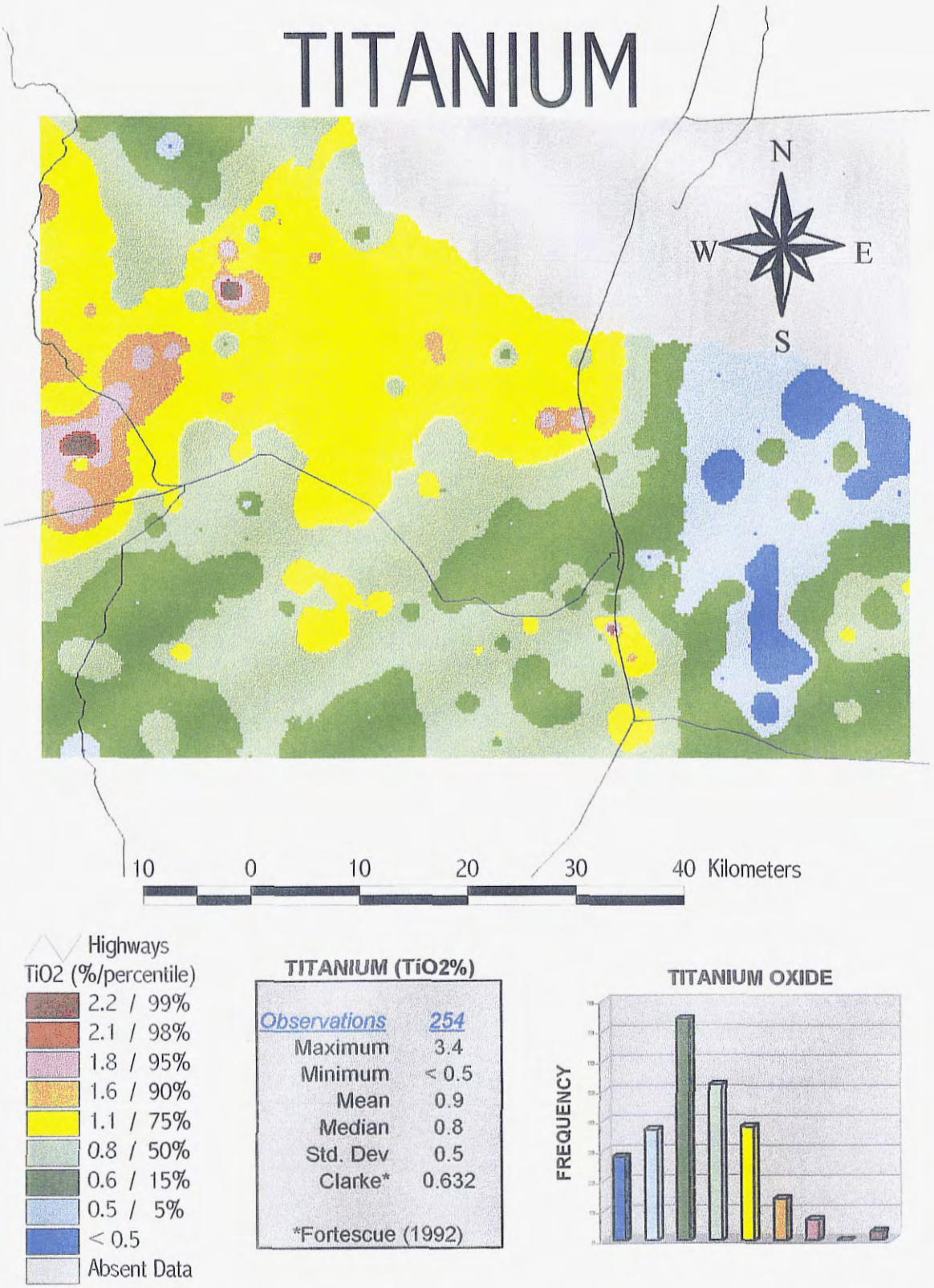

Figure 32. Titanium oxide distribution within the study area.

is uraninite (Wedepohl, 1978). In magmas the U^{4+} ion behaves incompatibly and becomes enriched in late-stage differentiates, typically in minerals such as zircon and allanite. Secondary enrichment of uranium may occur with the emplacement of acid volcanics and intrusives related to deuteric and hydrothermal activity (BGS, 1992). Uranium weathers to form complex carbonates, phosphates, vanadates, and silicates (Rose et al., 1979). Uranium in stream sediments may be present in resistant minerals such as zircon, monazite, and allanite. Further distribution of uranium in stream sediments is controlled by Eh and pH conditons with the main redox process being the oxidation of low solubility U^{4+} to the highly soluble uranyl cation UO_2^{2+}. The uranyl cation may then be reprecipitated by reduction at redox boundaries (BGS, 1992). Uranium is also strongly sorbed to both organic matter and iron oxides (Rose et al., 1979). Table 27 shows the concentrations of uranium in some typical rocks and soils.

Table 27 Uranium (ppm)

	Fortescue (1992)	Rose, Hawkes, and Webb (1979)	Wedepohl (1978)	Taylor and McLennan (1985)
Clarke	2.3			0.91
Ultramafic		0.03	0.84	
mafic		0.53		
granitic		3.9	2.2	
basalt				
andesite			0.8	
rhyolite			5.0	
sandstone		1.7	0.45-2.1	
limestone		2.2	2.2	
shale		3.7	3.2	
soils		1.0		
ores				

Data

Uranium concentrations within the study area range from less than 2 to 39 ppm with a mean of 3 ppm (Fig. 33). This value is slightly higher than Fortescue's (1992) Clarke of 2.3 ppm.

Uranium concentrations throughout much of the study area range from less than 2 to 3 ppm. Concentrations of 3 to 4 ppm occur in areas dominated by Tertiary rhyolites. This is consistent with the values for various rocks cited by Rose et al. (1979) and Wedepohl (1978). Uranium concentrations above 6 ppm occur in just a few places within the study area. These locations include the Hop Canyon, North Magdalena, and Water Canyon mining districts, as well as the Polvadera Mountain region. The highest concentrations of uranium within the study area are found within Copper Canyon.

VANADIUM

Geochemistry

Vanadium is a lithophile element associated with uranium in secondary uranium minerals of the Colorado Plateau, iron oxides, and organic matter in normal soils (Rose et al., 1979). V^{3+} has an ionic radius very similar to Fe^{3+} and therefore vanadium tends to follow iron in mineral formation (BGS, 1992; Wedepohl, 1978). There are no primary vanadium magmatic minerals. Instead the minerals magnetite and ilmenite are the primary carriers of vanadium. The vanadium minerals that are known are all secondary forming under surface conditions (Wedepohl, 1978). Vanadium is largely immobile during metamorphism (BGS, 1992). During weathering vanadium remains in the residual minerals or enters minerals in the silt or clay fraction. In the clay fraction

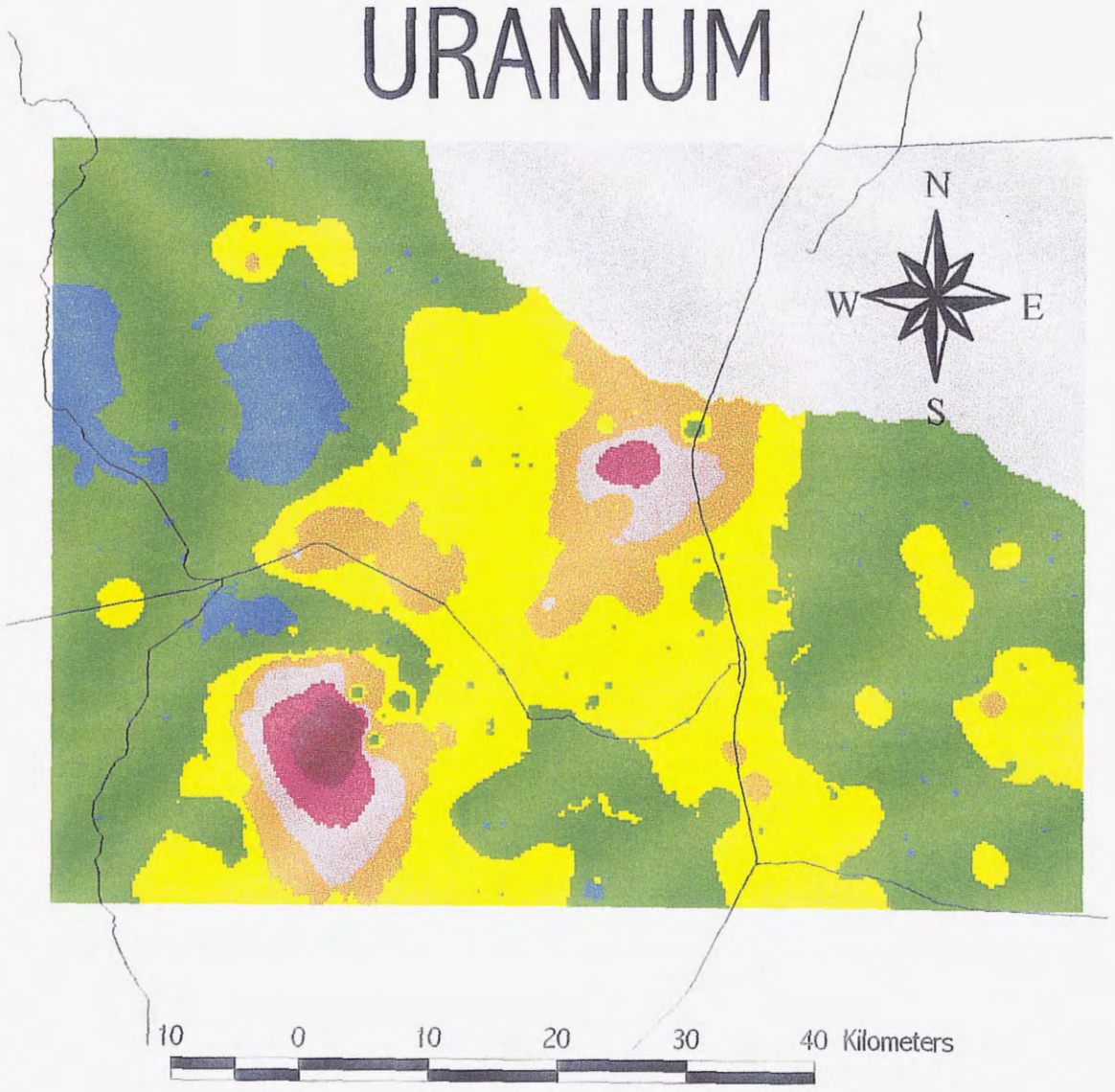

Figure 33. Uranium distribution within the study area.

vanadium may be adsorbed into clay mineral structures or in iron oxide coatings (Wedepohl, 1978). In sedimentary rocks vanadium concentrations reflect the abundance of detrital iron oxides, clay minerals, hydrous oxides of both iron and manganese, and organic matter content (BGS, 1992). Table 28 shows the concentrations of vanadium in some typical rocks and soils.

Exposure to high levels of vanadium may cause harmful health effects. High levels of vanadium that are inhaled may have major effects on the lungs, throat, and eyes. Animals that have ingested large quantities of vanadium have even died. However, the quantities ingested were much larger than those likely to occur in the environment (ATSDR, 1995b).

Table 28 Vanadium (ppm)

	Fortescue (1992)	Rose, Hawkes, and Webb (1979)	Wedepohl (1978)	Taylor and McLennan (1985)
Clarke	136.0			230.0
Ultramafic		40.0	40-100	
mafic		250.0		
granitic		44.0	72.0	
basalt			266.0	
andesite				
rhyolite				
sandstone		20.0	12.0	
limestone		20.0	10-80	
shale		130.0		
soils		57.0	56.0	
ores				

Data

Vanadium concentrations within the study area range from 28 to 478 ppm with a mean of 127 ppm (Fig. 34). This value is consistent with the Clarke value cited by Fortescue (1992) of 136 ppm.

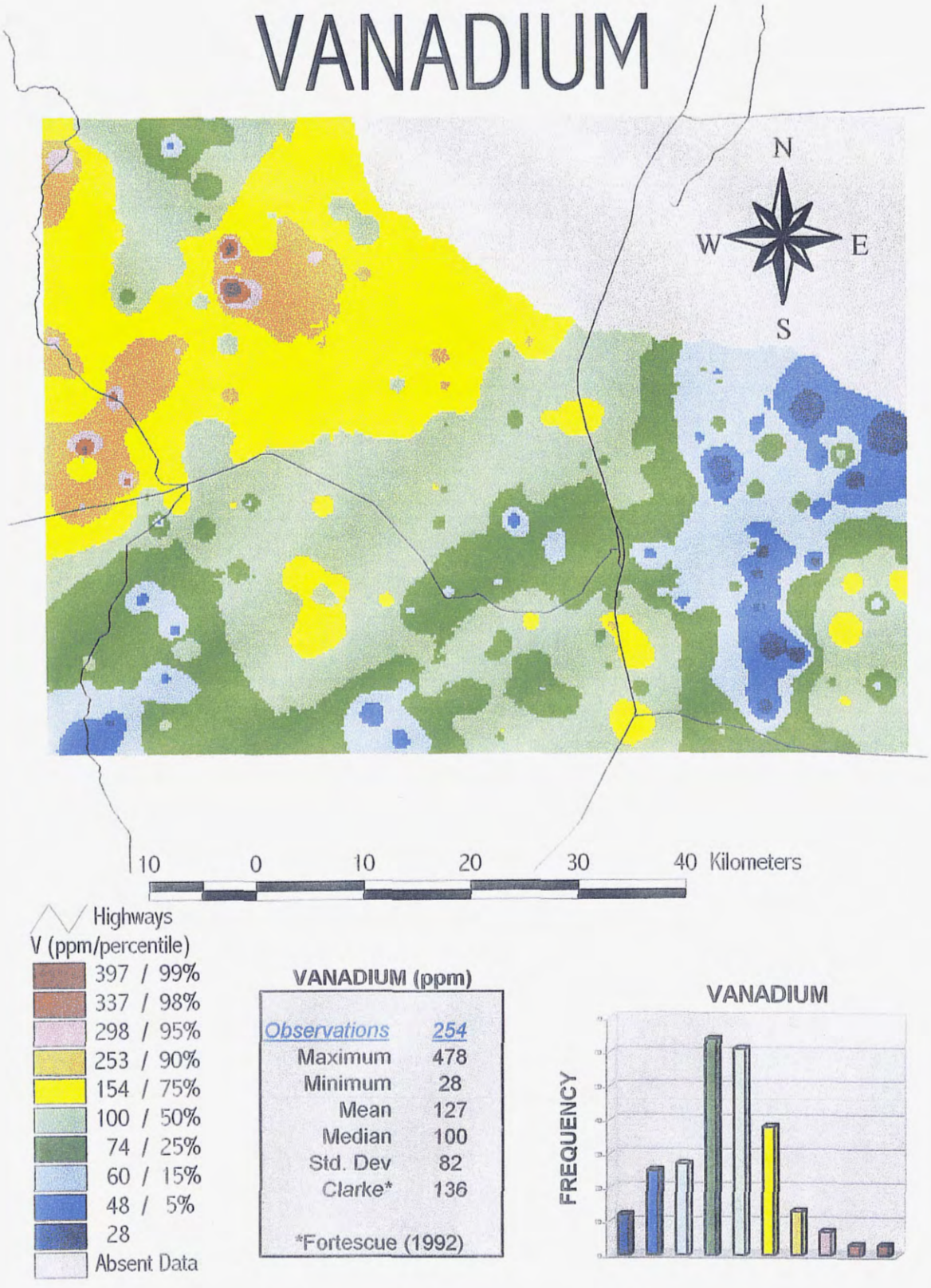

Figure 34. Vanadium distribution within the study area.

Vanadium concentrations across the Paleozoic sedimentary rocks east of the Rio Grande, Cretaceous sedimentary rocks in the northwest, and the Quaternary and Tertiary sediments in the southwest region range from 28 to 100 ppm.

Vanadium concentrations across Tertiary rhyolites range from 48 to 253 ppm. These values are consistent with those cited by Rose et al. (1979) and Wedepohl, (1979) for granitic rock types. Vanadium concentrations across the northwest region of the study area range from 154 to 478 ppm. This is due to the presence of Tertiary basaltic andesites within this area. The concentrations within this area once again match those cited for basalts by Rose et al. (1979) and Wedepohl, (1979).

YTTRIUM

Geochemistry

During magmatic processes yttrium is stongly partitioned into garnet, hornblende, clinopyroxene, and biotite. There is very little evidence for the mobility of yttrium during metamorphism. Yttrium in stream sediments is held in accessory minerals that are resistant to weathering such as garnet, apatite, sphene, monazite, and zircon. The concentration of yttrium in sedimentary rocks is determined by the abundance of the resistant minerals mentioned (BGS, 1992). Table 29 shows the concentrations of yttrium in some typical rocks and soils.

Table 29 Yttrium (ppm)

	Fortescue (1992)	BGS (1992)	Wedepohl (1978)	Taylor and McLennan (1985)
Clarke	31.0			20.0
Ultramafic				
mafic				
granitic		40.0	38.0	
basalt		32.0	32.0	
andesite				
rhyolite				
sandstone		15.0	15.0	
limestone		4.0	3.8	
shale		40.0	38.4	
soils				
carbonatite			35-95	

Data

Yttrium concentrations within the study area range from 13 to 233 ppm with a mean of 34 ppm (Fig. 35). This mean is consistent with the Clarke value cited by Fortescue (1992) of 31 ppm.

Yttrium concentrations across the Paleozoic sedimentary rocks east of the Rio Grande, Cretaceous sedimentary rocks in the northwest, and Tertiary basaltic andesites in the west range from 13 to 34 ppm. The sedimentary rocks have concentrations that generally range from 13 to 26 ppm while the basaltic rocks generally range from 26 to 34 ppm. These values are consistent with the cited values of the BGS (1992) and Wedepohl (1979) for sedimentary rocks and basalts. In regions dominated by Tertiary rhyolites yttrium concentrations range from 26 to 60 ppm.

Elevated concentrations of yttrium occur in the south central region, near Water Canyon, and at Polvadera Mountain. The maximum concentration of 233 ppm occurs at

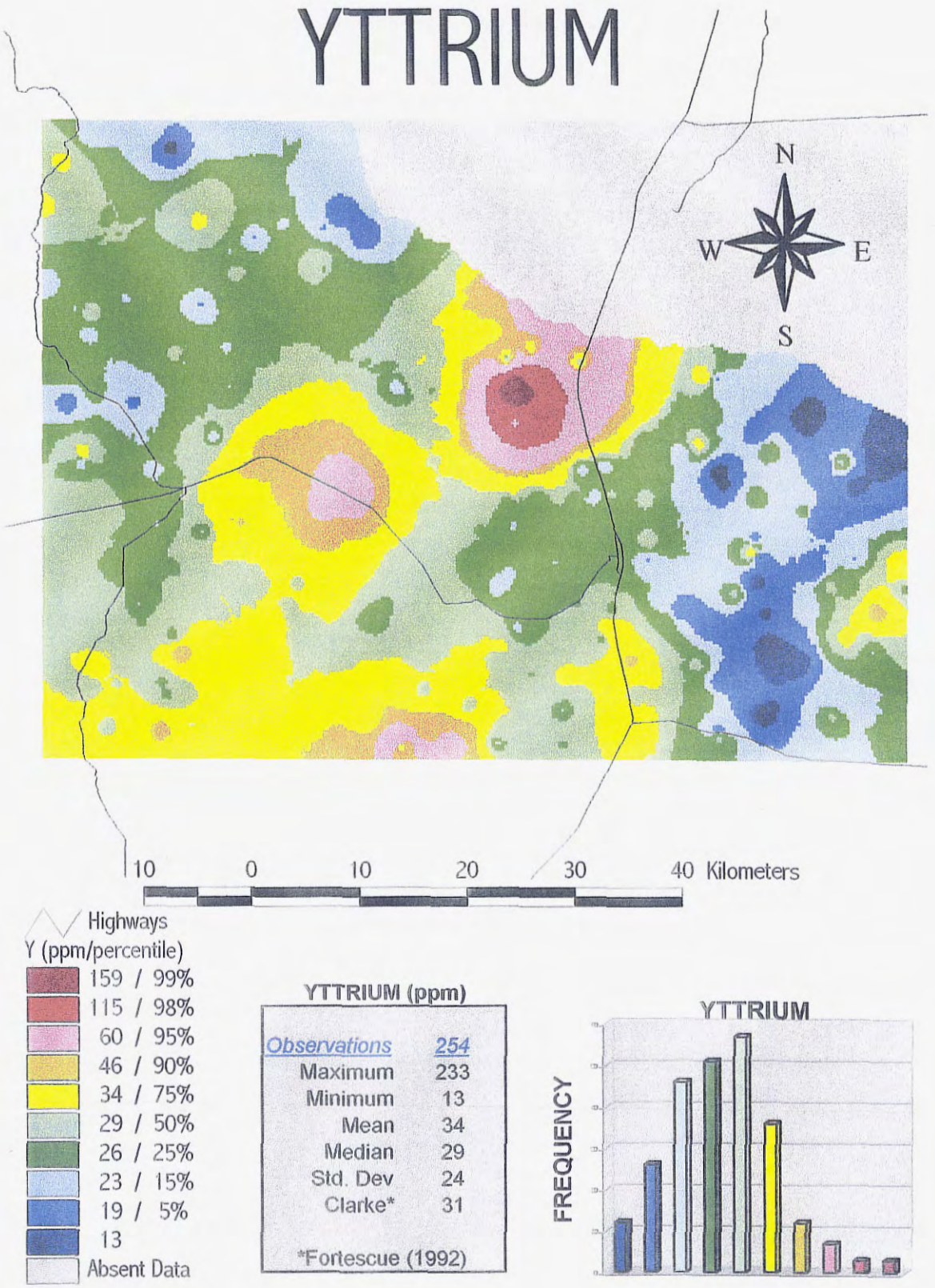

Figure 35. Yttrium distribution within the study area.

Polvadera Mountain. Yttrium enrichment in this area is the result of the presence of both Precambrian granites as well as carbonatite dikes.

ZINC

Geochemistry

Zinc is a chalcophile element associated with Cu, Pb, Ag, Au, Sb, As, and Se in both base and precious metal deposits (Rose et al., 1979). In magmatic processes zinc is enriched in early differentiates. Zinc becomes partitioned into silicates and oxides by substitution for both Fe^{2+} and Mg^{2+}. In mafic rocks the principal zinc bearing mineral is magnetite while in granites biotite is more important. Sphalerite is a common zinc mineral found in hydrothermal ore deposits (BGS, 1992). Zinc goes into solution during the weathering of silicates and oxides but has a low mobility and is easily adsorbed on clay minerals, iron oxides, and organic substances. Concentrations of zinc are commonly slightly higher in soils than in undecomposed rock. In streams sediments zinc principally occurs in detrital matter (Wedepohl, 1978). Table 30 shows the concentrations of zinc in some typical rocks and soils.

The breathing or ingesting of large quantities of zinc may result in stomach cramps, nausea, vomiting, anemia, pancreas damage, and a short term disease called metal fume fever. Because of the adverse health affects of zinc, the EPA has set a limit of 5 ppm of zinc in drinking water (ATSDR, 1995c).

Table 30 Zinc (ppm)

	Fortescue (1992)	Rose, Hawkes, and Webb (1979)	Wedepohl (1978)	Taylor and McLennan (1985)
Clarke	76.0			80.0
Ultramafic		58.0		
mafic		94.0		
granitic		51.0	75.0	
basalt			84.0	
andesite			69.9	
rhyolite			75.0	
sandstone		40.0	23.0	
limestone		21.0	20.0	
shale		100.0	93.0	
soils		36.0	44.0	

Data

Zinc concentrations within the study area range from 22 to 19,818 ppm with a median value of 74 ppm (Fig. 36). The median value of 74 ppm is consistent with the 76 to 80 ppm cited for the Clarke value (Table 30).

The lowest concentrations of zinc within the study area occur in the Paleozoic sedimentary rocks east of the Rio Grande and in the Cretaceous sedimentary rocks in the northwest. Concentrations of zinc in these regions range from 22 to 54 ppm. This range is consistent with that cited for sedimentary rocks by Rose et al. (1979). Zinc concentrations in areas dominated by Tertiary rhyolites and basaltic andesites range from 54 to 161 ppm. These values are again consistent with values cited for basalts, andesites, and rhyolites (Wedepohl, 1978).

Zinc concentrations exceed the 95th percentile in three regions. These include Polvadera Mountain, Socorro Peak, and a region extending from the town of Magdalena through Copper Canyon. The Socorro Peak and Magdalena regions coincide with the

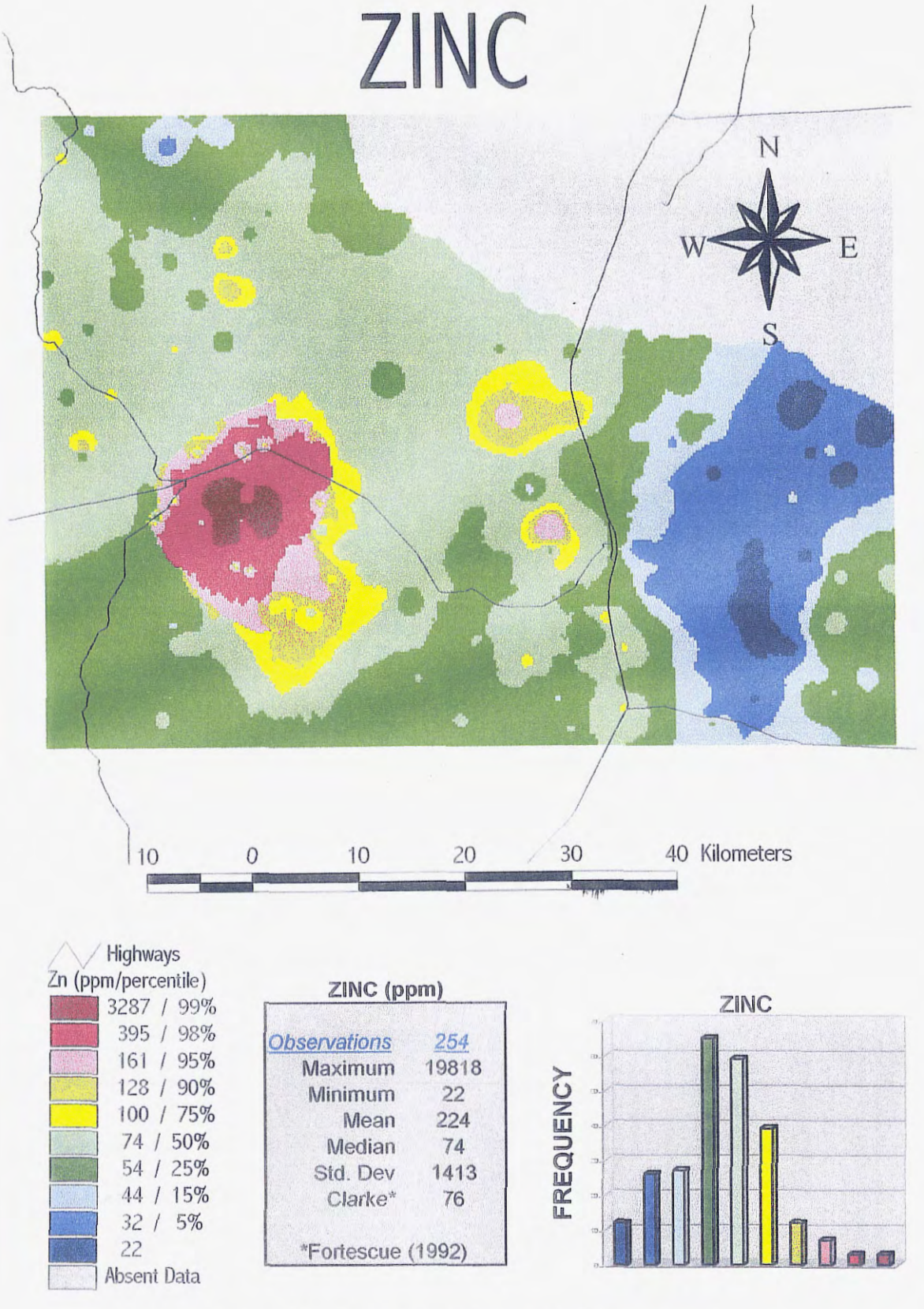

Figure 36. Zinc distribution within the study area.

Socorro Peak, North Magdalena, Magdalena, Hop Canyon, and Water Canyon mining districts.

ZIRCONIUM

Geochemistry

Zirconium is a lithophile element occurring in accessory zircon in igneous rocks (Rose et al., 1979). During magmatic processes the Zr^{4+} ion is incompatible with the lattice sites of most common rock forming silicates. Instead it is preferentially partitioned into accessory phases such as zircon, baddeleyite, and sphene (BGS, 1992). Zirconium may replace titanium, niobium, tantalum, iron, and the rare earth elements (Wedepohl, 1978). Zirconium may be remobilized during metasomatism and granite related hydrothermal alteration (BGS, 1992). During hydrothermal processes, Zr tends to concentrate in veins (Wedepohl, 1978). Zirconium accumulates in weathering profiles. This accumulation is due to the resistant nature of zircons, which may survive several cycles of erosion (Wedepohl, 1978). The abundance of zirconium in sedimentary rocks is due to the presence of detrital minerals such as zircon and sphene. Zirconium when mobilized is also rapidly adsorbed onto clays as $Zr(OH)_4$ (BGS, 1992). Table 31 shows the concentration of zirconium in some typical rocks and soils.

Table 31 Zirconium (ppm)

	Fortescue (1992)	Rose, Hawkes, and Webb (1979)	Wedepohl (1978)	Taylor and McLennan (1985)
Clarke	162.0			100.0
Ultramafic		45.0		
mafic		140.0	140.0	
granitic		175.0	175.0	
basalt				
andesite			120.0	
rhyolite			136.0	
sandstone		220.0	188-387	
limestone		19.0	18.0	
shale		160.0	197.0	
soils		270.0	264.0	
ores				

Data

Zirconium concentrations within the study area range from 216 to 3678 ppm with a mean of 619 ppm (Fig. 37). This value is much higher than the referenced Clarke values of either Fortescue (1992) or Rose et al. (1979). This is likely the result of zirconium being enriched in sediments due to weathering resistant minerals such as zircon.

Zirconium concentrations within the study area are variable and show no distinction with rock type. This is consistent with the very similar numbers given for various rock types by Rose et al. (1979) and Wedepohl (1979). The highest concentrations occur at Polvadera Mountain and are associated with the carbonatite dikes in this region.

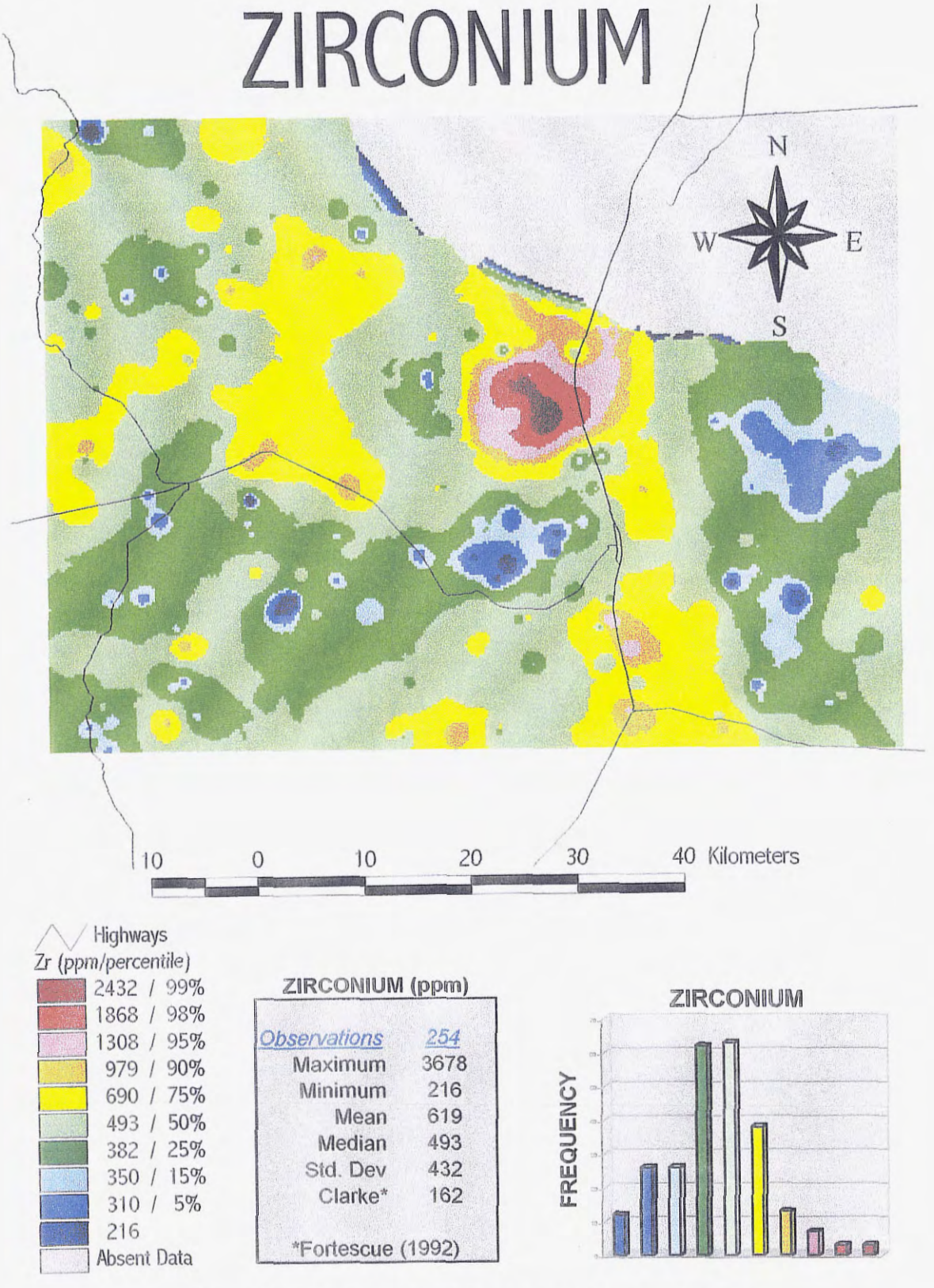

Figure 37. Zirconium distribution within the study area.

INTERPRETATIONS

The following paragraphs will briefly discuss a few of the observations that can be made about the data obtained from this project and how they relate to the geology of the study area. In particular, some general interpretations made on the data as a whole and then a discussion of the potassium metasomatized region that occurs within the study area. These brief comments are largely based on mapped element distribution as well as the statistical results obtained from the data set. Table 32 shows the results of the Spearman's correlation coefficients determined for the data set. In the Spearman's method a correlation of 1 tells us that y increases as x increases. This relationship does not have to fall on a straight line to be considered perfect.

General Interpretations

The first thing that is evident from looking at Table 32 is that the regional geology is strongly controlling the elemental relationships. This is reflected by the strong positive and negative correlations of Fe_2O_3, MnO, Na_2O, SiO_2, TiO_2, Cr, Ga, Ni, Sr, and V. With the exception of SiO2, which has a negative correlation with the other elements, the elements have low concentrations in the Paleozoic sediments, moderate concentrations in the Tertiary rhyolites, and the highest concentrations in the Tertiary basaltic andesites.

The correlation coefficients also emphasize geochemical relationships that have long been recognized. These relationships include potassium-rubidium, aluminum-gallium, and barium-strontium. The data from this project continue to reflect these relationships with strong correlations between the element pairs.

From simply looking at the data in map view it was evident that a relationship existed between iron-manganese oxides and many metals. This relationship is further

Table 32. Correlation Coefficients

SiO2	Al2O3	Fe2O3	CaO	K2O**	MgO	Na2O	TiO2*	P2O5	MnO	As	Ba	Cr	Cu	Ga	Mo	Nb	Ni	Pb	Rb	Sr	Th	U	V	Y	Zn	Zr	
1.0000	-0.5667	-0.7762	-0.2519	0.0467	-0.4892	-0.4937	-0.6553	-0.6469	-0.6601	-0.2707	-0.4426	-0.7420	-0.6343	-0.7514	0.2278	-0.1578	-0.8111	-0.2748	-0.0775	-0.6313	-0.2212	-0.0105	-0.7465	-0.1602	-0.6433	-0.0085	SiO2 (%)
	1.0000	0.5275	-0.4565	0.4435	0.1023	0.6996	0.4976	0.4367	0.5581	0.0930	0.4997	0.4106	0.5592	0.6630	-0.2251	0.4626	0.5680	0.5228	0.3972	0.5214	0.4174	0.0367	0.4390	0.3893	0.5809	-0.0797	Al2O3 (%)
		1.0000	-0.0160	0.0771	0.3033	0.6094	0.8467	0.5966	0.7692	0.3604	0.5293	0.6513	0.6169	0.7934	0.0703	0.3238	0.8116	0.3745	0.0295	0.6453	0.3346	0.1170	0.9635	0.3878	0.7601	0.4346	*Fe2O3 (%)**
			1.0000	-0.7155	0.5637	-0.3201	-0.1274	-0.0244	-0.2531	-0.1456	-0.2030	0.0784	-0.2078	-0.2836	-0.1629	-0.6267	0.0450	-0.5676	-0.5647	0.0147	-0.5372	-0.2982	0.0414	-0.5361	-0.3000	0.4685	CaO (%)
				1.0000	-0.5197	0.3325	0.1668	0.2878	0.3564	0.3151	0.3405	-0.0194	0.3653	0.3313	0.2061	0.7458	0.0390	0.7355	0.6937	0.0847	0.6766	0.4116	0.0141	0.6244	0.4128	0.0578	K2O (%)**
					1.0000	-0.0177	0.1692	0.2212	0.0340	-0.2330	-0.0876	0.4015	0.1534	0.2103	-0.3758	-0.4059	0.4969	-0.3519	-0.4171	0.1517	-0.3247	-0.1364	0.2644	-0.3115	0.0131	-0.1969	MgO (%)
						1.0000	0.6455	0.3860	0.6687	0.0178	0.4574	0.4575	0.4022	0.7698	-0.0832	0.4702	0.4656	0.4417	0.1421	0.7861	0.3492	-0.0313	0.5562	0.3997	0.6019	0.2887	Na2O (%)
							1.0000	0.5630	0.7754	0.3772	0.5664	0.6347	0.5612	0.7425	0.1179	0.4070	0.7371	0.3865	0.0536	0.6563	0.3379	0.1492	0.9450	0.4115	0.7661	0.5311	*TiO2 (%)**
								1.0000	0.5966	0.3205	0.5923	0.5708	0.6139	0.5461	-0.0427	0.2570	0.6184	0.4635	0.3530	0.4771	0.3362	0.2115	0.5987	0.2807	0.7016	0.0384	P2O5 (%)
									1.0000	0.3709	0.5107	0.6523	0.7163	0.7568	0.1125	0.5280	0.6891	0.6390	0.2903	0.5111	0.4614	0.1693	0.7436	0.5563	0.6865	0.3120	MnO (%)*
										1.0000	0.3499	0.3945	0.4009	0.1684	0.2230	0.3371	0.3560	0.4229	0.3725	0.1991	0.3198	0.1948	0.3902	0.3060	0.4350	0.1065	As (ppm)*
											1.0000	0.5196	0.5251	0.4611	-0.0484	0.1698	0.4920	0.3543	0.1675	0.6065	0.1647	-0.0344	0.5845	0.1340	0.5113	0.0804	Ba (ppm)*
												1.0000	0.5910	0.6178	-0.0190	0.1807	0.6811	0.2426	-0.0145	0.6106	0.1555	0.0516	0.6817	0.2341	0.6330	0.2906	Cr (ppm)*
													1.0000	0.6163	-0.0019	0.3268	0.7246	0.6413	0.3680	0.3928	0.4077	0.0949	0.5744	0.3853	0.7626	0.0078	*Cu (ppm)**
														1.0000	-0.0685	0.4509	0.7125	0.5360	0.2399	0.6381	0.4289	0.0238	0.7089	0.4365	0.7654	0.1797	Ga (ppm)*
															1.0000	0.3649	-0.1454	0.2735	0.2240	-0.2636	0.4283	0.4032	0.0325	0.3663	0.1901	0.5594	Mo (ppm)*
																1.0000	0.2150	0.7231	0.7047	0.1185	0.6073	0.4846	0.2478	0.7943	0.5409	0.3737	Nb (ppm)*
																	1.0000	0.3562	0.1225	0.5679	0.2334	0.0489	0.7778	0.2848	0.6996	0.0321	Ni (ppm)*
																		1.0000	0.6972	0.1840	0.7333	0.3446	0.3013	0.6879	0.7737	0.1434	Pb (ppm)*
																			1.0000	-0.1043	0.7027	0.4812	-0.0394	0.6203	0.3479	-0.0763	Rb (ppm)*
																				1.0000	0.0795	-0.2017	0.6952	0.0334	0.4829	0.1005	Sr (ppm)*
																					1.0000	0.5423	0.2438	0.6033	0.5468	0.3085	Th (ppm)*
																						1.0000	0.0950	0.4939	0.2139	0.2762	U (ppm)*
																							1.0000	0.2957	0.7241	0.4397	V (ppm)*
																								1.0000	0.5728	0.4093	*Y (ppm)**
																									1.0000	0.3140	Zn (ppm)*
																										1.0000	Zr (ppm)*

COLOR KEY

+/- 0.8 - 1.0

+/- 0.6 - 0.8

+/- 0.4 - 0.6

+/- 0.2 - 0.4

+/- 0.0 - 0.2

shown by the strong correlation coefficients between Fe_2O_3, MnO, Cr, Cu, Ga, Ni, Pb, V, and Zn. From this it is evident that both iron and manganese oxides are playing a major role in controlling the distribution of metals within the study area. This is likely the result of scavenging of metals by the Fe-Mn oxides. Phosphorus oxides are also related to the Fe-Mn oxides and may be the reason for the strong correlation between P_2O_5 and Cu.

Another interesting discovery concerning the manganese oxide distribution is the general lack of a MnO anomaly associated with the Luiz Lopez mining district. The principal product of this district is manganese and the bed material within streams sampled in this area contained pebbles with manganese oxide coatings. One explanation for this lack of anomaly is that the manganese oxides may be concentrated in the larger grain size fractions. Therefore, as a result of sampling the finer fractions as part of this work the manganese oxide anomaly is not observed.

Potassium Metasomatism

One of the principal reasons this study was conducted in this area was the presence of a region of potassium metasomatism. This region can be observed in the map of potassium distribution by airborne gamma-ray spectrometry (Fig. 38). However, in the soils work done by Shacklette and Boerngen (1984), the region is not observed. One explanation for the lack of a potassium anomaly in Shacklette's and Boerngen's work might be a lack of sample locations within this area.

The potassium metasomatized region is thought to have formed as a result of the downward percolation of alkaline, saline brines in a hydrologically closed basin. The potassium alteration is restricted to units from the Hells Mesa Tuff through the Basal

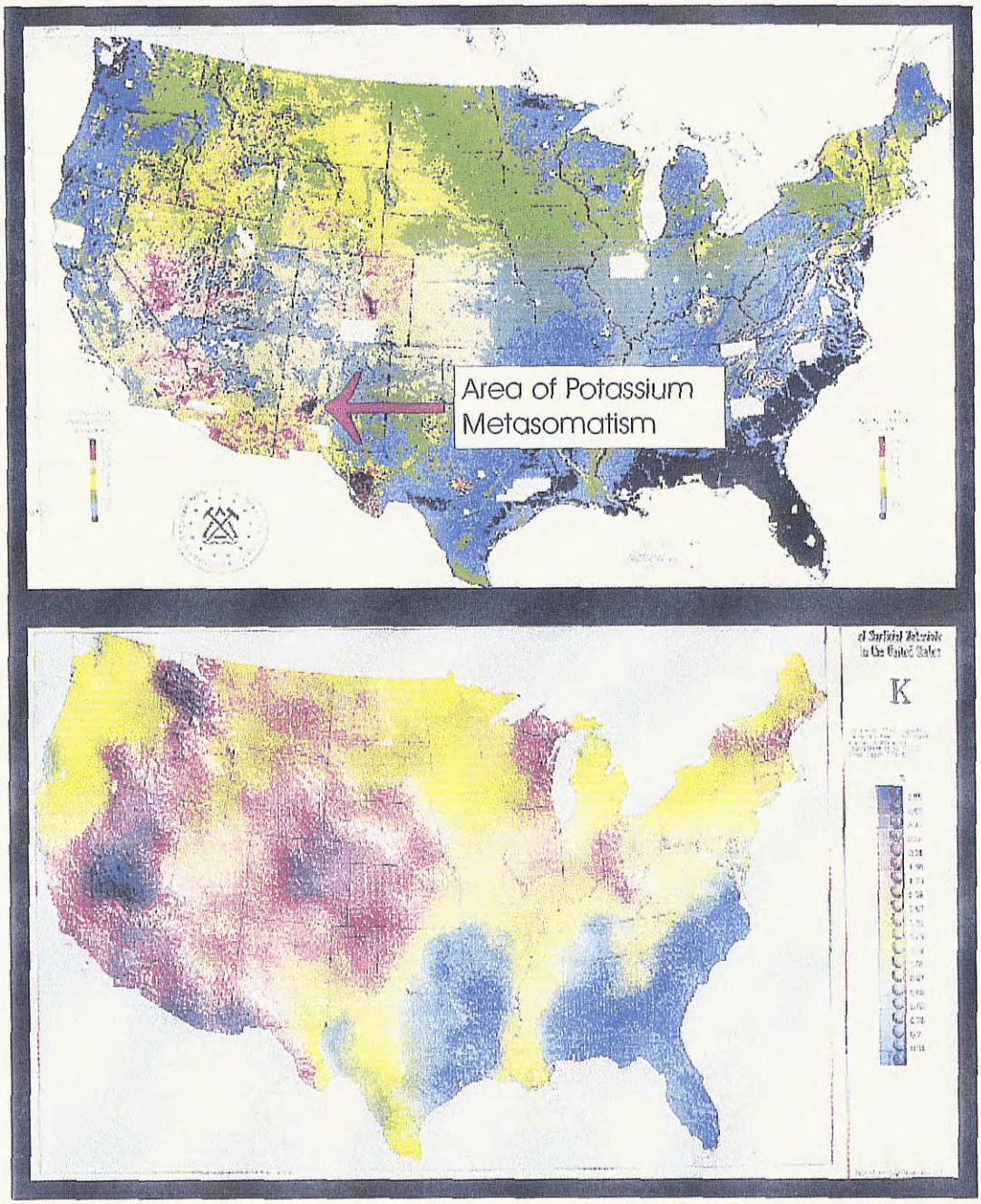

Figure 38. The top figure shows the potassium distribution of the United States observed by airborne gamma-ray spectrometry. The arrow points to a region of potassium metasomatism that occurs within the study area of this project. The bottom figure shows the potassium distribution from Shacklette and Boerngen, (1984) soils work. Note the absence of a potassium anomaly on this map (modified from, Darnley et al., 1995).

insert k2o map here

Popotosa Formation with K_2O concentrations being as high as 13.5 wt.% (Chapin and Dunbar, 1994). The trace elements As, Ba, and Rb also show significant enrichment in these rocks (Ennis, 1996).

While the maps of K_2O, As, Ba, and Rb produced in this study confirm the existence of the metasomatized region they do not precisely define its boundary (Figs. 12, 13, 26, and 27). The map of potassium oxide does not show the expected zone of enrichment shown by Ennis (1996). There are several possibilities for why this may be. The first is that the potassium metasomatism is restricted to lithology. Therefore, in regions where this lithology is not dominant the K_2O signal may be obscured. Another possibility is that the potassium may be removed as a free ion in stream water as opposed to remaining behind in the stream sediments. A final possibility is that during weathering the potassium in the rocks is being concentrated in the clay size fraction. Because, there was a general lack of the clay size fraction in the stream sediment samples the K_2O enrichment may not be observed.

The map of arsenic actually shows the best relationship to the metasomatized region (Fig. 12). This is likely the result of the increased concentration of arsenic in the metasomatized rocks as well as its strong tendency to sorb onto iron, manganese, and aluminum oxides as well as fine-grained sediments (Chapin and Dunbar, 1994).

RECOMMENDATIONS

Figure 39 shows an arsenic contamination map based on soil guidelines established by a British agency, the Interdepartmental Committee on the Redevelopment of Contaminated Lands (ICRCL). The guidelines used here are based on the maximum

SAMPLE LOCATIONS WITH HIGH ARSENIC VALUES

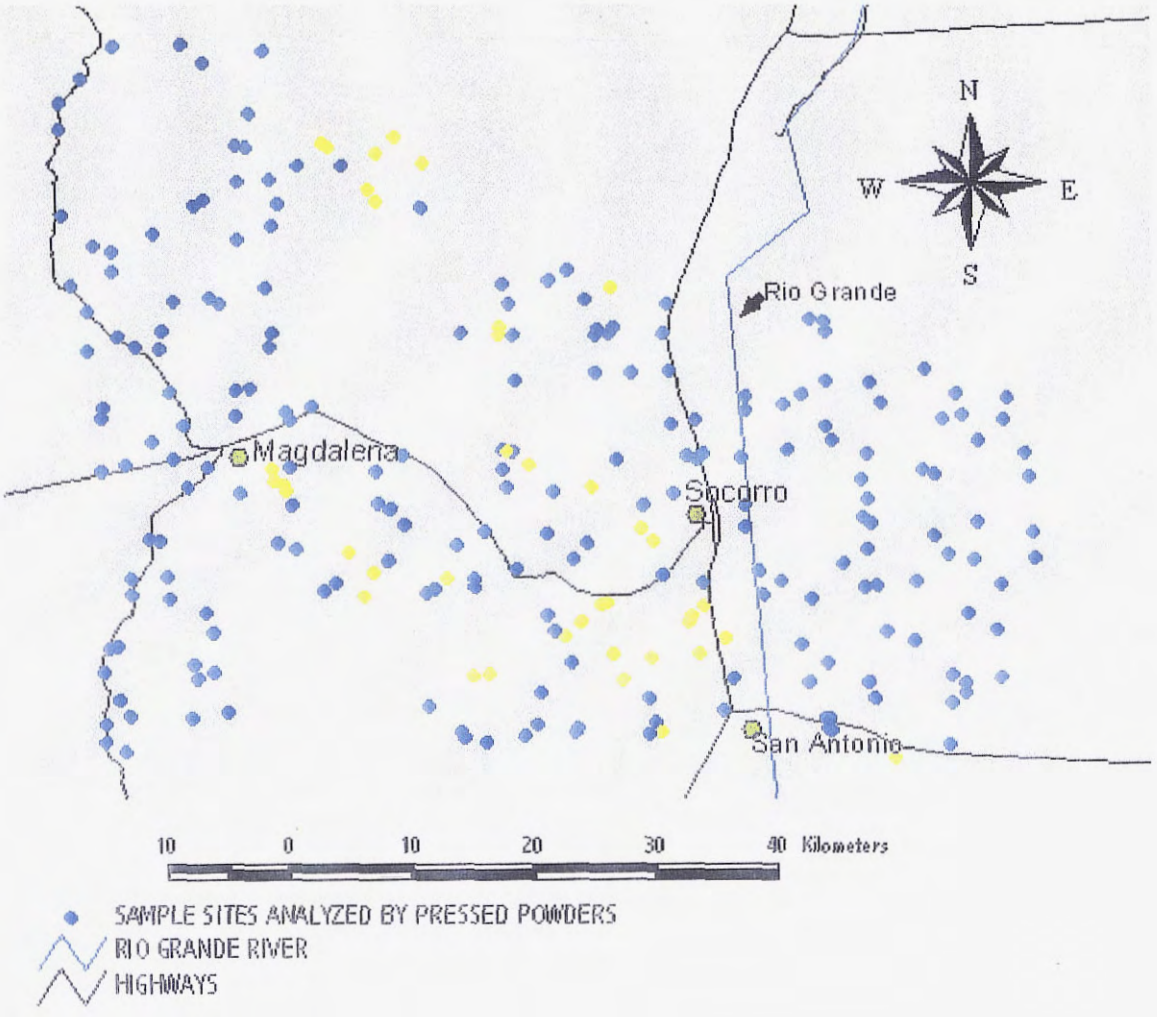

Figure 39. Map of sample locations (in yellow) that according to the ICRCL (Bell et al., 1996) guidelines for soils are considered too contaminated with arsenic for use as residential developments with gardens. Note that the samples above are stream sediments and the correlation between stream sediments and soils in not defined.

concentrations allowed, in soils, for residential developments with gardens. The maximum concentration allowed for arsenic is 10 ppm. Approximately 15 % of the 254 sample sites, in this study, have concentrations that exceed the guideline. However, the concentrations in this study are of stream sediments that may or may not reflect the concentrations of arsenic in soils. Also, the British guidelines were used because in the United States contamination is measured by ground water quality and a comparison with those numbers would not be meaningful. From an environmental standpoint alone this geochemical mapping project should continue within New Mexico. Recommendations for future work would include:

1). Further chemical analysis on the samples collected as part of this project. Other analytical methods should be employed to add to our understanding of the geochemistry within the study area. It is particularly important that we obtain data for other environmentally sensitive elements such as cadmium and selenium.

2). The continuation of this project to provide high quality, comparable data for the rest of New Mexico. The Environmental Protection Agency is considering lowering the allowable concentration of arsenic in drinking water. The results of our study reflect that the natural concentrations of arsenic within the study area are commonly higher than what other nations would consider threshold values for soil contamination. The high concentration of arsenic in rocks and sediments will likely effect the quality of drinking water. For this reason, it is important that data is gathered for the rest of New Mexico in order to fully understand how new water-

quality guidelines may be affected by the natural chemistry of the region.

3). One region within the state which could greatly benefit from this type of work is the Albuquerque Basin. The expansion of the Albuquerque metropolitan area, will continue to put a strain on the natural resources, namely water, within this region. A detailed geochemical survey of the region may assist with future land use decisions.

4). Expansion of the survey to look at other sampling media. Ideas for this include water sampling near Magdalena during the rainy season and sampling of soils within residential regions of Magdalena. The analysis of different size fractions of steam sediments may also be helpful. This would provide more details on the amount of mining related contamination near the town of Magdalena.

CONCLUSIONS

There are several conclusions that can be drawn from this study. The first is that the sampling strategy, sample preparation, and analytical methods used provided highly accurate and comparable data that may be incorporated into future studies of this type.

Results from this project indicate that nearly all elements have trends that are correlative with the varying geology of the region. The Paleozoic sedimentary rocks east of the Rio Grande are defined by all elements with the exception of Cr, Mo, SiO_2, U, and Zr. The Cretaceous sedimentary rocks in the northwest are defined by all elements with the exception of CaO, Cr, MgO, Mo, P_2O_5, SiO_2, U, and Zr. The Tertiary basaltic andesites and rhyolites can best be differentiated by Al_2O_3, Cr, Fe_2O_3, Ni, SiO_2, Na_2O_3,

Sr, TiO_2, and V. One caveat to these correlations is that most of the major elements were determined on approximately half of the sample sites due principally to time considerations for this study. Further analysis of the remainder of samples may reveal that some of the exceptions listed actually nicely define the geology of the region.

There are three multi-element anomalous regions within the study area. These regions include the northern Magdalena Mountains, Socorro Peak, and Polvadera Mountain. The Magdalenas have anomalous concentrations of many elements including As, Cu, Pb, U, and Zn. These anomalies are coincident with the Northern Magdalena, Magdalena, Hop Canyon, and Water Canyon mining districts. Socorro Peak contains anomalous concentrations of Ba, Pb, and Zn. This area is coincident with the Socorro Peak mining district. Polvadera Mountain has anomalous concentrations of Mo, Th, U, Y, and Zr. This is likely the result of sampling the Precambrian granites as well as the carbonatite dikes in this region.

A final conclusion is the presence of an arsenic anomaly within the Chupadera Mountains. This anomaly is coincident with the Luiz Lopez mining district. This anomaly is significant because of the environmental problems associated with arsenic.

REFERENCES CITED

ATSDR (Agency for Toxic Substances and Disease Registry), 1997. Top 20 Hazardous Substances: ATSDR/EPA Priority List for 1997. http://atsdr1.atsdr.cdc.gov:8080/cxcx3.html.

ATSDR, 1995a. Toxicological profile for barium. Public Health Statement, 4 pp.

ATSDR, 1995b. Toxicological profile for vanadium. Public Health Statement, 4 pp.

ATSDR, 1995c. Toxicological profile for zinc. Public Health Statement, 4 pp.

ATSDR, 1993a. Toxicological profile for arsenic. Public Health Statement, 4 pp.

ATSDR, 1993b. Toxicological profile for lead. Public Health Statement, 4 pp.

Armstrong, A.K., 1958. The Mississippian of West-Central New Mexico. New Mexico Bureau of Mines and Mineral Resources Memoir 5, 32 pp.

Bell, F.G., Duane, M.J., Bell, A.W., Hytiris, N., 1996. Environmental and Engineering Geoscience, v. 2, n. 3, p. 355-368.

BGS (British Geological Survey), 1992. Regional Geochemistry—Lake District. Natural Environment Research Council, Keyworth. 98 pp.

Bolviken, B., Bogen, J., Demetriades, A., De Vos, W., Ebbing, J., Hindel, R., Langedal, M., Locutura, J., O'Connor, P., Ottesen, R.T., Pulkkinen, E., Salminen, R., Schermann, O., Swennen, R., Van der Sluys, J., Volden, T., 1996. Regional geochemical mapping of Western Europe towards the year 2000. Journal of Geochemical Exploration, v. 56, p. 141-166.

Cather, S.M., Chamberlin, R.M., Chapin, C.E., McIntosh, W.C., 1994. Stratigraphic consequences of episodic extension in the Lemitar Mountains, central Rio Grande rift. Geological Society of America Special Paper 291, p. 157-170.

Chapin, C.E., and Cather, S.M., 1994. Tectonic setting of the axial basins of the northern and central Rio Grande rift. Geological Society of America Special Paper 291, p. 5-25.

Chapin, C.E., and Dunbar, N.W., 1994. A regional perspective on arsenic in waters of the middle Rio Grande Basin. New Mexico.

Chamberlin, R.M., 1983. Cenozoic domino style crustal extentsion in the Lemitar Mountains, New Mexico: A Summary. New Mexico Geological Society Guidebook 34. p. 111-118.

Darnley, A.G., 1995. International geochemical mapping—a review. Journal of Geochemical Exploration, v. 55, p. 5-10.

Darnley, A.G., Bjorklund, A., Bolviken, B., Gustavsson, N., Koval, P.V., Plant, J.A., Steenfelt, A., Tauchid, M., and Xie Xuejing, 1995. A global geochemical database for environmental and resource management: Final report of IGCP Project 259. United Nations Educational, Scientific, and Cultural Organization, France. 122 pp.

DOE (Department of Energy), 1979. National Uranium Resource Evaluation Report. 137 pp.

Eggleston, T.L., Norman, D.I., Chapin, C.E., and Savin, S., 1983. Geology, alteration, and genesis of the Luis Lopez Manganese District, New Mexico. New Mexico Geological Society Guidebook 34, p. 241-246.

Ennis, D.J., 1996. The effects of K-metasomatism on the mineralogy and geochemistry of silicic ignimbrites near Socorro, New Mexico. Unpublished Masters Thesis. 160 pp.

ESRI (Environmental Systems Research Institute Inc.), 1996. Arc View Spatial Analyst-Advanced Spatial Analysis Using Raster and Vector Data. Redlands, California, 148 pp.

Fletcher, W.K., 1981. Handbook of exploration geochemistry, volume 1: Analytical methods in geochemical prospecting. Elsevier Scientific Publishing Company, New York. 205 pp.

Fortescue, J.A.C., 1992. Landscape geochemistry: retrospect and prospect—1990. Applied Geochemistry, v. 7, p. 1-53.

Gibbs, R.B., 1989. The Magdalena District, Kelly, New Mexico. The Mineralogical record, v. 20, n. 1, p. 13-17.

Govindaraju, K., 1994. 1994 Compilation of working values and sample description for 383 geostandards. Geostandards Newsletter, v. 18, p. 29-45.

Jaworski, M.J., 1973. Copper Mineralization of the Upper Moya Sandstone, Chupadera mines area, Socorro County, New Mexico. Unpublished MS Thesis, 102 pp.

Johnson, W.R., 1988. Soil Survey of Socorro County Area, New Mexico. 328 pp.

Koval, P.V., Burenkov, E.K., and Golovin, A.A., 1995. Introduction to the program "Multipurpose Geochemical Mapping of Russia". Journal of Geochemical Exploration, v. 55, p. 115-123.

Labuschagne, L.S., Holdsworth, R., and Stone, T.P., 1993. Regional stream sediment geochemical survey of South Africa. Journal of Geochemical Exploration, v. 47, p. 283-296.

LASL (Los Alamos Scientific Laboratory), 1978. Field Procedures for The Uranium Hydrogeochemical and Stream Sediment Reconnaissance as Used by The Los Alamos Scientific Laboratory. 64 pp.

LASL (Los Alamos Scientific Laboratory), 1985. A computer assisted mineral resource assessment of Socorro and Catron Counties, New Mexico.

McLemore, V.T., 1980. Carbonatites in the Lemitar Mountains, Socorro County, New Mexico. New Mexico Geology, v. 2, n. 4, p. 49-52.

McLemore, V.T., in press. Silver and Gold Occurrences in New Mexico. New Mexico Bureau of Mines and Mineral Resources, Resource Map 21.

Merrill, G.K., 1986. Map location literacy-How well does Johnny Geologist read? Geological Society of America Bulletin, v. 97, p. 404-409.

North, R.M., 1985. Geology and Mineralogy of the Bear Mountains Mining district, Socorro County, New Mexico. Abstract, New Mexico Geology, v. 7, n. 2, p. 42.

North, R.M., 1983. History and Geology of the precious metal occurrences in Socorro County, New Mexico. New Mexico Geological Society Guidebook 34, p. 261-268.

O'Neill, P., 1985. Environmental Chemistry. Chapman and Hall, London, 268 pp.

ORGDP (Oak Ridge Gaseous Diffusion Plant), 1978. Procedures Manual for Stream Sediment Reconnaissance Sampling—Uranium Resource Evaluation Project. 19 pp.

Osburn, G.R., 1984. Geology of Socorro County. New Mexico Bureau of Mines and Mineral Resources, Open File Report # 238. 14 pp.

Osburn, G.R., and Chapin, C.E., 1983. Ash-Flow Tuffs and Cauldrons in the Northeast Mogollon-Datil Volcanic Field: A Summary. New Mexico Geological Society Guidebook 34, p. 197-204.

Reed, W.P., 1990. Certificate of analysis- standard reference material 2704 Buffalo River sediment. NIST Certificate. 3 pp.

Rose, A.W., Hawkes, H.E., and Webb, J.S., 1979. Geochemistry in Mineral Exploration. Academic Press Inc., San Diego, 657 pp.

Shacklette, H.T., and Boerngen, J.G., 1984. Element concentrations in soils and surficial materials of the conterminous United States. US Geological Survey, Professional Paper 574D, 70 pp.

Siegel, F.R., 1995. Environmental geochemistry in development planning: an example from the Nile delta, Egypt. Journal of Geochemical Exploration, v. 55, p. 265-273.

Siemers, W.T, 1973. Stratigraphy and Petrology of Mississippian, Pennsylvanian, and Permian Rocks in the Magdalena Area, Socorro County, New Mexico. Unpublished MS Thesis, 133 pp.

Simpson, P.R., Edmunds, W.M., Breward, N., Cook, J.M., Flight, D., Hall, G.E.M., and Lister, T.R., 1993. Geochemical mapping of stream water for environmental studies and mineral exploration in the UK. Journal of Geochemical Exploration, v. 49, p. 63-88.

SRL (Savannah River Laboratory), 1977. Field Manual for Stream Sediment Reconnaissance. 55 pp.

Taylor, S.R., and McLennan, S.M., 1985. The Continental Crust: Its Composition and Evolution. Blackwell Scientific Publishing, Oxford, England, 312 pp.

U.S. Bureau of Census, 1993. 1990 Census of Population—Social and Economic Characteristics New Mexico. 638 pp.

Wedepohl, K.H. (editor), 1978. Handbook of Geochemistry. Springer-Verlag, Berlin Heidelberg New York.

APPENDIX A

ORIENTATION SURVEY DETAILS

This project began with an orientation survey conducted on March 7, 1996. The primary goal of this survey was to establish the grain size fraction that would be collected during future work. The best sample size would be the size fraction that involved a reasonable sieving effort to obtain a required quantity and showed the overall highest elemental concentrations.

The Nogal Arroyo was chosen for the stream that would be used to conduct this survey. Samples were collected from three locations within the stream approximately 50 m apart. Samples consisted of a composite of three subsamples taken across the streambed. The samples were sieved and five size fractions were collected. The five size fractions were

> 500 μm
500 > x > 250
250 > x > 125
125 > x > 63
< 63 μm

Each of the size fractions was placed in a polyethylene sample bag and labeled with a sample number that is a combination of location and size fraction.

Sample Numbers: XXXZZZ

XXX is the location 0, 50, 100 meters
ZZZ is the size fraction 500, 250, 125, 063, L63

After returning from the field each size fraction was weighed and then the < 500 μm size fractions were analyzed by x-ray fluorescence spectrometry. Only one sample location

yielded enough of the < 63 μm size fraction for analysis. Table A-1 shows the results of the grain size analysis while Table A-2 shows the results of the geochemical analysis.

As a result of this survey, as well as a review of current literature regarding stream sediment sampling, it was decided that we would use a slightly larger fraction than the < 125 μm size fraction used in this survey. Therefore, the < 150 μm was chosen for use in the project.

TABLE A-1. SIZE FRACTION ANALYSIS.

SAMPLE #	WEIGHT (g)	% FINER THAN
000500	4553.2	24.87
000250	1161	5.72
000125	290	0.93
000063	52.3	0.07
000L63	4.3	
050500	5455.6	20.03
050250	1093	4.01
050125	235.3	0.56
050063	35.3	0.04
050L63	2.9	
100500	5406.4	15.3
100250	649.3	5.12
100125	247.2	1.25
100063	58.7	0.33
100L63	21	

TABLE A-2. ORIENTATION SURVEY GEOCHEMICAL DATA

	000250	000125	000063		050250	050125	050063
Fe2O3 (%)	2.76	4.34	10.6	Fe2O3 (%)	4.92	8.39	15.73
TiO2 (%)	0.5	0.67	1.64	TiO2 (%)	0.68	1.15	2.34
MnO (%)	0.05	0.061	0.12	MnO (%)	0.07	0.09	0.16
As (ppm)	4.6	5.4	7	As (ppm)	7.4	6.1	7.5
Ba (ppm)	862.5	867.9	933.1	Ba (ppm)	912.6	896.7	732.8
Cr (ppm)	47.8	54.6	165.8	Cr (ppm)	48.3	83	227
Cu (ppm)	12.5	17.1	25.2	Cu (ppm)	14.7	15.5	23.3
Ga (ppm)	12.5	12.9	16.6	Ga (ppm)	13.2	13.9	18
Mo (ppm)	3.6	2.2	4.2	Mo (ppm)	1.5	2.6	6.2
Nb (ppm)	11.5	12.1	22.3	Nb (ppm)	14.6	16.9	26.2
Ni (ppm)	15.3	16.5	31.7	Ni (ppm)	15.4	20.2	40.6
Pb (ppm)	17.6	20.4	28.1	Pb (ppm)	21.6	24.6	33.3
Rb (ppm)	146.2	110.6	102.4	Rb (ppm)	137.9	100.5	95
Sr (ppm)	362.2	420.2	427.4	Sr (ppm)	359.2	396.2	394.9
Th (ppm)	9.3	9.2	12.4	Th (ppm)	11.1	10.4	17.7
U (ppm)	1.5	2.3	4.5	U (ppm)	3.2	3.2	7
V (ppm)	55.9	87	229.3	V (ppm)	95.6	179.3	343.1
Y (ppm)	22.3	20.9	35.9	Y (ppm)	22.9	25.4	39.9
Zn (ppm)	44	55.8	110.4	Zn (ppm)	60.1	81.3	162.7
Zr (ppm)	160.2	215.4	967.8	Zr (ppm)	219.7	334.1	1635.2
	100250	100125	100063	100163			
Fe2O3 (%)	2.78	4.6	7.2	5.43			
TiO2 (%)	0.46	0.68	1.15	0.98			
MnO (%)	0.049	0.062	0.089	0.084			
As (ppm)	5.1	5.1	6.8	7			
Ba (ppm)	867.4	862.3	850	764			
Cr (ppm)	50.3	50	110	105.9			
Cu (ppm)	13.2	14.2	22.1	29.5			
Ga (ppm)	13.4	12.7	15.4	16.4			
Mo (ppm)	3	3.2	2.9	4			
Nb (ppm)	11.6	12.6	16.6	17.5			
Ni (ppm)	13.6	17.2	25.8	29.8			
Pb (ppm)	18.2	20.9	25.8	40.5			
Rb (ppm)	150.4	110.3	110.3	120.9			
Sr (ppm)	351.7	404.6	423.6	387.5			
Th (ppm)	9.7	9.3	11.2	12.7			
U (ppm)	3.4	2	3.1	3.8			
V (ppm)	56.3	92.8	147.9	109.3			
Y (ppm)	24.6	20.9	28.3	34.2			
Zn (ppm)	41.8	56	86.5	85.5			
Zr (ppm)	150.9	208.1	600.6	603.3			

APPENDIX B

DETAILED FIELD PROCEDURES

Equipment

1. GPS receiver
2. Maps
3. Field forms
4. Plastic bucket
5. Aluminum trowel
6. Stainless steel colander
7. Stainless steel sieves (60 and 100 mesh)
8. Stainless steel brush
9. Paintbrush
10. Rags
11. Polyethylene bags (1 gal.)
12. Pens

Procedure

1. Arrive at sampling location at least 50 m upstream from road and any contamination.

2. Turn on the GPS receiver and allow it to acquire satellites.

3. Fill out data form saving the location for last. This will allow the GPS time to stabilize.

4. Clean sampling apparatus
   a. Scoop up several trowels full of bed material. Pour this material through the colander into the plastic bucket.
   b. Swirl the collected material around the inside of the bucket allowing the material to completely coat the inside of the bucket.
   c. Dump the collected material into the sieves and sieve. After sieving is completed, discard all of the material collected.
   d. Brush the sieves mesh with the wire and paintbrushes until clean.
   e. Wipe all of the sampling equipment down with the rags.

5. Collect sample
   a. Scoop up equal proportions of bed material from 5 locations spaced approximately 10 m apart. Pour this material through the colander into the plastic bucket. This will effectively remove the very large particles.
   b. Pour the material collected into the sieves and sieve.
   c. Collect the material from the pan (<150 μm) as well as the 100 mesh sieve (150<x<250 μm).

d. Place the samples into polyethylene bags and label the bags as

SOC96XXX for the <150 μm sediment fraction
CSOCXXX for the 150<x<250 μm sediment fraction

6. Wipe down the sampling equipment before moving on to the next sample site.

7. At every 30th site sample the same as above except when finished repeat the procedure choosing 5 new locations.

DETAILED SAMPLE PREPARATION

Equipment

1. Microsplitter with two pans.
2. Polyethylene Pill Bottles
3. Tungsten-carbide Swing Mill
4. Alcohol
5. Kimwipes
6. Pressed Pellet Die, Sleeve, Cylinder
7. Scale
8. Weigh Paper
9. Agate Mortar and Pestle
10. 2% Polyvinyl alcohol solution
11. Boric Acid
12. Hydraulic Press
13. Hot plate
14. Acetone
15. Pt Crucibles, Casting Dish and Tongs
16. Spartan Fusion Machine
17. Lithium Borate Flux 12:22 (12 parts di-lithium tetraborate and 22 parts lithium metaborate)
18. Lithium Bromide
19. Ammonium Nitrate
20. Furnace and Drying Oven
21. Ceramic crucibles (L.O.I.)

Procedure

1. Split each < 150 μm sample using a non-contaminating microsplitter. Split the sample until left with approximately 25 g of sample in one pan. The remainder of the sample should be placed back in the sample bag. The 25 g split should be placed in a polyethylene pill bottle labeled with the sample number.

2. The samples contained in bags are placed in storage for future use while the samples in pill bottles undergo further sample preparation.

3. The samples are then ground in a tungsten-carbide swing mill. Between each sample the mill should be cleaned with a combination of water and alcohol to prevent cross-contamination. The ground sample is placed back in the pill bottle and is ready for the preparation of pressed pellets and fusion disks.

4. Pressed Pellet Creation (Follows in-house preparation handout of Philip Kyle)
   a. The Die, sleeve, cylinder, mortar, and pestle are all cleaned with acetone prior to sample preparation. The die is put together with the aluminum sleeve in place.

b. Seven grams of sample are weighed and placed into the agate mortar. Seven drops of the Polyvinyl alcohol solution are added and then homogenized with the sample using the pestle.
c. The sample is transferred into the die and then the steel cylinder is used to form the sample within the die. The aluminum sleeve and steel cylinder are then pulled out of the die.
d. A boric acid backing is then applied to cover the back and sides of the sample in the die.
e. The final die plunger is then added and the die is transferred to the hydraulic press where it is placed under ten tons of pressure for one minute.
f. The final pressed pellet is then labeled with the sample number and dried on a hot plate.

5. Fusion Disk Creation (Follows in-house preparation handout of Philip Kyle)
   a. Remove lithium bromide and ammonium nitrate from dessicator and place in drying oven for approximately 10 minutes.
   b. Fill flux bottle mixing thoroughly to ensure homogeneity and place near scale.
   c. Clean crucibles and casting dish and allow to dry.
   d. Follow directions to turn on Spartan fusion machine.
   e. Check the calibration of the balance (with one gram weight) to ensure tolerance of 1.0000 ± 0.0005 grams.
   f. Determine flux loss by
      1). Zero balance and weigh dry cool crucible recording weight.
      2). Place 4-6 grams of flux into crucible and reweigh recording weight of crucible plus flux.
      3). Using Pt tongs place crucible on fusion machine and leave for 3 to 5 minutes.
      4). Occasionally swirl the crucible to remove gas bubbles.
      5). After the flux has fully fused remove from fusion machine and allow to cool.
      6). When cool reweigh crucible recording flux loss using the following equation

      Weight of Flux = (Crucible+Flux)-(Crucible)
      Flux Weight Loss = (Crucible+Flux)-(Crucible+Flux after heating)
      Flux Loss as % = Flux weight loss * 100 / Weight of Flux

   g. Sample Preparation
      1). In crucible combine

      1.0000 ± 0.0005 grams of sample
      6.000 ± 0.001 grams of flux adjusted for flux loss
      0.050 ± 0.001 grams of lithium bromide
      0.05 ± 0.01 grams of ammonium nitrate

      2). Homogenize mixture in crucible.
      3). Place crucible on left burner of fusion machine and allow to fuse for 4 to 5 minutes.
      4). Occasionally swirl the crucible to remove gas bubbles.

5). After the sample has cooled transfer to casting dish on the right burner and apply air to cool.
6). After air cooling remove sample and place on paper towel to finish cooling.
7). Using sticky labels. Label the sample with sample number and final sample weight.

Final Flux Weight = Flux weight – (Flux weight x Flux loss as percentage)
Final Sample Weight = Sample Weight * (6.0000 / Final Flux Weight)

6. Loss on Ignition Determination (Follows in-house preparation handout of Philip Kyle)
   a. Remove clean crucibles from drying oven and place in dessicator to cool.
   b. Weigh crucible and record the weight
   c. Place 2 to 4 grams of sample in crucible and record the weight.
   d. Dry samples in oven at 110 °C for two hours.
   e. Remove samples from oven and place in dessicator to cool.
   f. When cool reweigh sample + crucible
   g. Place crucible in high temperature with the following settings

Initial Rate	20 °C/minute
Transitional Temperature	100 °C
Hold Time	1 minute
Final Rate	20 °C/minute
Final Temperature	1000 °C
Final Hold	120 minutes

   h. Allow samples to cool completely and reweigh.
   i. Calculate LOI and H2O-

LOI = 100 x [(crucible+sample)-(weight 1000 °C)] / [(crucible+sample)-(crucible)]

H2O- = 100 x [(crucible+sample)-(weight 110 °C)] / [(crucible+sample)-(crucible)]

APPENDIX C

POTASSIUM OXIDE CONVERSION

A zone of potassium-metasomatism has been identified within the study area for this project. Because of this zone it was decided that it would be nice to have potassium oxide data for all of the sample locations. In order to accomplish this a new program was written for the XRF that would enable the determination of K_2O on pressed powders. This program was tested by plotting the data determined on pressed powders against that of the traditional method of fusion disks (Fig. C-1a). The result was a consistent linear trend in the data. The trend of this line was determined to be

$$y = 0.8061x + 0.1744$$

where y = value from fusion disk
x = value from pressed powder.

In order to obtain the most accurate data possible, the values for pressed powders were converted to values closer to fusion disk with the use of the equation above. As a final check, the converted data for pressed powders was plotted against that of the fusion disks (Fig. C-1b). This time the equation of the line has a slope of one, which means the data is closer to the values obtained by fusion disks.

A second conversion was required due to a change in the program between sample runs. The details of this conversion are shown in figure C-2a-b. All of the samples were then converted using the data from the specific program they were determined under. Finally the converted K_2O data was used in the creation of the potassium oxide map.

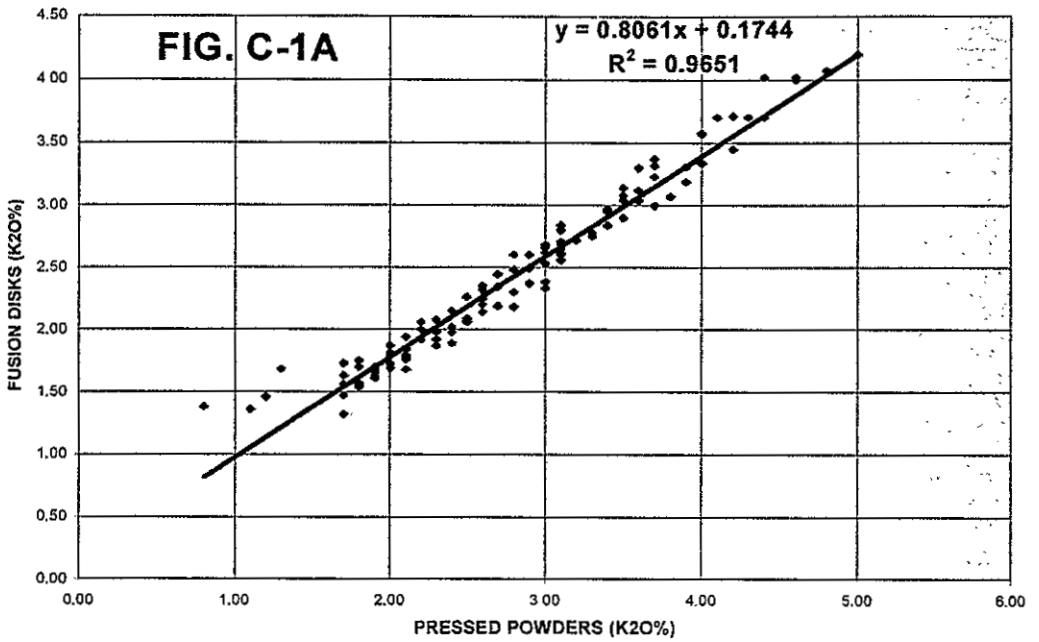
FIG. C-1A
y = 0.8061x + 0.1744
R2 = 0.9651
FUSION DISKS (K2O%)
PRESSED POWDERS (K2O%)
0.00
0.50
1.00
1.50
2.00
2.50
3.00
3.50
4.00
4.50
0.00
1.00
2.00
3.00
4.00
5.00
6.00

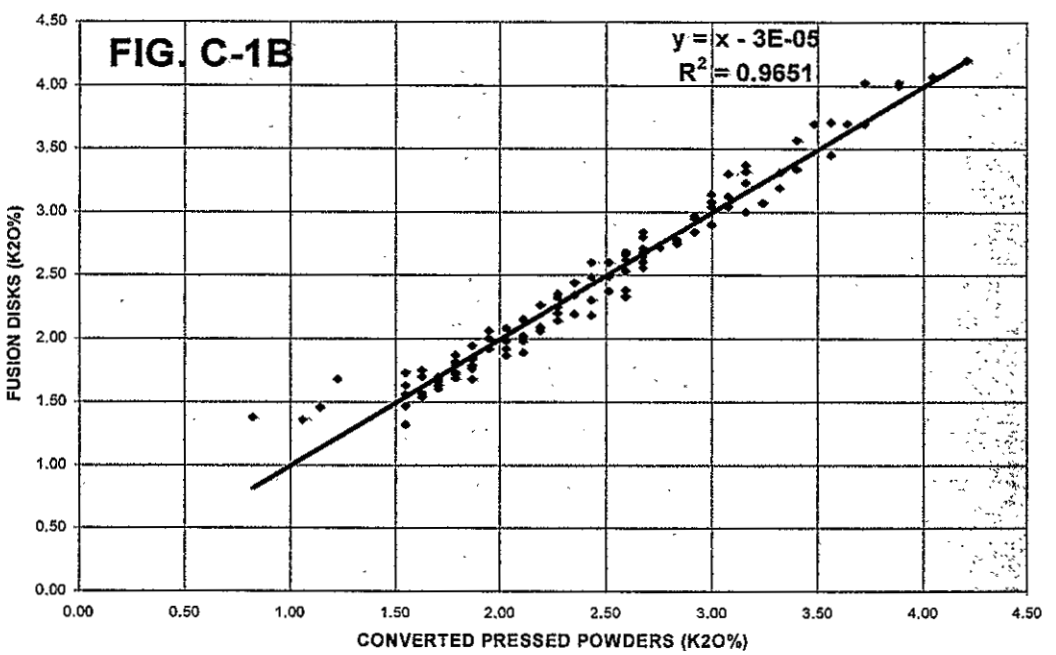
FIG. C-1B
y = x - 3E-05
R2 = 0.9651
FUSION DISKS (K2O%)
CONVERTED PRESSED POWDERS (K2O%)
0.00
0.50
1.00
1.50
2.00
2.50
3.00
3.50
4.00
4.50

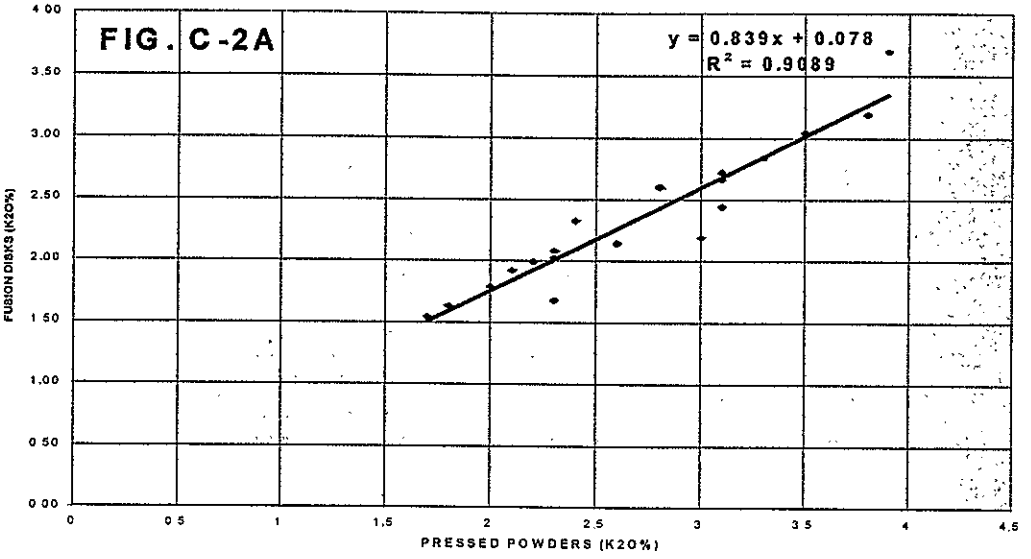
FIG. C-2A
y = 0.839x + 0.078
R² = 0.9089
FUSION DISKS (K2O%)
PRESSED POWDERS (K2O%)
4.00
3.50
3.00
2.50
2.00
1.50
1.00
0.50
0.00
0
0.5
1
1.5
2
2.5
3
3.5
4
4.5

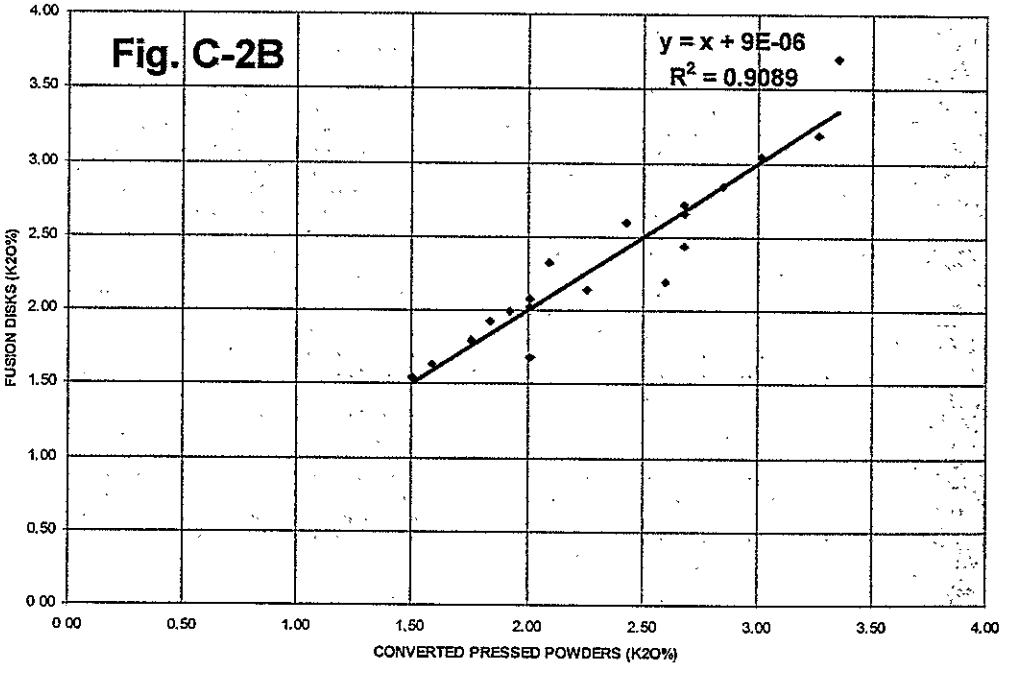
Fig. C-2B
y = x + 9E-06
R² = 0.9089
FUSION DISKS (K2O%)
CONVERTED PRESSED POWDERS (K2O%)
4.00
3.50
3.00
2.50
2.00
1.50
1.00
0.50
0.00
0.00
0.50
1.00
1.50
2.00
2.50
3.00
3.50
4.00

APPENDIX D

STANDARD REFERENCE MATERIALS

SOC96SRM1

SOC96SRM1 is an in-house reference material collected from within the study area. The sample was collected July 8, 1996. Approximately 2 kg of < 150 μm sediment was collected from the Arroyo de la Parida located east of the Rio Grande. The location of the sample site was UTM Zone 13S 330344m E, 3779324m N.

SOC96SRM2

SOC96SRM2 is an in-house reference material collected from within the study area. The sample was collected August 21, 1996. Approximately 10 kg of < 150 μm sediment was collected from San Lorenzo Arroyo located west of the Rio Grande. The location of the sample site was UTM Zone 13S 322556m E, 3788844m N.

NIST SRM 2704

SRM 2704 is a standard reference material issued by the National Institute of Standards and Technology. The river sediment for this SRM was collected from the Buffalo River near the Ohio Street Bridge in Buffalo, New York. The sediment was screened and passed through a 100 mesh (150 μm) sieve and collected on a 400 mesh sieve (38 μm). The sediment was radiation sterilized, blended, and bottled in 50 g units. The certified values for this standard are weighted means of results from two or more analytical methods. Noncertified values are provided for information only (Reed, 1990).

Jsd-1

Jsd-1 is a standard reference material issued by the Geological Survey of Japan. The river sediment for this SRM is a composite sample of the northern region, Ibaraki Prefecture. This sample was issued in 1988 (Govindaraju, 1994).

Jsd-2

Jsd-2 is a standard reference material issued by the Geological Survey of Japan. The river sediment for this SRM is a composite sample of the eastern region, Ibaraki Prefecture. This sample was issued in 1989 (Govindaraju, 1994).

Jsd-3

Jsd-3 is a standard reference material issued by the Geological Survey of Japan. The river sediment for this SRM is a composite sample of the central region, Ibaraki Prefecture. This sample was issued in 1988 (Govindaraju, 1994).

STSD-3

STSD-3 is a standard reference material issued by Canada Center for Mineral and Energy Technology, Mines and Resources. The river sediment for this SRM is a composite of the Hirok Stream and Lavant Creek (Govindaraju, 1994).

STSD-4

STSD-4 is a standard reference material issued by Canada Center for Mineral and Energy Technology, Mines and Resources (Govindaraju, 1994).

TABLE D-1 UNBALANCED TWO-LEVEL DESIGN

SAMPLE	SOC96030 A	SOC96030 B	SOC96030 C	MEAN OF A+B	ANALYTICAL VARIATION	WITHIN STREAM VARIATION
Fe2O3 (%)*	4.60	4.60	4.90	4.60	0.0	0.2
MnO (%)*	0.07	0.07	0.07	0.07	0.0	0.0
TiO2 (%)*	0.60	0.60	0.60	0.60	0.0	0.0
K2O (%)*	1.79	1.79	1.71	1.79	0.0	0.1
As (ppm)*	6	5	6	6	0.7	0.4
Ba (ppm)*	448	443	461	446	3.5	11.0
Cr (ppm)*	70	73	70	72	2.1	1.1
Cu (ppm)*	13	14	14	14	0.7	0.4
Ga (ppm)*	14	14	14	14	0.0	0.0
Mo (ppm)*	0	0	2	0	0.0	1.4
Nb (ppm)*	11	12	12	12	0.7	0.4
Ni (ppm)*	27	27	26	27	0.0	0.7
Pb (ppm)*	13	14	14	14	0.7	0.4
Rb (ppm)*	91	90	90	91	0.7	0.4
Sr (ppm)*	216	216	213	216	0.0	2.1
Th (ppm)*	8	7	10	8	0.7	1.8
U (ppm)*	3	3	3	3	0.0	0.0
V (ppm)*	81	76	81	79	3.5	1.8
Y (ppm)*	28	27	28	28	0.7	0.4
Zn (ppm)*	44	43	44	44	0.7	0.4
Zr (ppm)*	349	345	384	347	2.8	26.2

TABLE D-1 UNBALANCED TWO-LEVEL DESIGN

SAMPLE	SOC96060 A	SOC96060 B	SOC96060 C	MEAN OF A+B	ANALYTICAL VARIATION	WITHIN STREAM VARIATION
Fe2O3 (%)*	2.50	2.50	2.30	2.50	0.0	0.1
MnO (%)*	0.04	0.04	0.04	0.04	0.0	0.0
TiO2 (%)*	0.50	0.50	0.40	0.50	0.0	0.1
K2O (%)*	1.71	1.71	1.71	1.71	0.0	0.0
As (ppm)*	4	4	4	4	0.0	0.0
Ba (ppm)*	430	425	418	428	3.5	6.7
Cr (ppm)*	50	53	48	52	2.1	2.5
Cu (ppm)*	13	14	11	14	0.7	1.8
Ga (ppm)*	9	9	8	9	0.0	0.7
Mo (ppm)*	0	0	0	0	0.0	0.0
Nb (ppm)*	8	8	8	8	0.0	0.0
Ni (ppm)*	16	15	14	16	0.7	1.1
Pb (ppm)*	12	10	9	11	1.4	1.4
Rb (ppm)*	60	60	57	60	0.0	2.1
Sr (ppm)*	142	143	137	143	0.7	3.9
Th (ppm)*	4	4	3	4	0.0	0.7
U (ppm)*	2	2	2	2	0.0	0.0
V (ppm)*	48	50	47	49	1.4	1.4
Y (ppm)*	19	19	18	19	0.0	0.7
Zn (ppm)*	33	33	29	33	0.0	2.8
Zr (ppm)*	332	341	328	337	6.4	6.0

TABLE D-1 UNBALANCED TWO-LEVEL DESIGN

SAMPLE	SOC96090 A	SOC96090 B	SOC96090 C	MEAN OF A+B	ANALYTICAL VARIATION	WITHIN STREAM VARIATION
Fe2O3 (%)*	5.40	5.50	5.20	5.45	0.1	0.2
MnO (%)*	0.10	0.10	0.10	0.10	0.0	0.0
TiO2 (%)*	0.90	0.90	0.80	0.90	0.0	0.1
K2O (%)*	3.00	3.08	3.08	3.04	0.1	0.0
As (ppm)*	8	9	9	9	0.7	0.4
Ba (ppm)*	835	842	822	839	4.9	11.7
Cr (ppm)*	94	101	94	98	4.9	2.5
Cu (ppm)*	24	25	24	25	0.7	0.4
Ga (ppm)*	18	19	18	19	0.7	0.4
Mo (ppm)*	0	0	0	0	0.0	0.0
Nb (ppm)*	17	17	16	17	0.0	0.7
Ni (ppm)*	33	33	32	33	0.0	0.7
Pb (ppm)*	54	54	45	54	0.0	6.4
Rb (ppm)*	114	114	114	114	0.0	0.0
Sr (ppm)*	432	430	438	431	1.4	4.9
Th (ppm)*	12	12	11	12	0.0	0.7
U (ppm)*	3	4	3	4	0.7	0.4
V (ppm)*	114	107	112	111	4.9	1.1
Y (ppm)*	32	33	32	33	0.7	0.4
Zn (ppm)*	91	93	91	92	1.4	0.7
Zr (ppm)*	419	421	403	420	1.4	12.0

TABLE D-1 UNBALANCED TWO-LEVEL DESIGN

SAMPLE	SOC96120 A	SOC96120 B	SOC96120 C	MEAN OF A+B	ANALYTICAL VARIATION	WITHIN STREAM VARIATION
Fe2O3 (%)*	4.50	4.50	4.50	4.50	0.0	0.0
MnO (%)*	0.09	0.09	0.10	0.09	0.0	0.0
TiO2 (%)*	0.70	0.70	0.70	0.70	0.0	0.0
K2O (%)*	2.83	2.92	2.92	2.87	0.1	0.0
As (ppm)*	4	4	5	4	0.0	0.7
Ba (ppm)*	801	807	814	804	4.2	7.1
Cr (ppm)*	59	56	56	58	2.1	1.1
Cu (ppm)*	20	19	20	20	0.7	0.4
Ga (ppm)*	16	17	17	17	0.7	0.4
Mo (ppm)*	0	2	0	1	1.4	0.7
Nb (ppm)*	17	18	17	18	0.7	0.4
Ni (ppm)*	20	21	20	21	0.7	0.4
Pb (ppm)*	33	32	32	33	0.7	0.4
Rb (ppm)*	117	116	119	117	0.7	1.8
Sr (ppm)*	340	340	332	340	0.0	5.7
Th (ppm)*	12	11	11	12	0.7	0.4
U (ppm)*	3	3	2	3	0.0	0.7
V (ppm)*	82	82	84	82	0.0	1.4
Y (ppm)*	29	29	30	29	0.0	0.7
Zn (ppm)*	76	77	78	77	0.7	1.1
Zr (ppm)*	443	449	431	446	4.2	10.6

TABLE D-1 UNBALANCED TWO-LEVEL DESIGN

SAMPLE	SOC96150 A	SOC96150 B	SOC96150 C	MEAN OF A+B	ANALYTICAL VARIATION	WITHIN STREAM VARIATION
Fe2O3 (%)*	13.30	13.20	13.90	13.25	0.1	0.5
MnO (%)*	0.16	0.16	0.17	0.16	0.0	0.0
TiO2 (%)*	1.80	1.80	1.90	1.80	0.0	0.1
K2O (%)*	1.63	1.63	1.71	1.63	0.0	0.1
As (ppm)*	5	6	5	6	0.7	0.4
Ba (ppm)*	765	771	803	768	4.2	24.7
Cr (ppm)*	135	130	137	133	3.5	3.2
Cu (ppm)*	21	22	22	22	0.7	0.4
Ga (ppm)*	21	22	23	22	0.7	1.1
Mo (ppm)*	0	0	0	0	0.0	0.0
Nb (ppm)*	14	14	14	14	0.0	0.0
Ni (ppm)*	34	34	36	34	0.0	1.4
Pb (ppm)*	22	21	22	22	0.7	0.4
Rb (ppm)*	54	54	53	54	0.0	0.7
Sr (ppm)*	845	845	925	845	0.0	56.6
Th (ppm)*	9	8	8	9	0.7	0.4
U (ppm)*	2	3	2	3	0.7	0.4
V (ppm)*	314	319	335	317	3.5	13.1
Y (ppm)*	28	27	27	28	0.7	0.4
Zn (ppm)*	130	129	127	130	0.7	1.8
Zr (ppm)*	734	748	745	741	9.9	2.8

TABLE D-1 UNBALANCED TWO-LEVEL DESIGN

SAMPLE	SOC96180 A	SOC96180 B	SOC96180 C	MEAN OF A+B	ANALYTICAL VARIATION	WITHIN STREAM VARIATION
Fe2O3 (%)*	7.40	7.30	6.90	7.35	0.1	0.3
MnO (%)*	0.11	0.11	0.10	0.11	0.0	0.0
TiO2 (%)*	1.10	1.10	1.00	1.10	0.0	0.1
K2O (%)*	2.19	2.19	2.19	2.19	0.0	0.0
As (ppm)*	4	5	5	5	0.7	0.4
Ba (ppm)*	965	976	959	971	7.8	8.1
Cr (ppm)*	109	110	102	110	0.7	5.3
Cu (ppm)*	20	22	20	21	1.4	0.7
Ga (ppm)*	19	19	19	19	0.0	0.0
Mo (ppm)*	0	0	0	0	0.0	0.0
Nb (ppm)*	10	9	9	10	0.7	0.4
Ni (ppm)*	32	32	31	32	0.0	0.7
Pb (ppm)*	18	18	16	18	0.0	1.4
Rb (ppm)*	66	67	67	67	0.7	0.4
Sr (ppm)*	789	795	788	792	4.2	2.8
Th (ppm)*	9	8	7	9	0.7	1.1
U (ppm)*	2	3	3	3	0.7	0.4
V (ppm)*	164	157	150	161	4.9	7.4
Y (ppm)*	26	24	26	25	1.4	0.7
Zn (ppm)*	80	80	77	80	0.0	2.1
Zr (ppm)*	452	458	418	455	4.2	26.2

TABLE D-1 UNBALANCED TWO-LEVEL DESIGN

SAMPLE	SOC96210 A	SOC96210 B	SOC96210 C	MEAN OF A+B	ANALYTICAL VARIATION	WITHIN STREAM VARIATION
Fe2O3 (%)*	5.50	5.60	6.80	5.55	0.1	0.9
MnO (%)*	0.08	0.08	0.09	0.08	0.0	0.0
TiO2 (%)*	0.80	0.80	1.00	0.80	0.0	0.1
K2O (%)*	2.19	2.27	2.27	2.23	0.1	0.0
As (ppm)*	8	8	7	8	0.0	0.7
Ba (ppm)*	782	797	785	790	10.6	3.2
Cr (ppm)*	102	108	126	105	4.2	14.8
Cu (ppm)*	17	17	19	17	0.0	1.4
Ga (ppm)*	18	18	18	18	0.0	0.0
Mo (ppm)*	0	0	1	0	0.0	0.7
Nb (ppm)*	10	9	12	10	0.7	1.8
Ni (ppm)*	26	26	29	26	0.0	2.1
Pb (ppm)*	17	16	19	17	0.7	1.8
Rb (ppm)*	74	75	78	75	0.7	2.5
Sr (ppm)*	852	849	789	851	2.1	43.5
Th (ppm)*	6	6	8	6	0.0	1.4
U (ppm)*	2	2	2	2	0.0	0.0
V (ppm)*	120	115	152	118	3.5	24.4
Y (ppm)*	23	22	23	23	0.7	0.4
Zn (ppm)*	66	66	74	66	0.0	5.7
Zr (ppm)*	358	368	432	363	7.1	48.8

TABLE D-1 UNBALANCED TWO-LEVEL DESIGN

SAMPLE	SOC96240 A	SOC96240 B	SOC96240 C	MEAN A+B	ANALYTICAL VARIATION	WITHIN STREAM VARIATION
Fe2O3 (%)*	4.00	4.00	4.20	4.00	0.0	0.1
MnO (%)*	0.08	0.08	0.08	0.08	0.0	0.0
TiO2 (%)*	0.60	0.60	0.70	0.60	0.0	0.1
K2O (%)*	2.67	2.67	2.67	2.67	0.0	0.0
As (ppm)*	7	7	7	7	0.0	0.0
Ba (ppm)*	764	760	776	762	2.8	9.9
Cr (ppm)*	50	48	49	49	1.4	0.0
Cu (ppm)*	22	20	21	21	1.4	0.0
Ga (ppm)*	15	15	15	15	0.0	0.0
Mo (ppm)*	2	2	2	2	0.0	0.0
Nb (ppm)*	15	15	16	15	0.0	0.7
Ni (ppm)*	22	22	21	22	0.0	0.7
Pb (ppm)*	31	31	33	31	0.0	1.4
Rb (ppm)*	120	120	120	120	0.0	0.0
Sr (ppm)*	293	292	293	293	0.7	0.4
Th (ppm)*	11	12	12	12	0.7	0.4
U (ppm)*	3	3	4	3	0.0	0.7
V (ppm)*	74	79	79	77	3.5	1.8
Y (ppm)*	29	28	29	29	0.7	0.4
Zn (ppm)*	84	83	84	84	0.7	0.4
Zr (ppm)*	358	345	405	352	9.2	37.8

TABLE D-2. INTERNATIONAL SRM'S

Jsd-1				Jsd-2			
n=8				n=6			
	This Work		Ref. 1		This Work		Ref. 1
	Mean	STD			Mean	STD	
Fe2O3 (%)	4.95	0.0	4.889	Fe2O3 (%)	11.45	0.1	10.507
MnO (%)	0.09	0.0	0.0924	MnO (%)	0.13	0.0	0.12
TiO2 (%)	0.61	0.0	0.643	TiO2 (%)	0.65	0.0	0.614
As (ppm)	3	0.4	2.42	As (ppm)	36	0.5	38.6
Ba (ppm)	525	2.4	520	Ba (ppm)	1065	8.5	1199
Cr (ppm)	27	0.8	21.5	Cr (ppm)	143	3.6	108
Cu (ppm)	22	0.5	22	Cu (ppm)	1041	9.4	1117
Ga (ppm)	17	0.4	17.2	Ga (ppm)	14	0.4	15.3
Mo (ppm)				Mo (ppm)	15	0.4	11.5
Nb (ppm)	9	0.3	11.1	Nb (ppm)	2	0.6	4.56
Ni (ppm)	9	0.4	7.04	Ni (ppm)	100	0.9	92.8
Pb (ppm)	12	0.6	12.9	Pb (ppm)	156	1.0	146
Rb (ppm)	66	0.6	67.4	Rb (ppm)	26	0.5	26.9
Sr (ppm)	340	1.1	340	Sr (ppm)	206	1.4	202
Th (ppm)			4.44	Th (ppm)			2.33
U (ppm)			1	U (ppm)			1.1
V (ppm)	77	1.8	76	V (ppm)	150	3.9	125
Y (ppm)	13	0.4	14.8	Y (ppm)	18	0.6	17.4
Zn (ppm)	97	2.0	96.5	Zn (ppm)	1896	10.0	2056
Zr (ppm)	122	2.5	132	Zr (ppm)	107	1.3	111

TABLE D-2. Tables of international standard reference materials used in the study. Ref. 1 is values from Govindaraju (1994).

TABLE D-2. INTERNATIONAL SRM'S

Jsd-3				STSD-3			
	n=5				n=6		
	This Work		Ref. 1		This Work		Ref. 1
	Mean	STD			Mean	STD	
Fe2O3 (%)	4.27	0.0	4.218	Fe2O3 (%)	6.06	0.0	
MnO (%)	0.14	0.0	0.148	MnO (%)	0.39	0.0	0.34
TiO2 (%)	0.40	0.0	0.403	TiO2 (%)	0.61	0.0	0.72
As (ppm)	229	1.5	252	As (ppm)	25	0.5	28
Ba (ppm)	467	5.1	462	Ba (ppm)	1241	27.3	1490
Cr (ppm)	44	2.4	35.3	Cr (ppm)	79	1.1	80
Cu (ppm)	390	1.0	426	Cu (ppm)	38	0.7	39
Ga (ppm)	14	0.2	13.5	Ga (ppm)	15	0.4	
Mo (ppm)				Mo (ppm)	7	0.3	6
Nb (ppm)	6	0.6	7.8	Nb (ppm)	11	0.4	12
Ni (ppm)	20	0.5	19.6	Ni (ppm)	34	0.4	30
Pb (ppm)	84	0.5	82.1	Pb (ppm)	47	0.5	40
Rb (ppm)	282	1.7	285	Rb (ppm)	65	0.8	68
Sr (ppm)	57	0.3	58.7	Sr (ppm)	250	1.7	230
Th (ppm)	15	0.5	7.79	Th (ppm)	6	0.8	8.5
U (ppm)			1.66	U (ppm)	9	0.5	10.5
V (ppm)	82	2.1	70.4	V (ppm)	200	2.5	134
Y (ppm)	13	0.3	14.9	Y (ppm)	37	0.7	36
Zn (ppm)	134	0.8	136	Zn (ppm)	212	1.3	204
Zr (ppm)	120	1.7	124	Zr (ppm)	186	0.8	196

TABLE D-2. Tables of international standard reference materials used in the study. Ref. 1 is values from Govindaraju (1994).

TABLE D-2. INTERNATIONAL SRM'S

STSD-4			
	n=6		
	This Work		Ref. 1
	Mean	STD	
Fe2O3 (%)	5.49	0.0	
MnO (%)	0.21	0.0	0.19
TiO2 (%)	0.63	0.0	0.76
As (ppm)	13	0.2	15
Ba (ppm)	1483	25.5	2000
Cr (ppm)	93	3.7	93
Cu (ppm)	65	0.4	65
Ga (ppm)	14	0.3	
Mo (ppm)			
Nb (ppm)	5	0.4	9
Ni (ppm)	33	0.5	30
Pb (ppm)	18	0.4	18
Rb (ppm)	37	0.3	39
Sr (ppm)	373	1.5	350
Th (ppm)			4.3
U (ppm)			3
V (ppm)	124	2.4	106
Y (ppm)	25	0.4	24
Zn (ppm)	101	0.6	107
Zr (ppm)	172	3.0	190

TABLE D-2. Tables of international standard reference materials used in the study. Ref. 1 is values from Govindaraju (1994).

APPENDIX E

TABLE E-1. GEOCHEMICAL DATA

	SOC96001	SOC96002	SOC96003	SOC96004	SOC96005	SOC96006	SOC96007	SOC96008	SOC96009	SOC96010
UTM ZONE	13 S	13 S	13 S	13 S	13 S	13 S	13 S	13 S	13 S	13 S
EASTING	325000	327900	328000	330500	331800	332400	333400	333500	333400	336400
NORTHING	3775700	3780300	3779300	3779600	3780400	3786700	3786400	3785700	3781600	3781300
LAT. (N)	34.1075	34.1494	34.1404	34.1436	34.1510	34.2079	34.2053	34.1990	34.1621	34.1598
LONG (W)	106.8973	106.8668	106.8655	106.8384	106.8245	106.8192	106.8083	106.8071	106.8074	106.7748
TRACE ID	T1410	T1411	T1412	T1413	T1414	T1415	T1416	T1417	T1418	T1419
MAJOR ID	M1793	M1794	M1795	M1796	M1797	M1798	M1799	M1800	M1801	M1802
SiO2 (%)	70.68	70.33	68.58	66.42	67.27	67.67	72.04	67.61	65.53	66.16
Al2O3 (%)	9.61	7.64	7.94	6.95	9.84	10.29	8.35	9.04	10.68	8.11
Fe2O3 (%)	7.77	4.55	5.45	3.96	3.53	4.2	3.1	4.05	3.72	3.02
Fe2O3 (%)*	7.00	4.20	5.00	3.70	3.40	4.00	2.90	3.70	3.70	3.00
CaO (%)	3.05	5.85	4.97	7.03	3.88	3.96	4.15	5.02	5.25	6.58
K2O (%)	2.30	1.67	1.78	1.54	2.49	2.60	2.07	2.02	2.00	1.68
K2O (%)**	2.43	1.71	1.87	1.63	2.51	2.67	2.19	2.11	1.95	1.71
MgO (%)	1.02	1.34	1.21	1.52	1.36	1.82	1.19	1.55	1.45	2.55
Na2O (%)	1.67	1.27	1.55	1.14	1.70	1.99	1.41	1.29	1.30	1.06
TiO2 (%)	1.189	0.793	0.963	0.656	0.618	0.688	0.557	0.641	0.588	0.494
TiO2 (%)*	1.10	0.70	0.90	0.60	0.60	0.60	0.50	0.60	0.60	0.50
P2O5 (%)	0.120	0.085	0.101	0.065	0.090	0.117	0.096	0.119	0.142	0.080
MnO (%)	0.092	0.086	0.118	0.059	0.07	0.097	0.05	0.064	0.073	0.047
MnO (%)*	0.08	0.08	0.12	0.06	0.07	0.09	0.05	0.06	0.07	0.05
L.O.I.	3.49	6.79	5.76	8.2	6.85	5.41	5.98	6.82	7.75	9.45
SUM	101.199	100.577	98.62	97.707	97.848	99.01	99.394	98.586	98.656	99.368
As (ppm)*	7	6	6	6	4	5	4	5	6	4
Ba (ppm)*	757	682	811	633	509	649	486	566	885	426
Cr (ppm)*	112	58	60	57	53	95	50	60	53	55
Cu (ppm)*	16	14	17	13	17	20	13	17	19	14
Ga (ppm)*	13	10	10	9	14	14	10	11	13	9
Mo (ppm)*	3	2	3	2	2	2	2	0	0	0
Nb (ppm)*	15	12	14	9	16	19	10	10	10	8
Ni (ppm)*	22	15	18	15	18	38	13	18	17	18
Pb (ppm)*	24	15	17	13	24	22	14	14	17	12
Rb (ppm)*	89	59	60	56	90	100	72	72	83	64
Sr (ppm)*	316	204	225	213	243	402	295	342	306	172
Th (ppm)*	10	7	9	6	11	13	8	7	7	5
U (ppm)*	4	3	3	3	3	3	2	3	2	2
V (ppm)*	151	86	109	73	58	75	56	76	78	56
Y (ppm)*	30	27	29	24	36	40	23	24	26	20
Zn (ppm)*	76	48	58	42	66	74	44	52	55	37
Zr (ppm)*	885	676	776	605	492	513	494	491	346	312

* Analysis made on Pressed Powders

** Converted K2O%. Analysis on Pressed Powders

SUM is based on Fusion Disks and LOI

APPENDIX E

TABLE E-1. GEOCHEMICAL DATA

	SOC96011	SOC96012	SOC96013	SOC96014	SOC96015	SOC96016	SOC96017	SOC96018	SOC96019	SOC96020
UTM ZONE	13 S	13 S	13 S	13 S	13 S	13 S	13 S	13 S	13 S	13 S
EASTING	340200	342300	341400	342800	343800	330700	342600	342600	341700	342900
NORTHING	3782500	3780400	3778400	3778600	3776500	3775900	3755800	3756500	3757300	3762300
LAT. (N)	34.1712	34.1526	34.1345	34.1365	34.1177	34.1102	33.9309	33.9372	33.9443	33.9895
LONG (W)	106.7338	106.7106	106.7200	106.7049	106.6937	106.8355	106.7030	106.7031	106.7130	106.7009
TRACE ID	T1420	T1421	T1422	T1423	T1424	T1425	T1426	T1427	T1428	T1429
MAJOR ID	M1803	M1804	M1805	M1806	M1807	M1808	M1809	M1810	M1811	M1812
SiO2 (%)	72.52	73.01	70.58	56.05	74.06	71.83	63.65	65.45	67.11	59.94
Al2O3 (%)	5.33	8.65	8.38	13.73	7.08	6.73	10.18	9.94	10.47	11.32
Fe2O3 (%)	1.79	3.6	2.81	6.81	2.42	4.73	8.55	5.43	5.13	12.06
Fe2O3 (%)*	1.70	3.60	2.80	6.90	2.30	4.00	7.50	5.00	4.80	9.20
CaO (%)	5.66	3.60	5.55	7.01	4.63	6.09	5.80	5.40	4.17	4.44
K2O (%)	1.66	1.61	1.68	1.75	1.63	1.72	1.85	1.69	1.69	2.20
K2O (%)**	1.71	1.71	1.71	1.63	1.71	1.79	1.87	1.71	1.79	2.27
MgO (%)	1.68	2.14	2.26	2.95	2.06	1.20	1.89	1.96	1.99	1.89
Na2O (%)	0.65	1.03	1.27	0.77	1.14	0.91	1.94	0.92	0.62	2.11
TiO2 (%)	0.379	0.586	0.515	0.766	0.451	0.71	1.036	0.77	0.731	1.424
TiO2 (%)*	0.30	0.60	0.50	0.80	0.40	0.60	1.00	0.70	0.70	1.20
P2O5 (%)	0.057	0.066	0.075	0.079	0.064	0.083	0.170	0.107	0.093	0.212
MnO (%)	0.027	0.045	0.041	0.066	0.034	0.066	0.12	0.084	0.076	0.148
MnO (%)*	0.03	0.05	0.04	0.07	0.03	0.06	0.11	0.08	0.07	0.12
L.O.I.	8.53	6.13	7.83	10.74	6.57	6.68	5.81	8.11	7.95	4.44
SUM	99.068	100.589	101.094	100.827	100.406	100.921	101.19	100.047	100.247	100.419
As (ppm)*	0	5	5	6	4	6	6	6	6	6
Ba (ppm)*	329	391	376	401	368	639	796	1049	987	927
Cr (ppm)*	44	71	55	103	52	62	64	54	68	70
Cu (ppm)*	12	13	12	11	10	14	20	20	21	23
Ga (ppm)*	6	10	10	18	8	9	14	13	13	18
Mo (ppm)*	2	2	0	0	0	2	0	0	2	0
Nb (ppm)*	6	10	9	14	7	9	9	10	11	9
Ni (ppm)*	10	21	18	38	14	13	20	18	21	20
Pb (ppm)*	10	12	10	16	8	13	16	17	18	23
Rb (ppm)*	52	68	65	95	58	62	58	71	83	85
Sr (ppm)*	190	142	155	190	169	180	558	238	193	657
Th (ppm)*	3	7	5	11	4	6	7	8	9	12
U (ppm)*	2	2	3	4	2	3	2	3	3	3
V (ppm)*	30	59	48	115	38	87	180	110	96	231
Y (ppm)*	15	22	21	30	17	25	26	23	24	36
Zn (ppm)*	22	36	30	48	24	43	89	56	48	97
Zr (ppm)*	439	396	328	243	390	614	541	402	476	620

*** Analysis made on Pressed Powders**

**** Converted K2O%. Analysis on Pressed Powders**

SUM is based on Fusion Disks and LOI

APPENDIX E

TABLE E-1. GEOCHEMICAL DATA

	SOC96021	SOC96022	SOC96023	SOC96024	SOC96025	SOC96026	SOC96027	SOC96028	SOC96029	SOC96030 A
UTM ZONE	13 S	13 S	13 S	13 S	13 S	13 S	13 S	13 S	13 S	13 S
EASTING	344900	345100	318600	319200	326700	326250	327628	333387	333736	336102
NORTHING	3761000	3757100	3759250	3757200	3757100	3760400	3775380	3777810	3776597	3775412
LAT. (N)	33.9781	33.9430	33.9581	33.9398	33.9401	33.9698	34.1050	34.1279	34.1170	34.1067
LONG (W)	106.6790	106.6761	106.9632	106.9563	106.8752	106.8807	106.8687	106.8068	106.8028	106.7769
TRACE ID	T1430	T1431	T1432	T1433	T1434	T1435	T1436	T1437	T1438	T1439
MAJOR ID	M1813	M1814	M1815			M1816				M1817
SiO2 (%)	71.00	73.09	64.95			62.79				60.74
Al2O3 (%)	10.12	8.79	11.83			9.11				11.04
Fe2O3 (%)	6.34	3.9	4.06			12.43				4.58
Fe2O3 (%)*	5.10	3.60	3.90	3.90	3.90	11.20	5.00	1.70	2.10	4.60
CaO (%)	3.41	4.01	4.00			3.82				7.39
K2O (%)	2.18	2.06	3.70			2.34				1.79
K2O (%)**	2.43	2.19	3.48	2.59	2.43	2.35	1.87	2.51	2.11	1.79
MgO (%)	1.53	1.01	1.09			1.08				2.29
Na2O (%)	1.81	1.19	1.14			1.34				1.29
TiO2 (%)	1.008	0.666	0.656			1.832				0.657
TiO2 (%)*	0.80	0.60	0.60	0.60	0.70	1.70	0.80	0.30	0.40	0.60
P2O5 (%)	0.156	0.083	0.152			0.120				0.097
MnO (%)	0.087	0.056	0.143			0.201				0.066
MnO (%)*	0.08	0.05	0.13	0.15	0.09	0.19	0.07	0.03	0.04	0.07
L.O.I.	3.17	5.41	8.09			4.94				9.94
SUM	100.977	100.435	99.954			100.302				100.016
As (ppm)*	5	5	24	10	7	14	6	4	4	6
Ba (ppm)*	696	600	697	739	668	816	621	546	503	448
Cr (ppm)*	59	53	53	53	58	112	66	54	52	70
Cu (ppm)*	20	15	26	20	22	20	13	10	10	13
Ga (ppm)*	13	11	16	14	12	16	10	8	8	14
Mo (ppm)*	0	2	2	2	2	6	4	0	2	0
Nb (ppm)*	12	10	15	15	15	27	12	6	7	11
Ni (ppm)*	16	16	18	18	17	24	15	12	14	27
Pb (ppm)*	15	14	36	24	31	27	15	15	10	13
Rb (ppm)*	72	68	183	109	91	97	65	84	76	91
Sr (ppm)*	384	237	178	204	275	238	192	115	116	216
Th (ppm)*	7	7	11	10	9	17	8	3	3	8
U (ppm)*	3	2	3	3	3	5	3	2	3	3
V (ppm)*	118	70	74	73	80	252	102	33	42	81
Y (ppm)*	26	26	29	32	31	50	30	16	18	28
Zn (ppm)*	56	48	131	74	66	122	53	32	29	44
Zr (ppm)*	435	563	382	550	586	1614	1016	409	403	349

*** Analysis made on Pressed Powders**

**** Converted K2O%. Analysis on Pressed Powders**

SUM is based on Fusion Disks and LOI

APPENDIX E

TABLE E-1. GEOCHEMICAL DATA

	SOC96030 B	SOC96030 C	SOC96031	SOC96032	SOC96033	SOC96034	SOC96035	SOC96036	SOC96037	SOC96038
UTM ZONE	13 S	13 S	13 S	13 S	13 S	13 S	13 S	13 S	13 S	13 S
EASTING	336102	336102	335722	336051	336392	335788	336021	334336	332163	328861
NORTHING	3775412	3775412	3773286	3771739	3769769	3770254	3767626	3766484	3763591	3763923
LAT. (N)	34.1067	34.1067	34.0875	34.0736	34.0559	34.0602	34.0365	34.0259	33.9995	34.0020
LONG (W)	106.7769	106.7769	106.7806	106.7768	106.7727	106.7793	106.7763	106.7943	106.8173	106.8531
TRACE ID	T1440	T1441	T1442	T1443	T1444	T1445	T1446	T1447	T1448	T1449
MAJOR ID	M1818		M1819		M1820			M1821	M1822	
SiO2 (%)	60.66		68.99		71.64			59.75	72.65	
Al2O3 (%)	11.01		9.78		6.32			12.21	6.92	
Fe2O3 (%)	4.57		3.69		2.03			4.61	5.21	
Fe2O3 (%)*	4.60	4.90	3.70	2.90	2.00	4.60	2.00	4.60	3.80	4.90
CaO (%)	7.36		3.92		6.19			6.42	4.37	
K2O (%)	1.79		1.99		1.56			2.06	1.68	
K2O (%)**	1.79	1.71	2.03	1.87	1.63	1.79	1.63	1.95	1.71	1.87
MgO (%)	2.29		2.91		2.47			2.68	1.31	
Na2O (%)	1.30		1.09		0.62			0.88	1.08	
TiO2 (%)	0.657		0.685		0.442			0.675	0.831	
TiO2 (%)*	0.60	0.60	0.60	0.50	0.40	0.60	0.40	0.70	0.70	0.80
P2O5 (%)	0.098		0.075		0.076			0.090	0.059	
MnO (%)	0.066		0.059		0.034			0.057	0.063	
MnO (%)*	0.07	0.07	0.06	0.04	0.03	0.05	0.03	0.05	0.05	0.07
L.O.I.	9.94		7.87		8.78			10.56	5.78	
SUM	99.87		101.186		100.316			100.103	100.143	
As (ppm)*	5	6	4	5	4	5	5	6	5	6
Ba (ppm)*	443	461	527	505	354	567	360	367	583	1062
Cr (ppm)*	73	70	65	49	49	63	44	82	49	56
Cu (ppm)*	14	14	16	14	12	10	10	11	10	13
Ga (ppm)*	14	14	12	9	8	13	8	16	10	10
Mo (ppm)*	0	2	0	2	2	2	0	0	3	3
Nb (ppm)*	12	12	11	10	7	12	7	14	10	12
Ni (ppm)*	27	26	22	16	14	22	12	31	11	14
Pb (ppm)*	14	14	11	10	9	13	11	11	11	15
Rb (ppm)*	90	90	93	67	50	80	52	111	58	59
Sr (ppm)*	216	213	160	165	147	182	290	183	193	237
Th (ppm)*	7	10	7	5	0	10	3	9	5	8
U (ppm)*	3	3	3	3	3	3	2	4	2	3
V (ppm)*	76	81	66	54	36	80	45	78	81	110
Y (ppm)*	27	28	26	22	18	39	16	30	21	28
Zn (ppm)*	43	44	42	37	27	38	30	36	37	52
Zr (ppm)*	345	384	468	450	379	591	377	292	821	891

*** Analysis made on Pressed Powders**

**** Converted K2O%. Analysis on Pressed Powders**

SUM is based on Fusion Disks and LOI

APPENDIX E

TABLE E-1. GEOCHEMICAL DATA

	SOC96039	SOC96040	SOC96041	SOC96042	SOC96043	SOC96044	SOC96045	SOC96046	SOC96047	SOC96048
UTM ZONE	13 S	13 S	13 S	13 S	13 S	13 S	13 S	13 S	13 S	13 S
EASTING	331835	333106	333210	332896	336010	336288	332974	333275	341463	337591
NORTHING	3756712	3758309	3753862	3753801	3756682	3755329	3752984	3752888	3751540	3750431
LAT. (N)	33.9375	33.9521	33.9120	33.9114	33.9378	33.9257	33.9040	33.9032	33.8923	33.8817
LONG (W)	106.8195	106.8061	106.8041	106.8075	106.7744	106.7711	106.8065	106.8032	106.7145	106.7561
TRACE ID	T1450	T1451	T1452	T1453	T1454	T1455	T1456	T1457	T1458	T1459
MAJOR ID		M1823		M1824		M1825		M1826	M1827	
SiO2 (%)		75.06		70.82		72.74		69.43	75.62	
Al2O3 (%)		7.39		7.54		6.26		7.24	9.13	
Fe2O3 (%)		3.71		4.04		2.25		5.45	4.62	
Fe2O3 (%)*	3.90	2.90	3.90	3.10	2.70	2.00	5.20	4.20	3.90	5.20
CaO (%)		3.96		5.56		6.23		5.80	1.59	
K2O (%)		1.94		1.82		1.87		1.79	1.87	
K2O (%)**	2.11	1.87	1.95	1.79	1.71	1.79	1.87	1.79	2.03	2.11
MgO (%)		0.85		1.16		1.62		0.88	0.80	
Na2O (%)		1.17		1.14		0.86		1.15	1.29	
TiO2 (%)		0.703		0.706		0.458		1.073	0.751	
TiO2 (%)*	0.70	0.50	0.70	0.60	0.50	0.40	0.80	0.80	0.70	0.70
P2O5 (%)		0.068		0.078		0.064		0.092	0.075	
MnO (%)		0.059		0.058		0.037		0.101	0.056	
MnO (%)*	0.06	0.05	0.05	0.05	0.04	0.03	0.10	0.08	0.04	0.05
L.O.I.		5.11		7.09		7.46		6.66	3.94	
SUM		100.201		100.201		99.959		99.916	99.918	
As (ppm)*	4	4	6	5	5	4	5	5	7	11
Ba (ppm)*	632	539	659	689	499	407	805	738	571	704
Cr (ppm)*	57	56	55	55	48	42	53	52	44	61
Cu (ppm)*	12	10	11	12	15	9	13	10	13	18
Ga (ppm)*	10	9	10	10	10	7	11	10	11	16
Mo (ppm)*	4	2	3	2	0	0	2	4	2	2
Nb (ppm)*	16	10	10	9	8	6	11	12	11	12
Ni (ppm)*	14	11	12	12	16	11	17	11	14	19
Pb (ppm)*	16	12	14	14	11	10	17	16	14	22
Rb (ppm)*	74	66	65	64	63	59	81	67	72	90
Sr (ppm)*	208	211	192	213	158	153	246	230	193	289
Th (ppm)*	7	5	7	6	5	3	12	10	8	12
U (ppm)*	4	4	3	2	2	2	4	3	3	3
V (ppm)*	80	66	81	65	54	40	114	91	78	106
Y (ppm)*	29	21	23	21	20	15	32	28	26	27
Zn (ppm)*	50	35	42	40	35	31	59	45	50	76
Zr (ppm)*	830	672	667	600	312	375	1039	1090	569	483

*** Analysis made on Pressed Powders**

**** Converted K2O%. Analysis on Pressed Powders**

SUM is based on Fusion Disks and LOI

APPENDIX E

TABLE E-1. GEOCHEMICAL DATA

	SOC96049	SOC96050	SOC96051	SOC96052	SOC96053	SOC96054	SOC96055	SOC96056	SOC96057	SOC96058
UTM ZONE	13 S	13 S	13 S	13 S	13 S	13 S	13 S	13 S	13 S	13 S
EASTING	339175	337259	336629	335882	354826	341726	345216	341611	343315	340694
NORTHING	3759995	3760962	3764633	3764521	3755434	3754984	3764724	3767126	3766713	3768641
LAT. (N)	33.9682	33.9766	34.0096	34.0085	33.9294	33.9234	34.0117	34.0329	34.0294	34.0464
LONG (W)	106.7408	106.7617	106.7692	106.7772	106.5707	106.7123	106.6762	106.7157	106.6972	106.7259
TRACE ID	T1460	T1461	T1462	T1463	T1464	T1465	T1466	T1467	T1468	T1469
MAJOR ID		M1828	M1829					M1830		
SiO2 (%)		70.86	65.18					63.98		
Al2O3 (%)		6.44	6.81					12.22		
Fe2O3 (%)		2.17	2.46					6.08		
Fe2O3 (%)*	2.00	2.00	2.20	2.40	3.30	6.50	3.40	6.00	8.20	2.20
CaO (%)		6.41	7.30					3.44		
K2O (%)		1.73	1.81					2.08		
K2O (%)**	1.71	1.79	1.79	1.71	2.11	2.27	2.67	2.03	1.71	1.14
MgO (%)		2.08	2.42					2.21		
Na2O (%)		0.67	0.60					1.29		
TiO2 (%)		0.445	0.486					0.765		
TiO2 (%)*	0.40	0.40	0.40	0.50	0.50	0.80	0.60	0.80	1.00	0.50
P2O5 (%)		0.072	0.081					0.081		
MnO (%)		0.031	0.034					0.062		
MnO (%)*	0.03	0.03	0.03	0.04	0.06	0.07	0.06	0.06	0.12	0.03
L.O.I.		8.29	8.93					7.34		
SUM		99.381	97.126					99.682		
As (ppm)*	4	4	4	4	5	5	4	7	5	0
Ba (ppm)*	360	351	319	374	534	641	472	432	645	350
Cr (ppm)*	45	46	53	57	50	80	49	95	86	69
Cu (ppm)*	10	9	8	11	17	27	10	10	24	68
Ga (ppm)*	8	8	8	9	13	20	13	16	15	8
Mo (ppm)*	2	0	0	2	0	0	2	0	0	0
Nb (ppm)*	6	5	7	8	10	13	19	14	11	8
Ni (ppm)*	12	13	15	14	18	31	12	31	22	16
Pb (ppm)*	10	10	7	8	18	21	20	14	19	6
Rb (ppm)*	53	53	55	56	84	138	112	98	62	38
Sr (ppm)*	159	199	219	138	210	278	215	175	456	120
Th (ppm)*	4	5	3	5	8	11	15	10	9	4
U (ppm)*	2	2	3	2	2	4	4	5	4	2
V (ppm)*	38	38	48	47	60	122	61	100	192	42
Y (ppm)*	16	16	18	20	24	30	53	30	28	20
Zn (ppm)*	27	27	28	29	59	57	56	40	88	28
Zr (ppm)*	381	356	373	415	242	369	822	434	556	478

*** Analysis made on Pressed Powders**

**** Converted K2O%. Analysis on Pressed Powders**

SUM is based on Fusion Disks and LOI

APPENDIX E

TABLE E-1. GEOCHEMICAL DATA

	SOC96059	SOC96060 A	SOC96060 B	SOC96060 C	SOC96061	SOC96062	SOC96064	SOC96065	SOC96066	SOC96067
UTM ZONE	13 S	13 S	13 S	13 S	13 S	13 S	13 S	13 S	13 S	13 S
EASTING	339382	340692	340692	340692	339905	343642	337230	345637	347052	324763
NORTHING	3764974	3773718	3773718	3773718	3774068	3769741	3779668	3778186	3775398	3763050
LAT. (N)	34.0131	34.0921	34.0921	34.0921	34.0952	34.0567	34.1452	34.1332	34.1082	33.9934
LONG (W)	106.7394	106.7269	106.7269	106.7269	106.7354	106.6942	106.7655	106.6741	106.6582	106.8973
TRACE ID	T1470	T1471	T1472	T1473	T1474	T1475	T1477	T1478	T1479	T1480
MAJOR ID		M1831	M1832			M1833		M1834		
SiO2 (%)		69.39	69.28			67.20		65.88		
Al2O3 (%)		8.04	8.01			9.12		7.61		
Fe2O3 (%)		2.62	2.65			4.26		2.53		
Fe2O3 (%)*	4.90	2.50	2.50	2.30	5.20	3.90	5.10	2.50	2.50	13.60
CaO (%)		5.57	5.61			5.52		7.42		
K2O (%)		1.70	1.70			1.57		1.63		
K2O (%)**	1.95	1.71	1.71	1.71	1.22	1.63	1.87	1.54	1.38	2.27
MgO (%)		2.24	2.25			1.95		2.07		
Na2O (%)		1.24	1.24			0.75		1.03		
TIO2 (%)		0.487	0.486			0.66		0.456		
TiO2 (%)*	0.70	0.50	0.50	0.40	0.70	0.60	0.70	0.50	0.50	2.40
P2O5 (%)		0.087	0.086			0.114		0.085		
MnO (%)		0.044	0.044			0.069		0.051		
MnO (%)*	0.12	0.04	0.04	0.04	0.05	0.06	0.07	0.05	0.04	0.17
L.O.I.		8.36	8.36			8.62		10.12		
SUM		99.902	99.827			100.024		99.159		
As (ppm)*	4	4	4	4	6	6	6	4	5	11
Ba (ppm)*	626	430	425	418	432	712	404	469	549	608
Cr (ppm)*	57	50	53	48	85	59	80	37	44	173
Cu (ppm)*	22	13	14	11	13	18	9	12	12	19
Ga (ppm)*	17	9	9	8	15	11	15	9	8	16
Mo (ppm)*	0	0	0	0	0	2	0	0	0	8
Nb (ppm)*	12	8	8	8	13	10	13	8	8	36
Ni (ppm)*	22	16	15	14	31	19	28	12	13	27
Pb (ppm)*	18	12	10	9	14	15	13	13	13	31
Rb (ppm)*	104	60	60	57	76	64	100	55	59	87
Sr (ppm)*	235	142	143	137	209	182	204	219	233	242
Th (ppm)*	10	4	4	3	10	8	8	4	3	20
U (ppm)*	3	2	2	2	4	3	4	2	2	5
V (ppm)*	96	48	50	47	87	88	92	53	50	301
Y (ppm)*	24	19	19	18	28	23	29	17	19	47
Zn (ppm)*	38	33	33	29	47	49	39	34	39	143
Zr (ppm)*	258	332	341	328	331	484	341	335	448	1850

* Analysis made on Pressed Powders

** Converted K2O%. Analysis on Pressed Powders

SUM is based on Fusion Disks and LOI

APPENDIX E

TABLE E-1. GEOCHEMICAL DATA

	SOC96068	SOC96069	SOC96070	SOC96071	SOC96072	SOC96073	SOC96074	SOC96075	SOC96076	SOC96077
UTM ZONE	13 S	13 S	13 S	13 S	13 S	13 S	13 S	13 S	13 S	13 S
EASTING	324844	326012	321305	321765	320977	324453	321105	316390	317790	314124
NORTHING	3765119	3754597	3753622	3752774	3755701	3759244	3758985	3761932	3763396	3762646
LAT. (N)	34.0121	33.9174	33.9079	33.9003	33.9265	33.9591	33.9562	33.9819	33.9954	33.9880
LONG (W)	106.8968	106.8821	106.9328	106.9277	106.9368	106.8999	106.9361	106.9877	106.9728	107.0123
TRACE ID	T1481	T1482	T1483	T1484	T1485	T1486	T1487	T1488	T1489	T1490
MAJOR ID	M1835	M1836		M1837	M1838		M1839		M1840	
SiO2 (%)	70.32	64.52		64.84	71.73		65.38		63.57	
Al2O3 (%)	10.20	8.63		9.91	9.69		11.80		11.26	
Fe2O3 (%)	3.99	12.32		7.29	4.5		6.75		6.32	
Fe2O3 (%)*	3.70	10.50	5.10	6.50	3.90	5.30	6.00	4.10	5.70	5.40
CaO (%)	3.13	2.83		4.59	2.90		2.71		3.99	
K2O (%)	2.71	2.19		2.37	2.76		3.34		3.31	
K2O (%)**	2.67	2.35	2.59	2.51	2.83	2.75	3.40	3.32	3.32	3.24
MgO (%)	1.09	0.99		1.09	0.86		1.11		1.63	
Na2O (%)	1.49	1.41		1.70	1.54		2.05		1.24	
TiO2 (%)	0.691	1.81		1.222	0.758		1.073		1.125	
TiO2 (%)*	0.60	1.60	0.80	1.10	0.60	0.70	1.00	0.70	1.00	1.00
P2O5 (%)	0.114	0.109		0.097	0.082		0.129		0.134	
MnO (%)	0.087	0.158		0.112	0.077		0.121		0.092	
MnO (%)*	0.09	0.14	0.10	0.10	0.07	0.08	0.11	0.17	0.09	0.12
L.O.I.	5.69	4.2		6.03	4.76		4.49		6.72	
SUM	99.677	99.429		99.459	99.836		99.129		99.556	
As (ppm)*	8	9	8	13	5	10	10	21	21	8
Ba (ppm)*	727	629	677	721	626	624	834	900	718	831
Cr (ppm)*	72	106	71	83	58	64	80	62	92	71
Cu (ppm)*	17	20	20	22	14	22	23	16	25	15
Ga (ppm)*	14	15	15	15	12	17	17	14	15	16
Mo (ppm)*	2	6	2	2	2	0	2	3	2	3
Nb (ppm)*	16	26	20	20	15	17	23	18	17	23
Ni (ppm)*	17	23	20	22	15	24	23	17	27	19
Pb (ppm)*	27	22	22	25	19	23	27	63	31	20
Rb (ppm)*	103	86	111	102	103	117	142	143	149	119
Sr (ppm)*	262	240	359	334	274	194	330	231	338	392
Th (ppm)*	8	14	11	10	11	12	11	10	10	8
U (ppm)*	4	4	3	2	3	2	3	3	3	3
V (ppm)*	76	238	106	146	79	96	123	84	134	101
Y (ppm)*	28	46	34	34	26	35	36	35	24	32
Zn (ppm)*	57	121	73	83	52	80	78	86	86	66
Zr (ppm)*	449	1334	588	873	557	502	540	632	409	673

* Analysis made on Pressed Powders

** Converted K2O%. Analysis on Pressed Powders

SUM is based on Fusion Disks and LOI

APPENDIX E

TABLE E-1. GEOCHEMICAL DATA

	SOC96078	SOC96079	SOC96080	SOC96081	SOC96082	SOC96083	SOC96084	SOC96085	SOC96086	SOC96087
UTM ZONE	13 S	13 S	13 S	13 S	13 S	13 S	13 S	13 S	13 S	13 S
EASTING	315292	315716	313593	313231	315972	315873	312486	309865	308035	308321
NORTHING	3760806	3758752	3756282	3753718	3753278	3752970	3752792	3752278	3753128	3752570
LAT. (N)	33.9716	33.9531	33.9305	33.9073	33.9038	33.9011	33.8988	33.8937	33.9011	33.8961
LONG (W)	106.9993	106.9943	107.0167	107.0201	106.9904	106.9914	107.0280	107.0562	107.0761	107.0729
TRACE ID	T1491	T1492	T1493	T1494	T1495	T1496	T1497	T1498	T1499	T1500
MAJOR ID		M1841		M1842		M1843		M1844	M1845	
SiO2 (%)		64.95		69.79		63.91		72.00	71.98	
Al2O3 (%)		11.22		10.20		10.43		11.21	11.48	
Fe2O3 (%)		5.86		7.08		4.06		4.9	4.53	
Fe2O3 (%)*	4.40	5.20	4.10	6.40	7.10	3.50	5.50	4.10	3.90	3.20
CaO (%)		3.25		1.72		6.36		1.09	0.97	
K2O (%)		2.97		3.00		2.35		3.45	3.70	
K2O (%)**	3.48	2.92	2.59	3.16	2.59	2.27	3.24	3.56	3.72	3.00
MgO (%)		1.21		0.70		1.04		0.64	0.57	
Na2O (%)		1.59		1.77		1.74		1.99	2.13	
TiO2 (%)		0.975		1.171		0.655		0.911	0.837	
TiO2 (%)*	0.80	0.90	0.70	1.10	1.20	0.60	1.00	0.80	0.70	0.60
P2O5 (%)		0.123		0.080		0.093		0.061	0.050	
MnO (%)		0.097		0.121		0.062		0.148	0.106	
MnO (%)*	0.07	0.09	0.07	0.11	0.09	0.05	0.10	0.12	0.09	0.07
L.O.I.		7.05		3.3		8.89		3.15	2.94	
SUM		99.466		99.169		99.756		99.747	99.469	
As (ppm)*	13	9	8	7	6	5	5	8	6	6
Ba (ppm)*	701	688	744	708	600	581	817	699	508	570
Cr (ppm)*	76	78	66	70	82	44	56	49	42	45
Cu (ppm)*	17	20	15	15	16	16	13	15	11	14
Ga (ppm)*	14	16	14	14	15	14	16	15	17	14
Mo (ppm)*	2	2	2	4	2	0	4	3	2	2
Nb (ppm)*	17	20	16	29	19	13	32	25	31	18
Ni (ppm)*	17	22	20	18	17	14	16	14	12	14
Pb (ppm)*	23	21	17	23	20	20	21	24	23	19
Rb (ppm)*	141	146	113	120	111	116	117	140	156	127
Sr (ppm)*	231	274	312	245	390	466	274	228	188	215
Th (ppm)*	10	12	9	14	14	11	18	14	18	11
U (ppm)*	3	3	3	4	4	0	4	3	4	3
V (ppm)*	82	106	79	121	178	67	95	71	58	56
Y (ppm)*	31	34	31	58	32	24	77	62	104	37
Zn (ppm)*	75	78	59	86	74	52	74	64	62	54
Zr (ppm)*	648	623	542	986	758	377	1210	815	875	486

* Analysis made on Pressed Powders

** Converted K2O%. Analysis on Pressed Powders

SUM is based on Fusion Disks and LOI

APPENDIX E

TABLE E-1. GEOCHEMICAL DATA

	SOC96088	SOC96089	SOC96090 A	SOC96090 B	SOC96090 C	SOC96091	SOC96092	SOC96093	SOC96094	SOC96095
UTM ZONE	13 S	13 S	13 S	13 S	13 S	13 S	13 S	13 S	13 S	13 S
EASTING	314699	298604	293383	293383	293383	289820	288412	288521	289460	288981
NORTHING	3761298	3780143	3779502	3779502	3779502	3778650	3785077	3786508	3789070	3781522
LAT. (N)	33.9759	34.1428	34.1360	34.1360	34.1360	34.1276	34.1852	34.1981	34.2214	34.1533
LONG (W)	107.0058	107.1843	107.2407	107.2407	107.2407	107.2791	107.2960	107.2951	107.2856	107.2889
TRACE ID	T1501	T1502	T1503	T1504	T1505	T1506	T1507	T1508	T1509	T1510
MAJOR ID	M1846		M1847	M1848				M1849		M1850
SiO2 (%)	67.13		62.93	62.95				55.36		58.67
Al2O3 (%)	10.86		13.69	13.71				14.50		15.00
Fe2O3 (%)	8.09		5.59	5.7				14.74		10.31
Fe2O3 (%)*	6.80	7.80	5.40	5.50	5.20	10.50	11.50	12.00	12.50	9.40
CaO (%)	2.05		3.17	3.20				3.37		3.81
K2O (%)	3.07		3.04	3.04				1.68		2.09
K2O (%)**	3.24	2.83	3.00	3.08	3.08	2.51	1.95	1.87	1.79	2.19
MgO (%)	0.93		1.55	1.56				1.74		1.86
Na2O (%)	1.98		2.01	2.01				3.27		3.63
TiO2 (%)	1.328		0.904	0.914				2.001		1.573
TiO2 (%)*	1.20	1.00	0.90	0.90	0.80	1.50	1.80	1.80	1.90	1.50
P2O5 (%)	0.084		0.155	0.155				0.068		0.129
MnO (%)	0.12		0.098	0.098				0.16		0.123
MnO (%)*	0.10	0.11	0.10	0.10	0.10	0.13	0.13	0.13	0.15	0.11
L.O.I.	3.18		6.21	6.21				2.42		2.03
SUM	99.052		99.543	99.73				99.589		99.495
As (ppm)*	8	7	8	9	9	6	6	7	5	4
Ba (ppm)*	886	705	835	842	822	969	840	824	916	945
Cr (ppm)*	141	117	94	101	94	220	134	128	303	152
Cu (ppm)*	17	39	24	25	24	30	16	19	33	19
Ga (ppm)*	16	22	18	19	18	20	22	24	21	20
Mo (ppm)*	3	4	0	0	0	0	0	2	0	0
Nb (ppm)*	25	26	17	17	16	11	11	12	12	12
Ni (ppm)*	25	33	33	33	32	53	30	32	71	37
Pb (ppm)*	24	45	54	54	45	26	19	18	19	17
Rb (ppm)*	122	165	114	114	114	92	51	54	48	66
Sr (ppm)*	319	369	432	430	438	788	1153	1056	944	1019
Th (ppm)*	11	43	12	12	11	7	6	8	5	5
U (ppm)*	3	6	3	4	3	2	2	2	2	2
V (ppm)*	150	154	114	107	112	231	285	289	298	218
Y (ppm)*	44	58	32	33	32	25	22	24	27	26
Zn (ppm)*	83	135	91	93	91	101	89	100	107	87
Zr (ppm)*	842	1055	419	421	403	429	616	827	646	565

*** Analysis made on Pressed Powders**

**** Converted K2O%. Analysis on Pressed Powders**

SUM is based on Fusion Disks and LOI

APPENDIX E

TABLE E-1. GEOCHEMICAL DATA

	SOC96096	SOC96097	SOC96098	SOC96099	SOC96100	SOC96101	SOC96102	SOC96103	SOC96104	SOC96105
UTM ZONE	13 S	13 S	13 S	13 S	13 S	13 S	13 S	13 S	13 S	13 S
EASTING	286757	283627	285527	287680	284457	284372	293396	294460	291362	287306
NORTHING	3785314	3788250	3786111	3777459	3780335	3779490	3781604	3781686	3775192	3769431
LAT. (N)	34.1870	34.2128	34.1940	34.1164	34.1417	34.1341	34.1549	34.1559	34.0967	34.0440
LONG (W)	107.3140	107.3487	107.3275	107.3020	107.3377	107.3384	107.2411	107.2296	107.2616	107.3041
TRACE ID	T1511	T1512	T1513	T1514	T1515	T1516	T1517	T1518	T1519	T1520
MAJOR ID	M1851	M1852		M1853	M1854			M1855		M1856
SiO2 (%)	51.87	56.83		55.20	49.09			58.43		65.16
Al2O3 (%)	13.91	13.16		13.61	12.72			12.85		13.41
Fe2O3 (%)	16.26	12.91		13.54	20.71			6.16		4.63
Fe2O3 (%)*	14.40	11.40	8.00	12.40	17.80	6.30	6.40	5.40	8.40	4.40
CaO (%)	4.38	3.94		2.78	4.20			5.88		3.01
K2O (%)	1.56	1.98		2.44	1.47			2.34		2.49
K2O (%)**	1.54	2.11	2.51	2.35	1.54	2.19	2.59	2.35	2.27	2.51
MgO (%)	2.13	2.21		2.17	2.12			1.60		1.34
Na2O (%)	3.23	2.84		2.76	3.01			2.15		2.25
TiO2 (%)	2.16	1.849		1.793	3.444			0.923		0.773
TiO2 (%)*	2.10	1.80	1.30	1.80	3.40	1.00	1.00	0.80	1.20	0.70
P2O5 (%)	0.116	0.174		0.175	0.156			0.148		0.107
MnO (%)	0.177	0.151		0.153	0.225			0.083		0.095
MnO (%)*	0.16	0.14	0.11	0.15	0.20	0.09	0.11	0.08	0.12	0.09
L.O.I.	2.75	2.82		3.67	2.1			9.27		6.47
SUM	98.834	99.111		98.544	99.571			100.031		99.913
As (ppm)*	6	5	5	5	6	4	6	6	6	4
Ba (ppm)*	768	937	1021	910	579	929	926	765	859	829
Cr (ppm)*	177	193	152	370	164	68	128	81	133	62
Cu (ppm)*	21	22	26	33	19	15	32	24	22	18
Ga (ppm)*	23	20	19	20	25	20	18	17	18	16
Mo (ppm)*	2	2	0	0	2	0	0	0	0	0
Nb (ppm)*	13	13	10	11	28	10	14	13	16	14
Ni (ppm)*	44	46	42	74	42	21	48	25	31	21
Pb (ppm)*	19	19	16	21	20	16	124	29	22	19
Rb (ppm)*	45	61	70	98	47	55	96	88	81	91
Sr (ppm)*	1062	870	850	672	979	1106	462	553	628	460
Th (ppm)*	7	7	8	8	11	5	9	10	8	9
U (ppm)*	2	2	2	3	3	2	3	2	2	2
V (ppm)*	357	276	181	348	444	136	133	109	193	78
Y (ppm)*	26	29	27	27	39	23	32	24	28	28
Zn (ppm)*	126	104	83	107	163	63	110	84	93	67
Zr (ppm)*	891	678	466	585	1294	430	390	432	476	421

*** Analysis made on Pressed Powders**

**** Converted K2O%. Analysis on Pressed Powders**

SUM is based on Fusion Disks and LOI

APPENDIX E

TABLE E-1. GEOCHEMICAL DATA

	SOC96106	SOC96107	SOC96108	SOC96109	SOC96110	SOC96111	SOC96112	SOC96113	SOC96114	SOC96115
UTM ZONE	13 S	13 S	13 S	13 S	13 S	13 S	13 S	13 S	13 S	13 S
EASTING	286016	286036	284408	285020	283951	283940	283972	304674	303671	302892
NORTHING	3764830	3766159	3760492	3760679	3758591	3752774	3754212	3770260	3771571	3772019
LAT. (N)	34.0023	34.0143	33.9629	33.9647	33.9456	33.8932	33.9062	34.0549	34.0665	34.0704
LONG (W)	107.3170	107.3171	107.3333	107.3267	107.3378	107.3365	107.3365	107.1163	107.1274	107.1360
TRACE ID	T1521	T1522	T1523	T1524	T1525	T1526	T1527	T1528	T1529	T1530
MAJOR ID	M1857		M1858				M1859	M1860		M1861
SiO2 (%)	65.89		67.28				67.73	68.64		66.78
Al2O3 (%)	13.78		12.31				12.82	12.68		13.31
Fe2O3 (%)	4.67		6.07				3.69	6.12		5.3
Fe2O3 (%)*	4.40	4.70	5.40	4.40	4.00	3.10	3.50	5.70	7.30	5.40
CaO (%)	1.85		3.05				1.85	1.50		1.85
K2O (%)	2.68		2.56				3.30	2.72		2.62
K2O (%)**	2.67	2.51	2.67	3.08	2.51	3.24	3.08	2.75	2.27	2.59
MgO (%)	1.17		1.25				0.87	1.11		1.25
Na2O (%)	2.27		2.69				2.10	1.91		1.67
TiO2 (%)	0.765		1.058				0.636	1.054		0.998
TiO2 (%)*	0.70	0.70	1.00	0.90	0.70	0.50	0.60	1.00	1.00	0.90
P2O5 (%)	0.096		0.085				0.100	0.088		0.080
MnO (%)	0.103		0.1				0.093	0.106		0.093
MnO (%)*	0.10	0.12	0.09	0.08	0.09	0.07	0.09	0.11	0.14	0.09
L.O.I.	6.44		3.2				6.33	4.12		5.75
SUM	99.889		99.861				99.647	100.235		99.864
As (ppm)*	4	5	5	5	5	0	5	6	5	6
Ba (ppm)*	827	845	788	754	738	455	527	746	598	715
Cr (ppm)*	56	55	73	54	55	43	45	73	68	63
Cu (ppm)*	17	21	13	12	20	12	18	22	35	25
Ga (ppm)*	18	17	17	16	17	16	16	16	18	17
Mo (ppm)*	2	0	0	0	0	0	0	0	0	0
Nb (ppm)*	19	15	21	22	18	21	20	16	14	15
Ni (ppm)*	21	22	18	16	17	13	17	23	35	23
Pb (ppm)*	20	24	23	19	26	19	21	31	42	31
Rb (ppm)*	102	97	89	114	106	132	131	103	106	101
Sr (ppm)*	382	406	549	396	383	231	222	317	182	220
Th (ppm)*	11	10	10	12	12	12	12	11	10	10
U (ppm)*	3	2	3	3	2	3	3	3	3	2
V (ppm)*	78	81	115	86	71	51	55	109	132	100
Y (ppm)*	34	30	35	36	30	46	41	37	47	47
Zn (ppm)*	71	79	66	58	73	57	69	86	131	92
Zr (ppm)*	404	349	658	679	430	391	345	544	367	425

*** Analysis made on Pressed Powders**

**** Converted K2O%. Analysis on Pressed Powders**

SUM is based on Fusion Disks and LOI

APPENDIX E

TABLE E-1. GEOCHEMICAL DATA

	SOC96116	SOC96117	SOC96118	SOC96119	SOC96120 A	SOC96120 B	SOC96120 C	SOC96121	SOC96122	SOC96123
UTM ZONE	13 S	13 S	13 S	13 S	13 S	13 S	13 S	13 S	13 S	13 S
EASTING	302791	284137	285914	289124	288648	288648	288648	291566	289914	306555
NORTHING	3774580	3775059	3775473	3775948	3764488	3764488	3764488	3761695	3754585	3764867
LAT. (N)	34.0934	34.0941	34.0982	34.1031	33.9997	33.9997	33.9997	33.9752	33.9107	34.0066
LONG (W)	107.1377	107.3398	107.3207	107.2860	107.2884	107.2884	107.2884	107.2562	107.2723	107.0947
TRACE ID	T1531	T1532	T1533	T1534	T1535	T1536	T1537	T1538	T1539	T1540
MAJOR ID		M1862							M1863	
SiO2 (%)		56.67							64.81	
Al2O3 (%)		13.41							12.08	
Fe2O3 (%)		14.1							7.08	
Fe2O3 (%)*	9.40	12.20	10.50	4.90	4.50	4.50	4.50	7.80	6.00	6.60
CaO (%)		3.52							3.04	
K2O (%)		1.89							3.19	
K2O (%)**	2.11	2.11	2.67	2.59	2.83	2.92	2.92	3.16	3.32	4.04
MgO (%)		1.85							1.00	
Na2O (%)		3.09							2.38	
TiO2 (%)		2.2							1.239	
TiO2 (%)*	1.60	2.10	1.80	0.80	0.70	0.70	0.70	1.40	1.00	1.10
P2O5 (%)		0.165							0.100	
MnO (%)		0.158							0.133	
MnO (%)*	0.17	0.15	0.15	0.08	0.09	0.09	0.10	0.16	0.11	0.17
L.O.I.		2.48							4.52	
SUM		99.823							99.803	
As (ppm)*	4	6	9	5	4	4	5	6	4	8
Ba (ppm)*	556	828	879	899	801	807	814	792	694	1719
Cr (ppm)*	102	150	182	67	59	56	56	86	81	169
Cu (ppm)*	32	22	27	20	20	19	20	15	15	34
Ga (ppm)*	19	22	21	18	16	17	17	19	17	17
Mo (ppm)*	0	0	0	0	0	2	0	4	4	2
Nb (ppm)*	19	20	23	13	17	18	17	45	28	21
Ni (ppm)*	48	34	39	23	20	21	20	20	19	47
Pb (ppm)*	32	20	24	18	33	32	32	24	22	47
Rb (ppm)*	94	61	113	89	117	116	119	111	116	192
Sr (ppm)*	217	886	620	546	340	340	332	376	332	339
Th (ppm)*	9	10	16	9	12	11	11	16	17	12
U (ppm)*	3	3	4	2	3	3	2	4	4	5
V (ppm)*	174	303	265	94	82	82	84	137	105	146
Y (ppm)*	67	32	34	27	29	29	30	55	51	26
Zn (ppm)*	131	107	118	71	76	77	78	105	84	126
Zr (ppm)*	605	857	639	330	443	449	431	1149	1020	351

*** Analysis made on Pressed Powders**

**** Converted K2O%. Analysis on Pressed Powders**

SUM is based on Fusion Disks and LOI

APPENDIX E

TABLE E-1. GEOCHEMICAL DATA

	SOC96124	SOC96125	SOC96126	SOC96127	SOC96128	SOC96129	SOC96130	SOC96131	SOC96132	SOC96133
UTM ZONE	13 S	13 S	13 S	13 S	13 S	13 S	13 S	13 S	13 S	13 S
EASTING	305971	307434	309239	309371	295809	296679	296104	298057	295724	295951
NORTHING	3764572	3765805	3764956	3765635	3785155	3796848	3798744	3799898	3789938	3786321
LAT. (N)	34.0038	34.0152	34.0079	34.0140	34.1874	34.2930	34.3099	34.3207	34.2305	34.1979
LONG (W)	107.1010	107.0854	107.0657	107.0644	107.2158	107.2091	107.2158	107.1949	107.2178	107.2145
TRACE ID	T1541	T1542	T1543	T1544	T1545	T1546	T1547	T1548	T1549	T1550
MAJOR ID	M1864	M1865	M1866				M1867			M1868
SiO2 (%)	59.01	61.08	71.23				49.87			57.57
Al2O3 (%)	12.87	13.17	10.97				11.00			14.86
Fe2O3 (%)	6.84	8.16	3.51				20.21			11.85
Fe2O3 (%)*	6.60	7.70	3.50	4.10	11.40	10.20	16.90	6.70	5.50	10.40
CaO (%)	1.66	1.49	0.92				5.18			3.59
K2O (%)	4.02	4.20	2.60				1.68			1.92
K2O (%)**	3.88	4.20	2.51	3.08	2.27	2.27	1.22	1.87	2.51	2.03
MgO (%)	1.56	1.60	0.71				2.39			1.81
Na2O (%)	1.81	1.99	1.38				2.36			3.41
TiO2 (%)	1.126	1.346	0.727				2.209			1.656
TiO2 (%)*	1.10	1.30	0.70	0.80	1.70	1.50	2.10	0.90	0.80	1.50
P2O5 (%)	0.228	0.221	0.110				0.180			0.104
MnO (%)	0.177	0.154	0.098				0.213			0.139
MnO (%)*	0.19	0.16	0.10	0.12	0.14	0.13	0.19	0.09	0.08	0.12
L.O.I.	10.64	5.81	7.44				4.28			3.08
SUM	100.205	99.514	99.84				99.826			100.255
As (ppm)*	9	10	7	8	6	7	7	6	6	6
Ba (ppm)*	1731	1887	631	797	811	941	733	842	811	832
Cr (ppm)*	189	234	56	82	167	301	328	170	79	128
Cu (ppm)*	37	34	25	33	22	33	29	22	20	21
Ga (ppm)*	16	17	13	14	23	18	21	15	18	22
Mo (ppm)*	0	0	2	2	3	0	2	0	0	0
Nb (ppm)*	18	22	16	17	18	13	14	10	12	13
Ni (ppm)*	49	48	19	25	34	67	59	36	23	30
Pb (ppm)*	46	47	28	31	21	18	24	17	19	19
Rb (ppm)*	190	197	110	133	78	75	62	62	80	64
Sr (ppm)*	344	352	193	218	813	738	774	723	660	994
Th (ppm)*	10	13	10	10	11	9	12	8	9	9
U (ppm)*	4	3	3	3	2	2	3	2	2	0
V (ppm)*	145	174	65	82	281	245	443	156	109	245
Y (ppm)*	28	28	31	32	28	30	26	23	26	26
Zn (ppm)*	122	128	67	73	108	98	160	72	70	98
Zr (ppm)*	355	439	478	444	824	454	716	385	438	634

* Analysis made on Pressed Powders

** Converted K2O%. Analysis on Pressed Powders

SUM is based on Fusion Disks and LOI

APPENDIX E

TABLE E-1. GEOCHEMICAL DATA

	SOC96134	SOC96135	SOC96136	SOC96137	SOC96138	SOC96139	SOC96140	SOC96141	SOC96142	SOC96143
UTM ZONE	13 S	13 S	13 S	13 S	13 S	13 S	13 S	13 S	13 S	13 S
EASTING	292475	291906	296191	290982	291606	293971	294521	293912	294896	296488
NORTHING	3788772	3789297	3795045	3796824	3797322	3798707	3801540	3801610	3804278	3773672
LAT. (N)	34.2193	34.2240	34.2766	34.2916	34.2962	34.3092	34.3348	34.3353	34.3596	34.0841
LONG (W)	107.2528	107.2591	107.2140	107.2709	107.2643	107.2389	107.2336	107.2403	107.2302	107.2057
TRACE ID	T1551	T1552	T1553	T1554	T1555	T1556	T1557	T1558	T1559	T1560
MAJOR ID		M1869	M1870		M1871			M1872	M1873	
SiO2 (%)		56.02	45.71		61.85			73.19	72.74	
Al2O3 (%)		13.54	11.25		12.94			9.46	11.74	
Fe2O3 (%)		15.26	21.39		6.33			5.31	3.42	
Fe2O3 (%)*	9.80	13.10	18.80	6.60	5.80	7.50	4.20	4.50	3.50	15.90
CaO (%)		3.07	5.87		3.43			2.50	0.93	
K2O (%)		1.76	1.38		2.25			2.38	2.32	
K2O (%)**	2.11	1.87	0.82	2.11	2.27	2.35	2.35	2.59	2.27	1.30
MgO (%)		1.69	2.54		2.05			1.06	0.98	
Na2O (%)		2.94	2.40		2.15			0.92	0.98	
TiO2 (%)		2.118	2.687		0.973			0.782	0.708	
TiO2 (%)*	1.50	2.00	2.70	1.00	0.90	1.10	0.80	0.70	0.70	0.90
P2O5 (%)		0.078	0.139		0.184			0.103	0.090	
MnO (%)		0.175	0.216		0.094			0.059	0.035	
MnO (%)*	0.12	0.16	0.20	0.12	0.09	0.11	0.05	0.05	0.04	0.20
L.O.I.		3.01	4.95		7.44			4.69	5.41	
SUM		99.947	98.821		99.884			100.703	99.535	
As (ppm)*	6	6	5	8	6	6	7	6	7	253
Ba (ppm)*	802	738	526	788	767	917	1058	888	816	1258
Cr (ppm)*	116	148	366	70	126	209	91	71	57	112
Cu (ppm)*	18	20	29	29	27	30	20	21	21	1141
Ga (ppm)*	22	24	24	19	17	17	13	12	14	43
Mo (ppm)*	0	3	0	0	0	0	4	3	2	5
Nb (ppm)*	14	16	18	11	12	12	14	14	14	12
Ni (ppm)*	28	36	66	23	35	52	23	15	17	36
Pb (ppm)*	20	23	22	19	23	19	27	20	23	11258
Rb (ppm)*	59	61	44	78	79	74	86	106	89	85
Sr (ppm)*	997	880	831	711	507	665	204	437	177	285
Th (ppm)*	9	12	10	8	10	8	13	14	11	16
U (ppm)*	2	3	0	2	2	2	5	3	3	0
V (ppm)*	225	310	478	145	117	166	95	92	75	127
Y (ppm)*	26	31	29	28	27	29	34	36	30	51
Zn (ppm)*	87	122	174	86	75	80	79	52	76	19818
Zr (ppm)*	653	961	1047	330	432	377	855	771	438	405

*** Analysis made on Pressed Powders**

**** Converted K2O%. Analysis on Pressed Powders**

SUM is based on Fusion Disks and LOI

APPENDIX E

TABLE E-1. GEOCHEMICAL DATA

	SOC96144	SOC96145	SOC96146	SOC96147	SOC96148	SOC96149	SOC96150 A	SOC96150 B	SOC96150 C
UTM ZONE	13 S	13 S	13 S	13 S	13 S	13 S	13 S	13 S	13 S
EASTING	297032	297212	296094	285200	288121	285330	282465	282465	282465
NORTHING	3772050	3768377	3768850	3791515	3794571	3793247	3790471	3790471	3790471
LAT. (N)	34.0695	34.0365	34.0405	34.2426	34.2707	34.2582	34.2326	34.2326	34.2326
LONG (W)	107.1995	107.1967	107.2089	107.3324	107.3015	107.3314	107.3618	107.3618	107.3618
TRACE ID	T1561	T1562	T1563	T1564	T1565	T1566	T1567	T1568	T1569
MAJOR ID	M1874	M1875	M1876	M1877	M1878				
SiO2 (%)	56.79	63.30	62.12	60.85	66.66				
Al2O3 (%)	12.21	15.33	14.44	13.77	13.29				
Fe2O3 (%)	6.4	5.65	4.85	7.96	4.68				
Fe2O3 (%)*	6.30	5.30	4.60	7.00	4.60	10.70	13.30	13.20	13.90
CaO (%)	6.80	1.03	1.14	4.13	2.07				
K2O (%)	2.15	4.07	4.00	2.14	2.78				
K2O (%)**	2.11	4.04	3.88	2.27	2.83	2.19	1.63	1.63	1.71
MgO (%)	2.15	1.17	1.21	1.89	1.37				
Na2O (%)	1.50	1.88	1.89	2.67	2.23				
TiO2 (%)	0.76	0.747	0.74	1.182	0.91				
TiO2 (%)*	0.80	0.70	0.70	1.10	0.90	1.80	1.80	1.80	1.90
P2O5 (%)	0.160	0.232	0.210	0.145	0.135				
MnO (%)	0.149	0.111	0.11	0.104	0.089				
MnO (%)*	0.15	0.12	0.12	0.10	0.09	0.14	0.16	0.16	0.17
L.O.I.	9.95	6.84	9	5	5.64				
SUM	99.326	100.577	99.891	100.063	100.052				
As (ppm)*	0	4	4	5	4	0	5	6	5
Ba (ppm)*	986	868	820	942	1001	899	765	771	803
Cr (ppm)*	108	31	61	117	83	201	135	130	137
Cu (ppm)*	168	24	28	21	23	26	21	22	22
Ga (ppm)*	19	22	19	19	16	20	21	22	23
Mo (ppm)*	3	3	0	0	0	2	0	0	0
Nb (ppm)*	12	30	25	12	15	17	14	14	14
Ni (ppm)*	33	12	17	30	39	48	34	34	36
Pb (ppm)*	1192	79	62	17	17	20	22	21	22
Rb (ppm)*	115	238	219	67	96	66	54	54	53
Sr (ppm)*	298	153	183	816	502	726	845	845	925
Th (ppm)*	10	32	24	8	10	12	9	8	8
U (ppm)*	2	8	8	2	3	2	2	3	2
V (ppm)*	116	100	90	153	82	253	314	319	335
Y (ppm)*	35	32	30	25	26	32	28	27	27
Zn (ppm)*	2018	108	103	75	67	107	130	129	127
Zr (ppm)*	380	782	510	449	345	830	734	748	745

* Analysis made on Pressed Powders

** Converted K2O%. Analysis on Pressed Powders

SUM is based on Fusion Disks and LOI

APPENDIX E

TABLE E-1. GEOCHEMICAL DATA

	SOC96151	SOC96152	SOC96153	SOC96154	SOC96155	SOC96156	SOC96157	SOC96158	SOC96159	SOC96160
UTM ZONE	13 S	13 S	13 S	13 S	13 S	13 S	13 S	13 S	13 S	13 S
EASTING	282032	283446	322782	318861	317975	317877	319084	301814	300798	322442
NORTHING	3796181	3785042	3782517	3785830	3786034	3785604	3786197	3764394	3768024	3785691
LAT. (N)	34.2840	34.1839	34.1686	34.1978	34.1994	34.1955	34.2011	34.0015	34.0340	34.1971
LONG. (W)	107.3680	107.3498	106.9227	106.9659	106.9756	106.9765	106.9636	107.1459	107.1578	106.9270
TRACE ID	T1570	T1571	T1572	T1573	T1574	T1575	T1576	T1577	T1578	T1579
MAJOR ID	M1879					M1880	M1881	M1882		M1883
SiO2 (%)	60.44					59.03	59.70	53.34		66.81
Al2O3 (%)	13.91					12.90	12.07	16.62		11.50
Fe2O3 (%)	8.07					8.75	7.1	8.89		6.5
Fe2O3 (%)*	7.20	8.00	11.90	8.30	7.20	9.40	7.20	8.70	10.60	6.40
CaO (%)	4.50					3.50	5.07	2.84		2.79
K2O (%)	1.98					2.97	3.23	2.65		2.90
K20 (%)**	2.03	2.03	2.43	2.59	3.00	2.92	3.16	2.67	2.51	3.00
MgO (%)	1.97					2.19	1.72	1.50		1.56
Na2O (%)	2.94					1.85	1.76	2.50		1.98
TiO2 (%)	1.046					1.454	1.202	1.478		1.138
TiO2 (%)*	1.00	1.30	2.00	1.30	1.10	1.50	1.20	1.50	1.40	1.10
P2O5 (%)	0.132					0.278	0.213	0.465		0.175
MnO (%)	0.11					0.138	0.116	0.152		0.095
MnO (%)*	0.10	0.10	0.17	0.13	0.12	0.15	0.12	0.17	0.16	0.10
L.O.I.	4.99					6.23	7.48	9.54		4.05
SUM	100.312					99.685	99.982	100.174		99.828
As (ppm)*	6	5	6	5	5	5	8	16	18	5
Ba (ppm)*	868	909	707	903	576	481	742	786	780	654
Cr (ppm)*	94	101	110	80	56	92	100	102	106	87
Cu (ppm)*	20	15	27	29	27	31	25	59	48	20
Ga (ppm)*	19	20	18	19	21	22	19	21	22	17
Mo (ppm)*	0	0	7	13	7	8	5	0	2	7
Nb (ppm)*	11	11	21	26	31	39	25	16	18	20
Ni (ppm)*	26	25	27	32	22	36	32	31	36	25
Pb (ppm)*	16	17	62	46	48	39	34	21	830	45
Rb (ppm)*	61	50	118	185	238	294	223	105	125	166
Sr (ppm)*	884	1157	387	198	166	160	259	704	370	243
Th (ppm)*	8	7	20	52	40	55	34	9	10	36
U (ppm)*	0	2	6	12	8	11	9	2	2	8
V (ppm)*	159	187	228	131	84	125	125	222	220	104
Y (ppm)*	25	21	90	182	182	233	129	32	33	115
Zn (ppm)*	78	73	164	128	123	146	123	109	399	100
Zr (ppm)*	398	530	2122	3557	2198	2695	1682	517	520	1869

* Analysis made on Pressed Powders
** Converted K2O %. Analysis Made on Pressed Powders
Sum is Based on Fusion Disks and LOI

APPENDIX E

TABLE E-1. GEOCHEMICAL DATA

	SOC96161	SOC96162	SOC96163	SOC96164	SOC96165	SOC96166	SOC96167	SOC96168	SOC96169	SOC96170
UTM ZONE	13 S	13 S	13 S	13 S	13 S .	13 S	13 S	13 S	13 S	13 S
EASTING	322780	299028	299854	302491	303492	297110	291408	290410	289977	308970
NORTHING	3788183	3764921	3765506	3766314	3767334	3779093	3758322	3757866	3773636	3757674
LAT. (N)	34.2196	34.0057	34.0111	34.0189	34.0283	34.1330	33.9447	33.9404	34.0824	33.9422
LONG. (W)	106.9239	107.1762	107.1674	107.1390	107.1284	107.2003	107.2571	107.2678	107.2762	107.0670
TRACE ID	T1580	T1581	T1582	T1583	T1584	T1585	T1586	T1587	T1588	T1589
MAJOR ID		M1884		M1885		M1886	M1887		M1888	M1889
SiO2 (%)		48.87		65.61		65.09	65.43		63.77	70.69
Al2O3 (%)		12.20		12.74		13.37	12.97		13.06	11.46
Fe2O3 (%)		6.68		5.89		7.6	3.99		3.68	3.52
Fe2O3 (%)*	5.70	6.20	4.30	5.70	7.30	6.90	3.90	3.50	3.60	3.20
CaO (%)		3.10		2.55		2.18	2.43		3.53	1.07
K2O (%)		2.66		2.53		3.12	3.14		2.68	3.70
K20 (%)**	2.75	2.59	1.87	2.59	2.43	3.08	3.00	3.00	2.59	3.64
MgO (%)		2.25		1.16		1.19	1.07		1.41	0.75
Na2O (%)		1.41		1.39		2.45	1.64		1.99	1.57
TiO2 (%)		1.104		0.884		1.018	0.723		0.654	0.681
TiO2 (%)*	1.00	1.00	0.60	0.90	1.20	1.00	0.70	0.70	0.60	0.60
P2O5 (%)		0.326		0.118		0.213	0.119		0.136	0.082
MnO (%)		0.135		0.16		0.093	0.09		0.068	0.126
MnO (%)*	0.09	0.15	0.26	0.17	0.16	0.10	0.09	0.09	0.07	0.12
L.O.I.		21.11		7.16		3.58	8.51		8.86	6.77
SUM		100.046		100.36		100.182	100.27		100.012	100.578
As (ppm)*	6	7	5	15	6	6	5	4	4	11
Ba (ppm)*	814	1147	742	621	869	680	894	804	792	733
Cr (ppm)*	140	154	97	127	133	98	55	49	48	60
Cu (ppm)*	22	38	37	33	40	27	21	16	18	20
Ga (ppm)*	16	17	15	17	18	19	16	17	16	15
Mo (ppm)*	0	0	2	3	0	5	0	0	0	2
Nb (ppm)*	14	16	14	14	18	31	18	17	14	20
Ni (ppm)*	30	59	46	38	49	24	21	18	18	18
Pb (ppm)*	22	32	66	264	42	44	23	22	21	28
Rb (ppm)*	116	154	132	121	95	176	128	121	100	172
Sr (ppm)*	488	362	290	216	331	427	281	364	450	216
Th (ppm)*	10	12	10	12	10	43	11	10	10	14
U (ppm)*	2	12	39	3	2	7	2	3	2	2
V (ppm)*	132	141	120	122	170	140	70	64	58	61
Y (ppm)*	31	36	32	40	42	59	33	28	26	38
Zn (ppm)*	71	120	123	228	130	99	72	57	63	61
Zr (ppm)*	515	299	216	456	345	1349	341	355	314	476

* Analysis made on Pressed Powders
** Converted K2O %. Analysis Made on Pressed Powders
Sum is Based on Fusion Disks and LOI

APPENDIX E

TABLE E-1. GEOCHEMICAL DATA

	SOC96171	SOC96172	SOC96173	SOC96174	SOC96175	SOC96176	SOC96177	SOC96178	SOC96179	SOC96180 A
UTM ZONE	13 S	13 S	13 S	13 S	13 S	13 S	13 S	13 S	13 S	13 S
EASTING	310070	320197	317796	322838	324490	345935	347343	347426	347571	284152
NORTHING	3757842	3782489	3782539	3778111	3778442	3780008	3773538	3768875	3766871	3793726
LAT. (N)	33.9439	34.1679	34.1679	34.1289	34.1321	34.1496	34.0915	34.0495	34.0314	34.2623
LONG. (W)	107.0552	106.9507	106.9768	106.9212	106.9034	106.6712	106.6548	106.6530	106.6511	107.3443
TRACE ID	T1590	T1591	T1592	T1593	T1594	T1595	T1596	T1597	T1598	T1599
MAJOR ID	M1890	M1891		M1892			M1893		M1894	M1895
SiO2 (%)	59.58	60.94		66.81			71.60		57.64	60.01
Al2O3 (%)	12.32	10.80		11.63			8.78		11.55	14.15
Fe2O3 (%)	6.84	10.21		5			3.67		12.23	8.19
Fe2O3 (%)*	6.70	10.30	10.10	4.50	4.50	1.50	3.40	4.00	10.40	7.40
CaO (%)	4.42	3.77		4.47			3.89		5.10	3.82
K2O (%)	3.08	2.33		2.61			1.92		1.67	2.06
K20 (%)**	3.00	2.59	2.03	2.67	2.67	1.79	1.95	2.11	1.71	2.19
MgO (%)	1.89	1.73		1.20			1.42		2.75	1.98
Na2O (%)	1.43	1.74		2.33			1.12		2.25	2.80
TiO2 (%)	1.054	2.173		0.818			0.674		1.262	1.16
TiO2 (%)*	1.00	2.00	1.10	0.80	0.70	0.30	0.60	0.60	1.20	1.10
P2O5 (%)	0.217	0.352		0.154			0.093		0.253	0.136
MnO (%)	0.103	0.164		0.084			0.056		0.178	0.111
MnO (%)*	0.10	0.16	0.22	0.08	0.08	0.03	0.05	0.07	0.16	0.11
L.O.I.	8.94	4.96		4.59			6.71		4.97	5.12
SUM	100.075	99.699		99.914			100.105		100.073	99.774
As (ppm)*	12	6	4	8	6	0	4	5	4	4
Ba (ppm)*	901	699	600	925	776	334	573	638	797	965
Cr (ppm)*	172	121	65	88	90	44	58	47	98	109
Cu (ppm)*	32	31	32	18	19	8	14	16	32	20
Ga (ppm)*	17	17	21	15	15	6	11	13	19	19
Mo (ppm)*	0	12	4	3	0	0	2	0	0	0
Nb (ppm)*	15	24	19	10	10	4	10	10	9	10
Ni (ppm)*	71	26	24	23	24	11	16	13	26	32
Pb (ppm)*	16	32	39	18	22	10	17	19	19	18
Rb (ppm)*	139	112	146	98	105	49	72	100	54	66
Sr (ppm)*	331	256	199	588	494	308	200	298	718	789
Th (ppm)*	9	23	14	7	8	3	9	12	9	9
U (ppm)*	2	7	4	3	3	2	3	3	3	2
V (ppm)*	126	162	87	99	98	28	66	82	252	164
Y (ppm)*	30	139	113	24	24	13	26	43	28	26
Zn (ppm)*	82	156	223	55	61	26	46	54	112	80
Zr (ppm)*	512	3678	1516	350	352	368	651	591	495	452

* Analysis made on Pressed Powders

** Converted K2O %. Analysis Made on Pressed Powders

Sum is Based on Fusion Disks and LOI

APPENDIX E

TABLE E-1. GEOCHEMICAL DATA

	SOC96180 B	SOC96180 C	SOC96181	SOC96182	SOC96183	SOC96184	SOC96185	SOC96186	SOC96187	SOC96188
UTM ZONE	13 S	13 S	13 S	13 S	13 S	13 S	13 S	13 S	13 S	13 S
EASTING	284152	284152	282064	282010	283617	318312	323948	323855	320964	305977
NORTHING	3793726	3793726	3803251	3805274	3807356	3763491	3762334	3761808	3752634	3755249
LAT. (N)	34.2623	34.2623	34.3477	34.3659	34.3850	33.9963	33.9868	33.9821	33.8989	33.9198
LONG. (W)	107.3443	107.3443	107.3694	107.3705	107.3536	106.9672	106.9060	106.9069	106.9363	107.0989
TRACE ID	T1600	T1601	T1602	T1603	T1604	T1605	T1606	T1607	T1608	T1609
MAJOR ID	M1896			M1897			M1898			M1899
SiO2 (%)	60.08			63.63			67.54			73.89
Al2O3 (%)	14.25			11.75			10.69			10.27
Fe2O3 (%)	8.15			7.17			3.95			2.97
Fe2O3 (%)*	7.30	6.90	11.50	7.20	13.30	7.90	3.80	4.30	4.90	2.80
CaO (%)	3.79			4.06			3.50			0.81
K2O (%)	2.08			1.84			2.95			3.71
K20 (%)**	2.19	2.19	2.03	1.87	1.46	3.72	2.92	2.51	2.67	3.56
MgO (%)	1.98			2.89			1.13			0.55
Na2O (%)	2.79			1.84			1.55			1.47
TiO2 (%)	1.152			1.089			0.721			0.668
TiO2 (%)*	1.10	1.00	1.80	1.10	1.60	1.30	0.70	0.90	0.80	0.60
P2O5 (%)	0.136			0.168			0.115			0.059
MnO (%)	0.11			0.095			0.071			0.109
MnO (%)*	0.11	0.10	0.15	0.09	0.17	0.09	0.07	0.10	0.09	0.11
L.O.I.	5.12			4.65			6.16			5.02
SUM	99.853			99.413			98.547			99.669
As (ppm)*	5	5	6	7	6	15	11	10	8	9
Ba (ppm)*	976	959	843	872	1098	1538	755	766	870	542
Cr (ppm)*	110	102	220	280	175	112	58	68	62	38
Cu (ppm)*	22	20	24	32	26	22	17	14	21	16
Ga (ppm)*	19	19	19	15	19	15	13	11	14	14
Mo (ppm)*	0	0	2	0	2	2	0	2	0	2
Nb (ppm)*	9	9	17	11	9	18	15	17	17	23
Ni (ppm)*	32	31	46	58	36	24	17	15	19	12
Pb (ppm)*	18	16	19	18	23	30	20	18	23	26
Rb (ppm)*	67	67	66	60	56	186	118	92	94	181
Sr (ppm)*	795	788	753	475	657	376	311	310	449	173
Th (ppm)*	8	7	11	8	12	11	8	9	11	13
U (ppm)*	3	3	3	4	3	3	3	3	3	4
V (ppm)*	157	150	299	151	337	188	74	98	100	52
Y (ppm)*	24	26	35	29	35	28	27	32	28	37
Zn (ppm)*	80	77	106	82	121	95	60	55	65	64
Zr (ppm)*	458	418	703	529	1138	734	449	906	526	513

* Analysis made on Pressed Powders
** Converted K2O %. Analysis Made on Pressed Powders
Sum is Based on Fusion Disks and LOI

APPENDIX E

TABLE E-1. GEOCHEMICAL DATA

	SOC96189	SOC96190	SOC96191	SOC96192	SOC96193	SOC96194	SOC96195	SOC96196	SOC96197	SOC96198
UTM ZONE	13 S	13 S	13 S	13 S	13 S	13 S	13 S	13 S	13 S	13 S
EASTING	308111	290085	292270	291004	288489	310068	331365	330158	328669	327794
NORTHING	3768530	3758997	3755054	3763303	3766248	3769665	3759890	3765090	3765965	3769660
LAT. (N)	34.0399	33.9505	33.9154	33.9895	34.0156	34.0505	33.9660	34.0127	34.0204	34.0535
LONG. (W)	107.0787	107.2715	107.2470	107.2626	107.2906	107.0578	106.8252	106.8393	106.8556	106.8658
TRACE ID	T1610	T1611	T1612	T1613	T1614	T1615	T1616	T1617	T1618	T1619
MAJOR ID		M1900		M1901	M1902	M1903			M1904	
SiO2 (%)		70.91		69.29	68.06	63.80			75.44	
Al2O3 (%)		11.83		12.49	13.24	13.29			7.04	
Fe2O3 (%)		3.66		3.04	3.29	5.47			3.8	
Fe2O3 (%)*	5.10	3.30	4.20	2.90	3.20	5.20	4.20	2.50	3.30	2.80
CaO (%)		1.88		1.63	2.10	1.30			3.82	
K2O (%)		3.57		2.84	2.80	4.02			1.79	
K2O (%)**	3.16	3.40	3.16	2.67	2.67	3.72	2.03	1.71	1.87	1.95
MgO (%)		0.80		0.84	0.99	1.20			1.10	
Na2O (%)		2.29		2.32	2.16	1.64			1.11	
TiO2 (%)		0.673		0.616	0.609	0.897			0.703	
TiO2 (%)*	0.90	0.60	0.70	0.60	0.60	0.90	0.80	0.50	0.60	0.50
P2O5 (%)		0.060		0.072	0.089	0.202			0.081	
MnO (%)		0.094		0.091	0.065	0.149			0.06	
MnO (%)*	0.12	0.09	0.10	0.09	0.07	0.16	0.06	0.04	0.05	0.05
L.O.I.		4.73		6.75	6.42	7.96			5.08	
SUM		100.646		100.143	99.965	100.129			100.205	
As (ppm)*	8	5	7	4	5	9	5	4	5	5
Ba (ppm)*	834	552	703	764	773	1101	794	567	599	533
Cr (ppm)*	95	43	68	41	47	104	54	47	54	48
Cu (ppm)*	26	12	21	15	16	30	12	11	10	12
Ga (ppm)*	15	16	17	15	16	17	10	9	8	9
Mo (ppm)*	2	2	0	0	0	0	2	2	3	0
Nb (ppm)*	18	29	18	21	15	16	13	8	9	10
Ni (ppm)*	28	13	26	14	16	37	14	13	12	14
Pb (ppm)*	27	23	24	23	22	36	15	10	12	13
Rb (ppm)*	142	169	160	104	104	178	66	55	59	66
Sr (ppm)*	220	322	270	375	373	278	262	190	185	202
Th (ppm)*	10	16	12	9	8	9	8	5	7	7
U (ppm)*	3	3	3	3	2	3	3	2	3	3
V (ppm)*	106	57	76	52	54	106	89	51	71	56
Y (ppm)*	33	28	34	27	26	31	30	20	24	23
Zn (ppm)*	90	55	71	52	58	104	47	32	38	39
Zr (ppm)*	463	426	371	356	328	323	905	494	796	514

* Analysis made on Pressed Powders
** Converted K2O %. Analysis Made on Pressed Powders
Sum is Based on Fusion Disks and LOI

APPENDIX E

TABLE E-1. GEOCHEMICAL DATA

	SOC96199	SOC96200	SOC96201	SOC96202	SOC96203	SOC96204	SOC96205	SOC96206	SOC96207	SOC96208
UTM ZONE	13 S	13 S	13 S	13 S	13 S	13 S	13 S	13 S	13 S	13 S
EASTING	327827	285615	285019	285287	296838	296975	295825	293554	288024	296714
NORTHING	3771348	3754930	3756156	3751910	3779722	3775140	3774922	3772972	3769277	3773069
LAT. (N)	34.0687	33.9130	33.9239	33.8857	34.1386	34.0974	34.0952	34.0772	34.0428	34.0787
LONG. (W)	106.8658	107.3189	107.3256	107.3217	107.2033	107.2008	107.2132	107.2373	107.2963	107.2031
TRACE ID	T1620	T1621	T1622	T1623	T1624	T1625	T1626	T1627	T1628	T1765
MAJOR ID	M1905		M1906	M1907				M1908		
SiO2 (%)	72.48		68.10	68.49				65.10		
Al2O3 (%)	7.91		12.59	12.36				13.98		
Fe2O3 (%)	4.35		4.2	3.32				5.18		
Fe2O3 (%)*	3.80	3.30	3.90	3.10	8.80	4.60	11.50	4.80	4.40	5.50
CaO (%)	4.03		1.44	1.71				2.99		
K2O (%)	1.92		3.32	3.37				2.48		
K20 (%)**	2.03	3.24	3.16	3.16	2.51	2.11	2.11	2.43	2.43	2.19
MgO (%)	1.25		0.81	0.91				1.33		
Na2O (%)	1.29		2.21	1.87				2.57		
TiO2 (%)	0.831		0.801	0.604				0.812		
TiO2 (%)*	0.70	0.60	0.70	0.50	1.30	0.50	1.00	0.80	0.70	0.80
P2O5 (%)	0.087		0.098	0.088				0.097		
MnO (%)	0.074		0.114	0.094				0.082		
MnO (%)*	0.07	0.06	0.11	0.09	0.11	0.16	0.18	0.08	0.11	0.11
L.O.I.	5.69		6.1	6.85				4.95		
SUM	100.113		99.955	99.794				99.774		
As (ppm)*	4	4	7	5	7	5	23	4	4	11
Ba (ppm)*	603	499	690	503	752	476	805	864	766	678
Cr (ppm)*	60	49	51	41	103	81	122	62	54	72
Cu (ppm)*	11	14	22	16	28	62	794	17	23	21
Ga (ppm)*	11	15	16	16	20	14	24	17	17	18
Mo (ppm)*	3	0	2	0	2	2	4	0	0	0
Nb (ppm)*	15	17	22	21	17	11	19	13	16	13
Ni (ppm)*	14	22	16	14	29	32	33	20	20	24
Pb (ppm)*	16	22	26	23	28	317	2762	32	21	179
Rb (ppm)*	70	143	128	136	101	127	132	88	93	114
Sr (ppm)*	200	210	298	318	521	209	328	556	376	283
Th (ppm)*	10	12	11	15	13	10	26	10	10	9
U (ppm)*	3	3	3	3	3	3	2	2	3	4
V (ppm)*	79	45	68	52	190	69	164	85	77	102
Y (ppm)*	31	31	36	36	33	34	37	26	29	39
Zn (ppm)*	47	59	71	64	108	547	4718	73	76	207
Zr (ppm)*	878	350	505	341	751	231	552	414	397	362

* Analysis made on Pressed Powders
** Converted K2O %. Analysis Made on Pressed Powders
Sum is Based on Fusion Disks and LOI

APPENDIX E

TABLE E-1. GEOCHEMICAL DATA

	SOC96209	SOC96210 A	SOC96210 B	SOC96210 C	SOC96211	SOC96212	SOC96213	SOC96214	SOC96215	SOC96216
UTM ZONE	13 S	13 S	13 S	13 S	13 S	13 S	13 S	13 S	13 S	13 S
EASTING	295814	293900	293900	293900	304676	301066	303360	304582	306422	299672
NORTHING	3774001	3794018	3794018	3794018	3775989	3799901	3800821	3802099	3799889	3801693
LAT. (N)	34.0869	34.2669	34.2669	34.2669	34.1065	34.3213	34.3300	34.3418	34.3222	34.3372
LONG. (W)	107.2131	107.2386	107.2386	107.2386	107.1176	107.1622	107.1375	107.1245	107.1040	107.1777
TRACE ID	T1766	T1767	T1768	T1769	T1770	T1771	T1772	T1773	T1774	T1775
MAJOR ID					M1909	M1910		M1911	M1912	M1913
SiO2 (%)					65.71	54.38		48.32	47.78	66.11
Al2O3 (%)					12.54	9.94		7.32	7.80	12.04
Fe2O3 (%)					7.38	13.99		5.28	4.75	4.61
Fe2O3 (%)*	12.30	5.50	5.60	6.80	7.10	11.50	8.20	4.70	4.40	4.60
CaO (%)					1.95	6.02		17.07	16.68	3.25
K2O (%)					2.84	1.70		1.36	1.46	2.26
K20 (%)**	1.71	2.19	2.27	2.27	2.92	1.63	1.46	1.06	1.14	2.19
MgO (%)					1.25	2.12		1.11	1.07	1.59
Na2O (%)					1.67	1.73		1.20	1.20	1.13
TiO2 (%)					1.498	1.659		0.837	0.718	0.784
TiO2 (%)*	1.00	0.80	0.80	1.00	1.30	1.50	1.20	0.80	0.70	0.80
P2O5 (%)					0.104	0.158		0.147	0.150	0.128
MnO (%)					0.12	0.154		0.08	0.089	0.055
MnO (%)*	0.18	0.08	0.08	0.09	0.12	0.13	0.09	0.07	0.09	0.05
L.O.I.					4.24	7.44		16.68	17.61	7.43
SUM					99.561	99.535		99.582	99.49	99.565
As (ppm)*	73	8	8	7	7	8	10	10	10	10
Ba (ppm)*	1152	782	797	785	715	800	1122	685	975	818
Cr (ppm)*	105	102	108	126	82	252	190	110	103	98
Cu (ppm)*	543	17	17	19	24	29	22	18	21	21
Ga (ppm)*	32	18	18	18	18	17	14	10	10	15
Mo (ppm)*	4	0	0	0	4	2	2	0	0	2
Nb (ppm)*	19	10	9	12	27	13	12	9	8	12
Ni (ppm)*	34	26	26	29	29	46	38	26	29	29
Pb (ppm)*	6690	17	16	19	49	20	13	15	16	19
Rb (ppm)*	89	74	75	78	120	63	79	65	76	86
Sr (ppm)*	367	852	849	789	240	553	418	347	334	251
Th (ppm)*	11	6	6	8	17	10	7	6	6	10
U (ppm)*	0	2	2	2	6	3	2	2	2	3
V (ppm)*	123	120	115	152	125	283	200	111	103	105
Y (ppm)*	47	23	22	23	95	28	23	21	21	28
Zn (ppm)*	9824	66	66	74	131	107	71	65	54	74
Zr (ppm)*	552	358	368	432	1206	761	615	416	319	433

* Analysis made on Pressed Powders
** Converted K2O %. Analysis Made on Pressed Powders
Sum is Based on Fusion Disks and LOI

APPENDIX E

TABLE E-1. GEOCHEMICAL DATA

	SOC96217	SOC96218	SOC96219	SOC96220	SOC96221	SOC96222	SOC96223	SOC96224	SOC96225	SOC96226
UTM ZONE	13 S	13 S	13 S	13 S	13 S	13 S	13 S	13 S	13 S	13 S
EASTING	300068	317221	316057	314770	319059	324572	295998	291886	290427	285797
NORTHING	3801282	3788585	3790990	3790210	3789597	3775235	3809253	3808357	3809921	3809916
LAT. (N)	34.3336	34.2223	34.2438	34.2365	34.2317	34.1032	34.4046	34.3957	34.4095	34.4085
LONG. (W)	107.1733	106.9843	106.9974	107.0112	106.9646	106.9018	107.2194	107.2639	107.2802	107.3305
TRACE ID	T1776	T1777	T1778	T1779	T1780	T1781	T1782	T1783	T1784	T1785
MAJOR ID			M1914					M1915		M1916
SiO2 (%)			61.68					74.34		58.72
Al2O3 (%)			11.91					7.65		14.09
Fe2O3 (%)			9.72					2.86		5.25
Fe2O3 (%)*	13.00	4.20	8.00	7.70	10.00	4.10	4.70	2.90	5.40	5.50
CaO (%)			4.07					3.61		3.96
K2O (%)			2.75					1.32		2.60
K20 (%)**	0.90	2.51	2.83	2.92	2.43	2.35	2.03	1.54	1.71	2.43
MgO (%)			1.30					1.62		2.45
Na2O (%)			2.72					0.46		0.55
TiO2 (%)			1.518					0.439		0.675
TiO2 (%)*	1.70	0.70	1.30	1.20	1.60	0.80	0.70	0.50	0.70	0.70
P2O5 (%)			0.155					0.110		0.139
MnO (%)			0.144					0.038		0.086
MnO (%)*	0.16	0.09	0.12	0.12	0.13	0.07	0.06	0.04	0.09	0.08
L.O.I.			3.38					6.86		10.82
SUM			99.576					99.445		99.499
As (ppm)*	11	6	7	8	10	7	4	6	5	7
Ba (ppm)*	1386	1090	837	959	864	750	813	431	1124	650
Cr (ppm)*	274	73	141	260	298	73	95	56	72	66
Cu (ppm)*	32	17	20	35	31	14	21	12	26	29
Ga (ppm)*	16	16	18	18	17	11	13	10	15	17
Mo (ppm)*	0	0	2	0	0	2	3	2	0	0
Nb (ppm)*	15	18	21	16	20	13	10	8	11	12
Ni (ppm)*	54	20	29	54	49	16	20	17	25	27
Pb (ppm)*	19	22	25	21	23	18	14	11	16	17
Rb (ppm)*	50	167	155	150	117	82	88	55	80	145
Sr (ppm)*	409	635	465	632	556	284	182	147	221	258
Th (ppm)*	9	10	11	11	13	8	8	6	9	10
U (ppm)*	4	3	4	3	4	3	2	2	3	3
V (ppm)*	332	92	192	199	272	90	93	58	95	105
Y (ppm)*	25	28	35	35	36	28	24	18	25	24
Zn (ppm)*	112	75	83	81	99	52	47	39	54	52
Zr (ppm)*	857	357	698	410	699	663	959	419	372	252

* Analysis made on Pressed Powders
** Converted K2O %. Analysis Made on Pressed Powders
Sum is Based on Fusion Disks and LOI

APPENDIX E

TABLE E-1. GEOCHEMICAL DATA

	SOC96227	SOC96228	SOC96229	SOC96230	SOC96231	SOC96232	SOC96233	SOC96234	SOC96235	SOC96236
UTM ZONE	13 S	13 S	13 S	13 S	13 S	13 S	13 S	13 S	13 S	13 S
EASTING	302785	303264	306330	317002	316040	314308	317411	314759	313193	319203
NORTHING	3797802	3796944	3796319	3768512	3767257	3769342	3773006	3772695	3774905	3775372
LAT. (N)	34.3027	34.2951	34.2900	34.0413	34.0299	34.0483	34.0819	34.0786	34.0983	34.1036
LONG. (W)	107.1430	107.1376	107.1042	106.9824	106.9926	107.0118	106.9789	107.0076	107.0250	106.9600
TRACE ID	T1786	T1787	T1788	T2025	T2026	T2027	T2028	T2029	T2030	T2031
MAJOR ID		M1976		M1917					M1918	
SiO2 (%)		55.31		62.09					58.77	
Al2O3 (%)		9.76		12.38					11.18	
Fe2O3 (%)		12.98		4.52					8.35	
Fe2O3 (%)*	12.40	11.30	10.30	4.40	3.90	4.70	3.50	4.90	7.10	4.70
CaO (%)		6.74		4.01					5.31	
K2O (%)		1.73		2.58					2.71	
K20 (%)**	1.71	1.54	1.79	2.43	1.95	2.19	2.11	2.51	2.75	2.03
MgO (%)		1.81		1.68					1.33	
Na2O (%)		1.68		1.64					1.72	
TiO2 (%)		1.576		0.618					1.297	
TiO2 (%)*	1.70	1.50	1.60	0.60	0.60	0.70	0.60	0.80	1.10	0.90
P2O5 (%)		0.155		0.115					0.151	
MnO (%)		0.142		0.075					0.143	
MnO (%)*	0.14	0.13	0.12	0.08	0.06	0.08	0.08	0.08	0.13	0.05
L.O.I.		7.91		9.8					8.26	
SUM		100.046		99.661					99.419	
As (ppm)*	11	11	7	7	6	6	12	7	10	4
Ba (ppm)*	829	767	721	660	651	639	806	778	838	856
Cr (ppm)*	169	269	180	72	48	51	38	70	103	72
Cu (ppm)*	23	27	18	25	22	22	24	21	27	13
Ga (ppm)*	16	16	15	15	14	15	15	16	16	12
Mo (ppm)*	4	0	2	2	2	2	2	2	3	3
Nb (ppm)*	15	14	14	14	13	13	13	14	21	13
Ni (ppm)*	33	47	30	20	20	19	16	26	32	15
Pb (ppm)*	23	19	20	21	18	19	34	19	24	15
Rb (ppm)*	69	72	65	107	89	89	91	111	120	76
Sr (ppm)*	397	507	646	371	366	450	320	487	399	316
Th (ppm)*	15	10	9	11	11	11	9	10	13	10
U (ppm)*	3	3	4	3	3	3	3	4	7	5
V (ppm)*	324	287	259	81	72	91	54	103	144	111
Y (ppm)*	34	29	27	26	25	27	26	29	34	27
Zn (ppm)*	111	110	88	71	59	65	107	68	99	49
Zr (ppm)*	1377	777	1003	277	305	304	317	361	576	665

* Analysis made on Pressed Powders
** Converted K2O %. Analysis Made on Pressed Powders
Sum is Based on Fusion Disks and LOI

APPENDIX E

TABLE E-1. GEOCHEMICAL DATA

	SOC96237	SOC96238	SOC96239	SOC96240 A	SOC96240 B	SOC96240 C	SOC96241	SOC96242	SOC96243	SOC96244
UTM ZONE	13 S	13 S	13 S	13 S	13 S	13 S	13 S	13 S	13 S	13 S
EASTING	320657	320842	323939	322982	322982	322982	321474	312121	322122	311438
NORTHING	3769600	3771467	3775529	3772432	3772432	3772432	3768561	3766498	3765747	3776190
LAT. (N)	34.0518	34.0686	34.1058	34.0777	34.0777	34.0777	34.0426	34.0223	34.0173	34.1096
LONG. (W)	106.9431	106.9415	106.9087	106.9185	106.9185	106.9185	106.9340	107.0348	106.9264	107.0443
TRACE ID	T2032	T2033	T2034	T2035	T2036	T2037	T2038	T2039	T2040	T2041
MAJOR ID		M1919					M1920	M1921		
SiO2 (%)		66.71					72.39	64.79		
Al2O3 (%)		11.62					9.40	12.54		
Fe2O3 (%)		3.86					5.04	4.33		
Fe2O3 (%)*	3.60	3.80	4.30	4.00	4.00	4.20	4.30	4.40	4.40	8.20
CaO (%)		3.51					2.23	1.88		
K2O (%)		4.01					4.43	2.94		
K20 (%)**	2.92	4.04	2.51	2.67	2.67	2.67	4.45	2.59	2.67	2.83
MgO (%)		1.01					0.54	1.09		
Na2O (%)		1.59					1.16	1.23		
TiO2 (%)		0.633					0.915	0.739		
TiO2 (%)*	0.60	0.70	0.70	0.60	0.60	0.70	0.90	0.70	0.70	1.30
P2O5 (%)		0.170					0.157	0.162		
MnO (%)		0.105					0.069	0.078		
MnO (%)*	0.07	0.10	0.06	0.08	0.08	0.08	0.06	0.08	0.08	0.12
L.O.I.		5.47					3.12	9.44		
SUM		99.165					99.755	99.361		
As (ppm)*	11	9	7	7	7	7	11	6	8	8
Ba (ppm)*	890	2789	725	764	760	776	1413	697	683	773
Cr (ppm)*	39	38	62	50	48	49	56	68	61	133
Cu (ppm)*	21	31	19	22	20	21	15	29	22	25
Ga (ppm)*	15	15	13	15	15	15	12	16	15	18
Mo (ppm)*	2	2	2	2	2	2	3	3	3	3
Nb (ppm)*	14	16	14	15	15	16	15	17	17	22
Ni (ppm)*	17	16	21	22	22	21	11	25	21	35
Pb (ppm)*	28	183	21	31	31	33	30	30	27	25
Rb (ppm)*	148	220	102	120	120	120	197	122	113	125
Sr (ppm)*	490	213	339	293	292	293	224	191	230	391
Th (ppm)*	11	11	10	11	12	12	10	13	12	15
U (ppm)*	4	3	2	3	3	4	4	3	3	4
V (ppm)*	65	72	81	74	79	79	93	71	78	164
Y (ppm)*	26	28	24	29	28	29	28	32	29	35
Zn (ppm)*	74	328	62	84	83	84	130	84	67	104
Zr (ppm)*	284	297	382	358	345	405	694	403	412	667

* Analysis made on Pressed Powders
** Converted K2O %. Analysis Made on Pressed Powders
Sum is Based on Fusion Disks and LOI

APPENDIX E

TABLE E-1. GEOCHEMICAL DATA

	SOC96245	SOC96246	SOC96247	SOC96248	SOC96249	SOC96250	SOC96251	SOC96252	SOC96253	SOC96254
UTM ZONE	13 S	13 S	13 S	13 S	13 S	13 S	13 S	13 S	13 S	13 S
EASTING	312086	311748	311444	311653	308809	312028	311715	312320	311297	311367
NORTHING	3776079	3776036	3774667	3773081	3785949	3788390	3789983	3785768	3786443	3785686
LAT. (N)	34.1087	34.1082	34.0958	34.0816	34.1970	34.2196	34.2339	34.1960	34.2019	34.1951
LONG. (W)	107.0373	107.0409	107.0439	107.0413	107.0750	107.0406	107.0443	107.0368	107.0481	107.0472
TRACE ID	T2042	T2043	T2044	T2045	T2046	T2047	T2048	T2049	T2050	T2051
MAJOR ID		M1922				M1923	M1924			M1925
SiO2 (%)		63.25				51.70	57.34			50.35
Al2O3 (%)		11.04				11.38	12.74			11.82
Fe2O3 (%)		10.08				11.82	12.3			9.05
Fe2O3 (%)*	4.00	7.90	7.00	5.10	6.30	10.40	9.80	10.40	7.80	8.10
CaO (%)		2.95				6.42	4.59			10.06
K2O (%)		2.75				3.02	1.86			2.53
K20 (%)**	2.51	2.92	2.83	2.75	2.03	3.24	2.11	3.16	2.35	2.35
MgO (%)		1.12				2.80	1.76			1.48
Na2O (%)		1.86				1.73	2.94			2.21
TiO2 (%)		1.488				1.782	1.835			1.403
TiO2 (%)*	0.70	1.30	1.00	0.80	1.00	1.70	1.70	1.60	1.30	1.30
P2O5 (%)		0.101				0.260	0.087			0.256
MnO (%)		0.138				0.154	0.137			0.185
MnO (%)*	0.08	0.11	0.12	0.09	0.07	0.15	0.10	0.15	0.17	0.19
L.O.I.		4.68				7.9	3.48			9.61
SUM		99.667				99.201	99.332			99.179
As (ppm)*	7	11	7	6	6	8	6	8	10	11
Ba (ppm)*	625	770	745	709	855	968	773	973	991	1003
Cr (ppm)*	56	99	76	59	109	451	176	356	249	254
Cu (ppm)*	24	19	27	23	17	44	16	46	30	30
Ga (ppm)*	14	16	16	15	16	18	20	19	16	16
Mo (ppm)*	3	3	2	3	2	2	2	2	0	1
Nb (ppm)*	17	25	19	17	14	17	17	15	12	12
Ni (ppm)*	20	25	26	20	25	70	30	79	54	54
Pb (ppm)*	29	25	31	26	18	20	19	23	18	20
Rb (ppm)*	111	125	116	111	74	156	68	149	121	121
Sr (ppm)*	262	397	316	301	693	492	898	534	669	688
Th (ppm)*	12	19	14	13	11	12	10	14	10	10
U (ppm)*	3	3	4	4	3	4	3	3	3	3
V (ppm)*	68	162	127	91	142	283	250	268	203	206
Y (ppm)*	30	36	33	31	25	32	31	36	30	28
Zn (ppm)*	87	94	94	84	68	97	84	103	87	90
Zr (ppm)*	426	807	540	526	501	472	719	528	315	326

* Analysis made on Pressed Powders
** Converted K2O %. Analysis Made on Pressed Powders
Sum is Based on Fusion Disks and LOI

APPENDIX E

TABLE E-1. GEOCHEMICAL DATA

	SOC96255
UTM ZONE	13 S
EASTING	312311
NORTHING	3781974
LAT. (N)	34.1618
LONG. (W)	107.0361
TRACE ID	T2052
MAJOR ID	M1977
SiO2 (%)	64.30
Al2O3 (%)	12.24
Fe2O3 (%)	5.38
Fe2O3 (%)*	5.30
CaO (%)	2.73
K2O (%)	2.93
K20 (%)**	2.83
MgO (%)	1.56
Na2O (%)	1.74
TiO2 (%)	0.912
TiO2 (%)*	0.90
P2O5 (%)	0.184
MnO (%)	0.089
MnO (%)*	0.09
L.O.I.	6.98
SUM	99.228
As (ppm)*	6
Ba (ppm)*	745
Cr (ppm)*	118
Cu (ppm)*	26
Ga (ppm)*	15
Mo (ppm)*	2
Nb (ppm)*	15
Ni (ppm)*	38
Pb (ppm)*	24
Rb (ppm)*	125
Sr (ppm)*	358
Th (ppm)*	13
U (ppm)*	4
V (ppm)*	99
Y (ppm)*	33
Zn (ppm)*	88
Zr (ppm)*	439

* Analysis made on Pressed Powders
** Converted K2O %. Analysis Made on Pressed Powders
Sum is Based on Fusion Disks and LOI